EXHIBIT A

Narasimhan, "The effect of copper and gallium compounds on ribonucleotide reductase", UMI, Order Number 9302808, pp. 1-138 (1992).

Order Number 9302808

The effect of copper and gallium compounds on ribonucleotide reductase

Narasimhan, Jana, Ph.D.

The Medical College of Wisconsin, 1992

U·M·I
300 N. Zeeb Rd.
Ann Arbor, MI 48106

THE EFFECT OF COPPER AND GALLIUM COMPOUNDS ON RIBONUCLEOTIDE REDUCTASE

by

Jana Narasimhan

BSc. Chemistry, University of Madras, India, 1986

A Dissertation submitted to the faculty of

The Division of Graduate Studies of

The Medical College of Wisconsin in

Partial Fulfillment of the Requirement for

the Degree of Doctor of Philosophy

Milwaukee, Wisconsin

March, 1992

ABSTRACT

The mode of action of copper complexes (CuL and CuKTS) and gallium compounds (gallium nitrate and citrate) in cytotoxicity was studied. The effects of these agents on the enzyme ribonucleotide reductase was investigated by monitoring the tyrosyl free radical present in the active site of the enzyme through electron spin resonance spectroscopy. Ribonucleotide reductase is a key enzyme in cellular proliferation since it catalyzes the conversion of ribonucleotides to deoxyribonucleotides, which are the precursors in DNA synthesis. Ribonucleotide reductase consists of two subunits namely M1 and M2. M1 is a dimer of molecular weight 170,000, which has the substrate and effector binding sites. M2 subunit is a dimer of molecular weight 88000, which contains non-heme iron and tyrosyl free radical essential for the activity of the enzyme.

In the studies using copper complexes, the cellular oxidative chemistry was examined by ESR studies on adduct formation with membranes, and oxidation of thiols. Membrane thiols were shown to be oxidized through the reduction of the ESR signal of the thiol adduct and the analysis of sulfhydryl content. Using the radiolabel ^{59}Fe, the inhibitory action of copper thiosemicarbazones on cellular iron uptake was shown. The inhibitory action of CuL on ribonucleotide reductase was shown by the quenching of the tyrosyl free radical in the M2 subunit of the enzyme.

The effect of gallium compounds on the tyrosyl radical signal from ribonucleotide reductase was monitored both in intact cells and in a cell free system. The hypothesis that gallium directly interacts with the smaller iron containing subunit of the enzyme and displaces the iron from it was proven to be true. Using a cell free system, it was shown that gallium specifically acts at the level of the M2 subunit by limiting the amount of intracellular iron needed for its activity. The tyrosyl free radical signal from cell lysates was shown to be inhibited by the direct addition of gallium nitrate or gallium citrate. Furthermore, the signal was regenerated upon addition of soluble iron to the cell lysates. Gallium content in the cells was measured by a fluorimetric method, to ensure the presence of sufficient amounts of gallium to compete with the iron in the M2 subunit of ribonucleotide reductase. The enzyme activity, measured by the conversion of ^{14}C-CDP to the labeled deoxy CDP, was shown to be inhibited by the addition of gallium nitrate in a cell free assay system. The immunoprecipitation studies of the ^{59}Fe labeled M2 protein using the monoclonal antibody directed against this subunit suggested that gallium releases iron from the M2 subunit. Purification of ribonucleotide reductase from L1210 cells was attempted. The affinity column, dATP-sepharose, was synthesized for the purpose of purification of this enzyme. The effect of chelating agents or other inhibitors of the enzyme in combination with gallium on the enzyme activity and the tyrosyl radical signal was examined.

ACKNOWLEDGEMENTS

I am very grateful to all the members of my committee for their invaluable insights in my dissertation work. My special thanks to Drs. William Antholine and Christopher Chitambar for their encouragement and enthusiam in this project. Their easy accesibility at all times made it convenient for our interactions regarding the project. They have taught me the different approaches of addressing a scientific problem.

My sincere thanks to Dr. Larry Hopwood, Barbara Davies, and Donna Volk, who introduced me to the techniques of cell culture. My special thanks to Drs. William O'Brien and Jerry Taylor for their invaluable input in the establishment of the assay for ribonucleotide reductase obtained from cultured cells. I especially appreciate the help rendered by Dr. Joy Joseph with the modification of the assay for the measurement of gallium in cells, and the synthesis of the dATP affinity column.

I would like to acknowledge Dr. Claire Kennedy for the helpful discussions on related subjects. A special thanks to Dr. Helmut Beinert for letting me use liquid helium purchased to perform his studies, and for giving me a copper standard.

I am very thankful to Dr. Mark Newton, who suggested the use of Q-band for the system used in my studies, and to Dr. Christopher Felix for all the help he has rendered while carrying out ESR measurements at liquid helium temperatures

and Q-band. Special thanks to the engineering staff for all their help at times of problems with the spectrometer. It was a pleasure to work with the people of different nationalities at the ESR center.

A special thank you to Karen Hyde, who did a lot of the graphics presented in this dissertation. Also, a special thank you to Yvonne Morauski, Margaret Wold, and Marion Krug for their assistance with abstract and manuscript preparations.

Thanks are also due to Richard Tonkyn and Richard Johnson who made accessory tools needed for my experiments.

Last, but not the least, I would like to thank my husband, Nachu, for his continuous support, guidance, and patience, without which it would have been difficult to accomplish this project. I am indebted to my brother, Ravi, and my parents, Ramasamy and Rajalakshmi, for their support and guidance throughout my education.

TABLE OF CONTENTS

LIST OF FIGURES

LIST OF TABLES

I. GENERAL INTRODUCTION

Cancer cells are different from the normal cells in that they are biochemically transformed. These cells are committed to a gradual increase in their neoplastic properties, i.e., an amplification of the biochemical transformations, to maintain continued cellular replication. The biochemical transformations are manifested through alterations in the enzymic and metabolic pattern of cancer cells. A variety of cellular enzymes and metabolites have been linked to neoplastic transformations (1). A few of those enzymes are very stringently linked with transformation and progression in cancer cells, some of which are involved in the purine and pyrimidine metabolism and some in carbohydrate metabolism. Ribonucleotide reductase is among the key enzymes whose activity is markedly altered in the process of neoplastic transformation. DNA polymerase, the enzyme that utilizes the dNTPs for DNA synthesis, is another enzyme that is increased during transformation in cancer cells. The ribonucleotide reductase (CDP reductase) activity was shown to be increased by an order of magnitude in slow growing hepatomas, and by two orders of magnitude in rapidly growing tumors (2,3).

The biochemical basis for chemotherapy is to induce a change in the cancer cells which would selectively interfere

with the transformations in these cells, resulting in cell death (1). The chemotherapeutic drug or combination of drugs are targeted specifically at one or more of the key enzymes that are altered during neoplastic transformations. The normal cells should adapt and recover from toxicity.

The effect of compounds of two metals on the enzyme ribonucleotide reductase from leukemic cells (both human and murine) is studied in this dissertation. The first set, mono- and bis- thiosemicarbazone copper complexes, (via the redox reactions that take place) leads to inhibition of cellular iron uptake, followed by an attack on ribonucleotide reductase. The second set of compounds studied is that of gallium, whose direct effect on the iron binding subunit of the enzyme is examined.

A. Introduction to ribonucleotide reductase

Ribonucleotide reductases play a vital role in DNA biosynthesis by catalyzing the conversion of nucleotide phosphates (di- or tri- i.e., NDP or NTP) to deoxynucleotide phosphates (dNDP or dNTP), the phosphorylation state depending on the organism, Eq. (1).

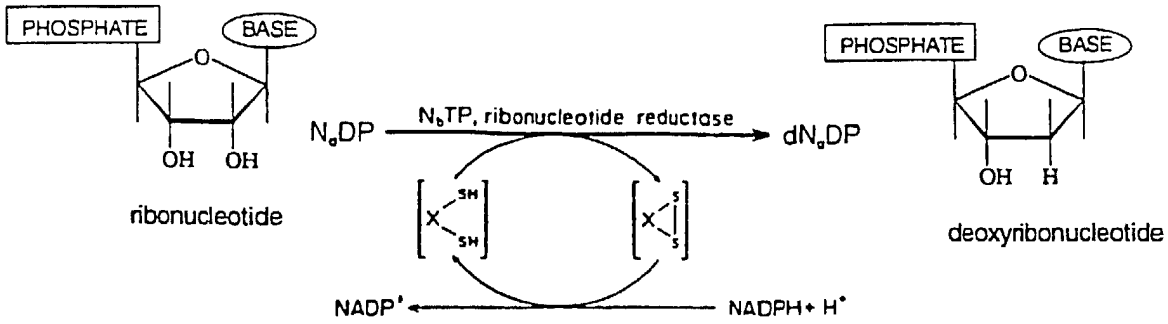

Eq 1. Enzymatic reaction catalyzed by ribonucleotide reductase. Scheme taken from (4).

The replication of DNA prior to cell division requires the presence of a balanced supply of deoxyribonucleotides (provided by the catalytic action of ribonucleotide reductase) for DNA polymerase. While the intracellular concentrations of ribonucleotides are in the millimolar range, the concentrations of the deoxyribonucleotide pools are extremely low (micromolar range). In both procaryotes and eukaryotes, the formation of deoxyribonucleotides occurs by the direct reduction of the 2'-position of the corresponding ribonucleotides. The reduction of a particular substrate, N_aDP, requires the presence of an appropriate N_bTP as the

allosteric effector. The electrons involved are transferred from the catalytic site of ribonucleotide reductase through a reducing agent thioredoxin (or glutaredoxin) to NADPH via thioredoxin reductase (or glutaredoxin reductase) (Fig. I.1 taken from (21)).

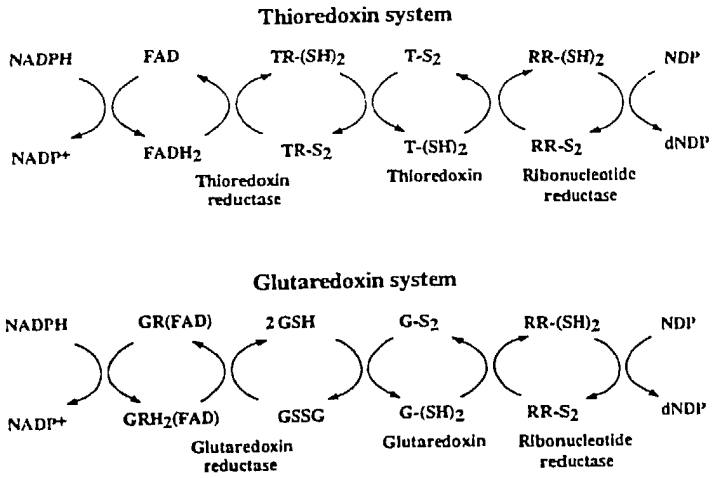

Fig I.1. Cofactors involved in the ribonucleotide reduction.

There are at least three distinct ribonucleotide reductase systems which have been identified. The ribonucleotide reductase from *L. leichmannii* is a single polypeptide of molecular weight 76,000. The enzymes from *L. leichmannii* and *Euglena glacillis* require as the substrate, ribonucleoside triphosphate, and have an absolute requirement for 5'-deoxyadenosylcobalamin (4). 5'-deoxyadenosylcobalamin functions as the intermediate between thioredoxin and ribonucleotide reductase. The enzymes from *Rhizobium meliloti*, *Bacillus megaterium*, and *Corynebacterium nephridii* require ribonucleoside diphosphates as substrates and likewise

have an absolute requirement for 5'-deoxyadenosylcobalamin.

The ribonucleotide reductase from *Escherichia coli* has been extensively investigated and is the prototype for the mammalian, yeast, and Herpes simplex virus I and II proteins. The enzyme consists of two subunits B1 (172 kD) and B2 (87 kD), each of which is composed of two equivalent protomers. There is one binuclear iron center and one tyrosyl radical per B2 protomer.

Ribonucleotide reductase from *Brevibacterium ammoniagenes* has been shown to be composed of an $\alpha\beta_2$ subunit structure, α (80 kD) and β (100 kD) (4). The cofactor is known to contain manganese, but the structure of the cofactor involved in this class of reductase remains to be established.

B. Ribonucleotide reductase from Escherichia coli

Ribonucleotide reductase from *Escherichia coli* consists of two non identical subunits B1 and B2. The active site of the enzyme is made up from both the subunits. In the presence of Mg^{2+}, dithiothreitol and dNTP, proteins B1 and B2 combine to yield a catalytically active complex. Protein B1 contains the binding sites for the ribonucleoside diphosphate substrates and for the ribo- and deoxyribonucleoside triphosphates that act as allosteric effectors. These

allosteric effectors, ATP, dATP, dGTP, and dTTP, regulate the level of activity as well as the substrate specificity of the reductase. Equilibrium dialysis experiments showed that protein B1 contains two binding sites for the four substrates, one site per polypeptide chain. Thelander demonstrated that in the absence of an external hydrogen donor, ribonucleotide reductase reduces approximately two moles of CDP per mole of B1, suggesting that each polypeptide chain contains a redox active thiol (5).

Protein B2 contains two apparently identical polypeptide chains. Protein B2 is a non-heme iron protein containing two iron atoms per molecule and an intrinsic organic free radical which gives a characteristic (g=2.0047) EPR signal (6). By isotopic substitution experiments this radical was shown to be located on the β position of a tyrosine residue (7). The major hyperfine doublet splitting of 19 G arises from one of the β methylene protons. The ring numbering system is shown in figure I.2.

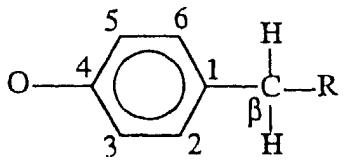

Fig I.2. The ring numbering of the tyrosine residue.

The hyperfine coupling for the second methylene proton has not

been resolved (8). The inequivalence of the two methylene protons even at room temperature was demonstrated (9). It was deduced that one of the β methylene hydrogen couplings would be much less than 1 G and hence too small to resolve. The minor hyperfine coupling of 7 G observed at 20 K is assigned to the 3,5 protons on the benzene ring.

ENDOR studies of the tyrosyl free radical (10) in ribonucleotide reductase from E.coli established that the tyrosyl radical has characteristics of a seven membered odd alternate species with a spin density distribution of 0.16 (phenolic oxygen), 0.26 (ortho), -0.07 (meta), -0.03 (ring carbon carrying phenolic oxygen), and 0.49 (para). It was suggested that the tyrosyl radical of ribonucleotide reductase is uncharged and not hydrogen bonded to donors in its environment within the protein (10).

Protein B2 has a characteristic electronic absorption spectrum with maxima at 370 nm (ϵ= 8.7 $\times$ 10^3), 410 nm (ϵ= 6.6 $\times$ 10^3) and 600 nm (ϵ= 0.6 $\times$ 10^3) and shoulders at 325 nm (ϵ= 10 $\times$ 10^3), 390 nm (ϵ= 7.2 $\times$ 10^3) and 500 nm(ϵ= 0.9 $\times$ 10^3) (11) (fig. I.3). The 410 nm band is attributed to the tyrosyl radical (6). The ferric iron center absorbs at 325 nm, 370 nm, 500 and 600 nm (6,11). There is some contribution from the tyrosyl radical in the 600 nm region (λ_{max}= 590 nm, ϵ= 200). A representative electronic spectrum of the native B2 protein from (6) is shown below.

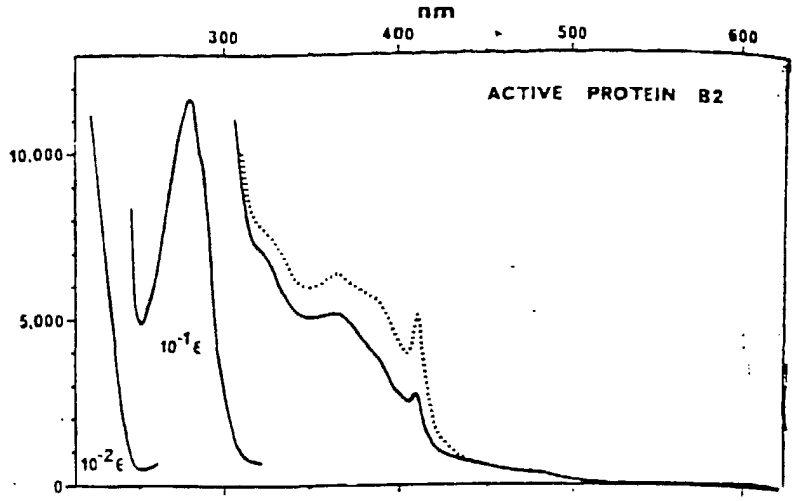

Fig I.3. Electronic spectrum of active E. coli B2 taken from reference (6).

Different forms of the B2 subunit have been shown to exist based on the states of the iron and the tyrosyl radical in the protein (12). The active form of B2 protein has the tyrosyl free radical and the intact diferric iron center. The B2 protein has a fully reduced state, denoted reduced B2, characterized by a normal nonradical tyrosine-122 residue and a dimeric ferrous iron center. The tyrosyl radical can be selectively reduced by one electron reduction in the presence of a suitable mediator, yielding met B2, a nonradical form with an intact ferric iron center. The apo B2 form exists without both the free radical and the iron atoms in the iron center. A mixed valence semi-met form of the iron cluster Fe(III)-Fe(II) in the B2 protein of ribonucleotide reductase

has been isolated and characterized by exposing met B2 to ionizing radiation from an x-ray source (13).

The iron center in protein B2 has been investigated by a variety of techniques. The Mössbauer analysis of [^{57}Fe]protein B2, and the striking similarity between the electronic spectrum of protein B2 and those of the oxidized forms of hemerythrin, favored the presence of an antiferromagnetically coupled pair of high spin ferric ions (6,11). Paramagnetic susceptibility measurements of protein B2 indicated a deviation from the Curie law at high temperatures. This deviation is consistent with the structure of an antiferromagnetically coupled pair of high spin ferric ions with an exchange coupling of $-J = 108$ cm^{-1} (11). Sjöberg and coworkers concluded that the resonance Raman characteristics of the Fe-O-Fe center in protein B2 are similar to those of the previously reported μ-oxo bridged binuclear iron center in hemerythrin (14). It was demonstrated by resonance Raman study that hydroxide ion is a ligand of the B2 iron center (15). The electron spin-lattice relaxation and spectral diffusion properties for tyrosine radicals in ribonucleotide reductase, photosystem II and a in model system were examined by Beck and coworkers (16). For the UV-generated model tyrosine radical, the dominant contribution to spectral diffusion occurred on a time scale of T_2 (electron spin-spin relaxation time) and was shown to saturate with a microwave pulse lasting only 50 μsec. For the tyrosine radicals in

proteins (ribonucleotide reductase and photosystem II), the spectral diffusion process was shown to occur on the time scale of T_1 (spin-lattice relaxation time), and was saturable with a microwave pulse of duration greater than 3-5 msec. When very long saturating pulses were applied, single-exponential relaxation kinetics were predominant for the tyrosine radical in ribonucleotide reductase (16).

A new protein to iron ratio of 1:4 was demonstrated with the E.coli ribonucleotide reductase using Mössbauer and EPR studies. It was proposed that the subunit B2 has two binuclear iron clusters , each associated with its own tyrosyl radical in contradistinction to the then prevailing model (17). The determination of the three dimensional structure of protein B2 (met form, i.e., reduction of the tyrosyl radical to a normal tyrosine) by X-ray crystallography published soon after (18), endorsed the presence of the two iron centers 25 Å apart (and 3.3 Å between the two iron atoms within one center) in the dimeric molecule B2 in *E. coli*. The tyrosine 122, which harbors the stable free radical, was shown to be buried inside the protein (about 10 Å from the closest surface) and located 5 Å from the closest iron atom (18). One glutamic acid residue at position 115 is ligated to both iron atoms forming a bridge between them. Glutamate 238 is bound to Fe2 and points towards Fe1, but is not close enough for direct coordination to Fe1. Fe1 is also ligated to His 118 and Asp 84, and Fe2 to His 241 and Glu 204. Two other non-protein

ligands, one for each iron atom, have been interpreted as being water molecules. Fe1 could have either trigonal bipyramidal or octahedral coordination features, and Fe2 has a regular octahedral coordination, with angles close to 90°. The schematic diagram (18) shows the coordination of the iron atoms at each iron center.

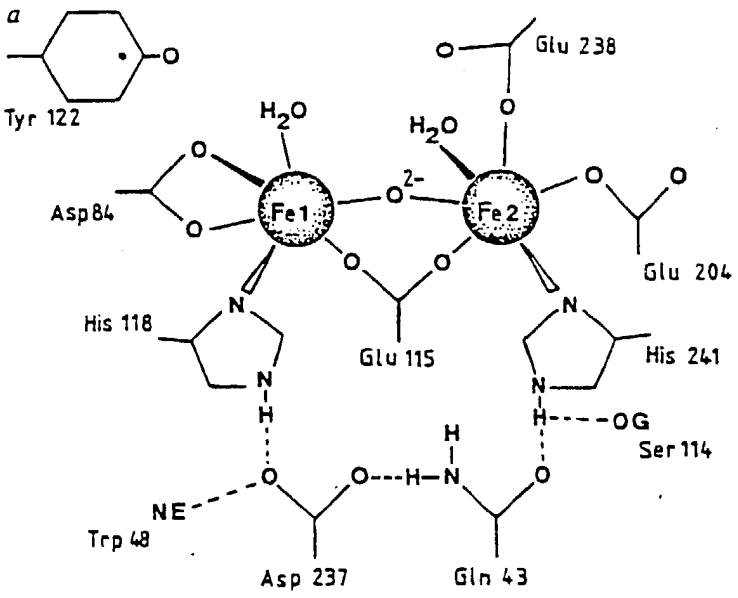

Fig I.4. The iron center in one monomer of E. coli B2 subunit; schematic taken from reference (18)

The mechanism of assembly of the tyrosyl radical-dinuclear iron cluster cofactor of ribonucleotide reductase was predicted to involve two intermediates (19). The first is

a μ-peroxo diferric complex, the second is an iron coupled EPR detectible radical (19). Electron transfer between the iron clusters in the B2 dimer is suggested upon invoking dioxygen activation catalyzed by the B2 subunit of ribonucleotide reductase from E. coli (20). 3.1 Fe(II) and 0.8 Tyr^{122} is shown to be oxidized per mole of oxygen reduced (20).

C. Mammalian ribonucleotide reductase

In mammalian cells, the synthesis of DNA requires a continuous supply of deoxyribonucleoside triphosphates (dNTP). The formation of the dNTPs can be either through the *'de novo'* pathway, in which the ribonucleotides are converted to the corresponding deoxyribonucleotides by ribonucleotide reductase; or through the 'salvage' pathway, wherein the preformed deoxyribonucleosides are converted to the deoxyribonucleotides by nucleoside kinases. The contribution of either pathway to the overall dNTP formation depends on the type of the cell, the amounts of the enzyme involved, and the environment of the cells (21).

Mammalian ribonucleotide reductase (RR) is a highly regulated enzyme that catalyses the conversion of ribonucleoside diphosphates (CDP, UDP, ADP, GDP) to deoxy-ribonucleotides (dCDP, dUDP, dADP, dGDP) (via the *de novo*

pathway), required for the synthesis of DNA. The reaction is rate limiting for DNA synthesis, and therefore, the enzyme plays an important role in cellular proliferation. The overall activity of the reductase is generally related to the growth rate of cells. Quiescent cells do not contain detectable reductase activity. Several studies have demonstrated the relationship of ribonucleotide reductase activity, the S phase of the cell cycle and the onset of DNA synthesis (22). Reductase activity is very low during the G_2, M and G_1 phases of the cell cycle, and increases in the late G_1 prior to the S phase (23). While dNTP pool sizes, DNA synthesis and ribonucleotide reductase activities increase in the S phase of the cell cycle, no strict correlation exists among them. This may be related to the fact that deoxyribonucleoside triphosphates are rapidly utilized during DNA synthesis thereby depleting dNTP pools. Thus, simultaneous rises in dNTP pools and DNA synthesis may not be expected. Furthermore, ribonucleotide reductase activity apparently reaches its maximum after the peak of DNA synthesis (21).

The mammalian ribonucleotide reductase consists of two non-identical subunits termed M1 and M2. In addition to components M1 and M2, a hydrogen donor system is required for ribonucleotide reduction. The function of the hydrogen donor system is to maintain the thiol groups of reductase in a reduced state for catalysis. Hydrogen donor systems are provided by either thioredoxin and thioredoxin reductase (24)

or glutaredoxin (25). Glutaredoxin has been purified from calf thymus (25) and unlike the thioredoxin system, utilizes glutathione as a hydrogen source. The reduction of ribonucleoside diphosphates also requires a cation (e.g. Mg^{2+}) as cofactor (26).

The M1 subunit is a dimer, with a molecular weight of 170,000, containing the substrate and the effector binding sites and redox active thiols. The M2 subunit is also a dimer with a molecular weight of 88,000; each one of the monomers contains a pair of μ-oxo bridged non-heme iron atoms and a tyrosyl free radical, which gives a characteristic signal using electron paramagnetic resonance (EPR) spectroscopy. The stable tyrosyl radical in the M2 subunit of ribonucleotide reductase does not saturate as easily as other tyrosyl radicals because of the nearness of a pair of μ-oxo bridged high spin ferric ions (27). Mouse fibroblast 3T6 cells, selected for resistance to hydroxyurea, were shown to overproduce protein M2, the non-heme iron containing subunit of the mammalian ribonucleotide reductase (28). Packed resistant cells gave an EPR signal at 77 K resembling the signal given by the tyrosyl free radical of the B2 subunit of E. coli ribonucleotide reductase. Also, the M2 specific free radical was shown to be located at a tyrosine residue (29). Studies of the temperature dependence of EPR relaxation and line shape reveal significant differences between the free radicals in the proteins B2 and M2. From the temperature

dependence studies it was deduced that the tyrosyl free radical and the iron center are close enough in space to exhibit magnetic interaction (27). For protein M2 the effects are more pronounced than for protein B2, indicating a stronger magnetic interaction (27).

To study the mechanism of tyrosyl radical formation, substoichiometric amounts of Fe(II) were added to recombinant mouse R2 apoprotein under strictly anaerobic conditions, and then exposed to air. Low temperature EPR spectroscopy has shown that the signal from the generated tyrosyl radical correlated well with a stoichiometry of 3 Fe(II) (or 2 Fe(II) and an electron donor) per tyrosyl radical, as indicated in the equation below,

$$3\ Fe(II) + P + O_2 + Tyr\text{-}OH + H^+ \rightarrow Fe(III)\text{-}O^{2-}\text{-}Fe(III)\text{-}P + H_2O + Tyr\text{-}O^{\bullet} + Fe(III),$$

where P is an iron binding site of protein R2. It was suggested that each dimeric Fe(III) center, during its formation, can generate a tyrosyl radical and that binding of iron to the apoprotein is highly cooperative (30).

Immunocytochemical studies, using two different monoclonal antibodies against the M1 and M2 subunits of ribonucleotide reductase (31,32), indicated the exclusively cytoplasmic localization of M1 in MDBK and mouse 3T6 cells. More recently, epitope-specific antibodies to the M1 and M2 subunits of mammalian ribonucleotide reductase were used in immunofluorescent staining studies to show that both M1 and M2

subunits are localized both in the cytoplasm and in the nuclear regions of a number of cell types (33). B77 avian sarcoma virus transformed NRK cells, T51B rat liver cells, 5123tc hepatoma cells, and rat liver cells in vivo were used in the above study. Furthermore, the M1 subunit was suggested to be glycosylated protein and localized around isolated rat liver nuclei. In the case of rat liver cells, about 40% of the total cellular ribonucleotide reductase activity was shown to be present in the nuclear membrane extract, and 60% in the cytosol. During liver regeneration, the activity of the enzyme in the nuclear membrane fraction increased 5-fold during DNA replication (measured by incorporation of tritiated thymidine), while the activity in the cytosolic fraction increased 11 to 12-fold (33).

D. Ribonucleotide reductase as a target for cancer chemotherapy

Ribonucleotide reductase, because of the critical role that it plays in DNA replication, provides a unique metabolic target for chemotherapeutic approaches to cancer treatment. The reduction of the intracellular pools of all four dNTPs through the inhibition of ribonucleotide reductase has the effect of reducing DNA polymerase activity. Since DNA

polymerase activity is critically related to the concentrations of the dNTPs, small decreases in the intracellular concentrations of dNTPs cause remarkably large decreases in DNA synthesis and hence cell replication.

Chemotherapeutic agents can be targeted independently at the individual subunits of ribonucleotide reductase, namely, the non-heme iron and the effector binding subunits. Combinations of ribonucleotide reductase inhibitors were shown to result in synergistic inhibition of cell growth with concurrent cytotoxicity (34). The drugs used in combination were targeted at the individual subunits of ribonucleotide reductase and at differential sensitivities of the substrate reductions. The specificity of inhibition of the enzyme were shown by utilizing [^{14}C]cytidine as the precursor and measuring the conversion of cytidine to deoxycytidine.

E. Effectors of the B2/M2 subunit of ribonucleotide reductase

The requirement of the tyrosyl radical in the small subunit for the activity of the enzyme has been the basis for the use of radical scavengers, antioxidants and reductants as inhibitors of ribonucleotide reductase. The activity of ribonucleotide reductase has also been inhibited by aiming at

the B2/M2 subunit using various iron chelating agents. In studies using the isolated enzyme, hydroxyurea, 2,3-dihydro-1H-imidazo[1,2-b]pyrazole (IMPY), guanazole, 1-formylisoquinoline thiosemicarbazone (IQ), 4-methyl-5-aminoisoquinoline thiosemicarbazone (MAIQ) and 1-isoquinolinoyl-methylene-N-hydroxy-N'-aminoguanidinetosylate (HAG-IQ) have been shown to be specific inhibitors of the non-heme iron containing subunit (B2/M2) of ribonucleotide reductase (35). In the presence of iron chelating agents such as EDTA, desferal, or 8-hydroxyquinoline (8-HQ) at a concentration that did not affect the ribonucleotide reductase activity, HU, guanazole, and IMPY inhibited the reductase activity more effectively than when used alone (36). The targeting of both the radical and the iron site simultaneously, thus results in enhanced inhibition of the enzyme.

The mechanism of inhibition of ribonucleotide reductase by hydroxyurea and IMPY is distinct from that of the thiosemicarbazones. The difference in mechanisms is expressed by the difference in responses to catalase and peroxidase (35). The inhibition of ribonucleotide reductase by hydrogen peroxide is completely reversed by catalase. Neither peroxidase nor superoxide dismutase alters the degree of inhibition caused by H_2O_2. The free radical scavengers, mannitol and sodium formate has no effect on the inhibition by H_2O_2. Peroxidase has no effect on the inhibition of CDP

reductase by IMPY or hydroxyurea, while causing a marked decrease in the inhibition by MAIQ. Catalase serves to potentiate the inhibition of CDP reductase by MAIQ in marked contrast to its reversal of the inhibitory effect caused by IMPY or hydroxyurea (35).

Hydrogen peroxide (2.5 and 5 mM) was shown to activate the met form of B2 protein to the active form containing the tyrosyl radical (37). This activation process was found to be counteracted by the peroxide-dependent inactivation of the protein at higher concentrations of H_2O_2 (37). A ferric peroxide intermediate followed by a high valent iron-oxo intermediate was proposed for the activation process of met B2 to active B2 by H_2O_2 (37).

The rate constants for the reduction of the tyrosine radical in the B2 subunit of E. Coli with various reductants (hydroxyurea, didox, N-methylhydroxylamine, acetohydroxamic acid, and hydroxamic acid derivatives) were shown to be of similar magnitude (e.g. 0.44 $M^{-1}s^{-1}$ for hydroxyurea) (38). The low reactivity of these reductants with tyrosine radical is attributed to the radical being buried within the protein (38). Both the tyrosine radical and the iron in the B2 subunit were shown to be reduced by methyl viologen, benzyl viologen, and phenosafarin under reducing and anaerobic conditions (39).

The free radical scavengers, hydrazines and hydroxylamines, quench the tyrosyl radical in ribonucleotide

reductase (6,40). Recently, it has been demonstrated that monosubstituted hydrazines and hydroxylamines are able to reduce the tyrosyl radical and the ferric ions, under anaerobic conditions (41). A mixed valence state of the binuclear iron center, which indicates a Fe(III)-Fe(II) complex, is formed transiently during the reduction of the protein by hydrazine (41).

The activity of ribonucleotide reductase has been demonstrated to be inhibited by NO synthase product(s) (42). Nitric oxide generated by donors such as sodium nitroprusside, S-nitrosoglutathione and the sydnonimine SIN-1 has been shown to inhibit the ribonucleotide reductase activity present in cytosolic extracts of TA3 mammary tumor cells (43). The tyrosyl radical of the small subunit in E. coli or mammalian reductase is efficiently scavenged by these nitric oxide donors (43).

It was demonstrated that ribonucleotide reductase activity was inhibited by peptides corresponding to the C-terminal of the small subunit B2/M2 (44). The peptide is able to interfere with the normal subunit association that takes place through the C-terminal of the small subunit (45). This inhibitory phenomenon observed with C-terminal peptides appeared to be specific to the primary sequence of the enzyme. The nonapeptide corresponding to the bacterial C-terminal sequence was found to inhibit the E.coli ribonucleotide reductase but had no effect on the activity of the mammalian

enzyme (44).

F. Regulation of B1/M1 subunit of ribonucleotide reductase

Even prior to the knowledge of the regulation of ribonucleotide reductase by dNTPs, deoxyadenosine, deoxythymidine and deoxyguanosine were shown to be inhibitors of cell growth in culture. The activity of *E.coli* ribonucleotide reductase is influenced by differential binding of allosteric effectors (nucleoside triphosphates) to the enzyme. Specific nucleoside triphosphates are required for substrate reduction. The prime activators for CDP, UDP, GDP and ADP reduction are ATP, ATP, dTTP and dGTP, respectively (4). dATP is a strong inhibitor of the reduction of all four substrates, while dTTP is a negative effector of UDP, CDP and ADP reductions. It has been demonstrated that the *mammalian* ribonucleotide reductase is also strongly regulated by nucleoside triphosphates. There is no reduction of substrate in the absence of the appropriate nucleoside triphosphate. The model proposed as a result of the kinetic studies with partially purified ribonucleotide reductase from different mammalian sources is shown below (21). This scheme

illustrates the complexity involved in the regulation of the key enzyme in DNA synthesis by positive, negative and feedback effectors of the enzyme during the catalytic reduction of the nucleoside diphosphates.

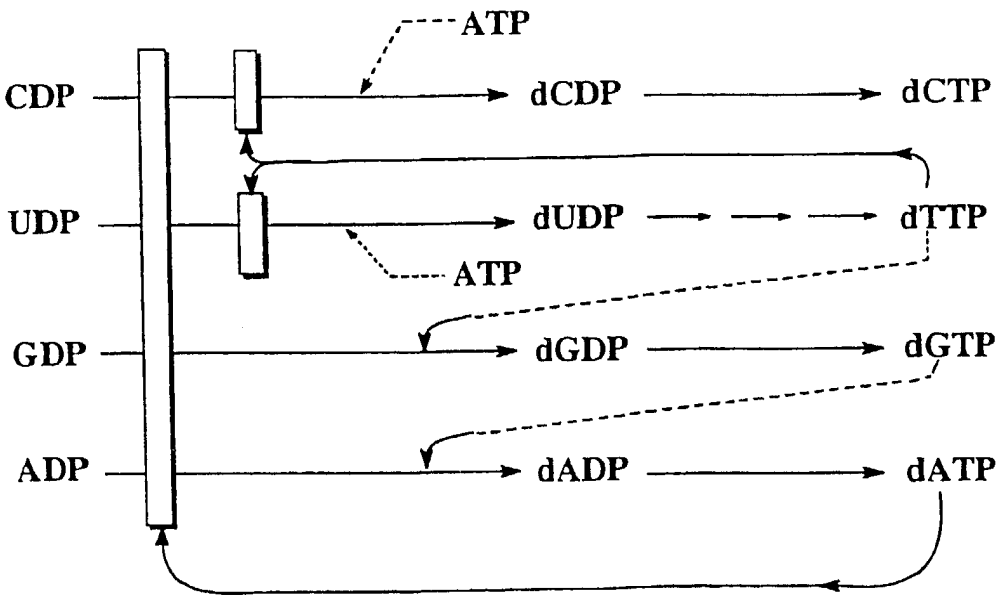

Fig I.5. Allosteric regulation of deoxyribonucleotide synthesis by ribonucleoside diphosphate reductase of E. coli. Solid lines with arrows leading to solid blocks indicate negative effects; dashed lines with arrows indicate positive effects. This schematic is taken from reference (21).

The concentrations of dNTP required to affect the regulation of ribonucleotide reductase are probably not achieved in

cells. In the cell however, the ribonucleotide reductase would 'see' the entire nucleotide pool consisting of mono-, di-, and triphosphates of both the ribo- and deoxyribo-nucleosides. Suggestions in the literature exist on compartmentalization, which would allow the concentrations of dNTP's to reach the appropriate level (21).

Nucleoside 5'-diphosphates have also been shown to be allosteric effectors of mammalian ribonucleotide reductase (21). ADP, for example, activated both CDP and UDP reductions; dADP, on the other hand, inhibited the reduction of all four substrates. However, the complete regulatory system of this enzyme in the cell, in terms of all the molecules capable of regulating it, is not yet defined.

Deoxyadenosine in combination with EHNA [erythro-9-(2-hydroxy-3-nonyl) adenine] resulted in synergistic inhibition of L1210 cell growth (34). In this case, deoxyadenosine was targeted at ribonucleotide reductase and EHNA was targeted at adenosine deaminase activity (Adenosine deaminase is an enzyme that deaminates deoxyadenosine to deoxyinosine). The specific inhibition of adenosine deaminase activity by EHNA results in the accumulation deoxyadenosine, which in turn leads to the accumulation of sufficient levels of dATP necessary for the feedback inhibition of ribonucleotide reductase (34). Another combination of agents based on a similar idea is the use of deoxyguanosine in combination with 8-aminoguanosine, wherein the accumulation of dGTP results in the feedback inhibition of

ribonucleotide reductase (34). 8-amino-guanosine is a specific inhibitor of purine nucleoside phosphorylase, an enzyme which degrades deoxyguanosine to guanine and deoxyribose-1-phosphate.

Analogues of the substrates for ribonucleotide reductase have been used to target the enzyme through the M1 subunit, since the substrate and effector binding sites are located on this subunit. 2'-Halo-2'-deoxynucleotides and 2'-azido-2'deoxynucleotides have been shown to be potent mechanism based inhibitors of ribonucleotide reductase (46,47). 2-F-ATP and 2-F-araATP also inhibit ribonucleotide reductase via the M1 subunit. Dialdehyde derivatives of inosine (Inox) and 5'-deoxyinosine (5'-dInox), are also specific inhibitors of the M1 subunit of ribonucleotide reductase.

II. GENERAL METHODOLOGY

A. Cell culture

1. Maintenance of cells in culture - Murine (mouse) leukemic **L1210 cells** were obtained from American Type Culture Collection (ATCC, Rockville, MD) and were maintained in suspension culture in an atmosphere of 6% CO_2 at 37°C in RPMI 1640 medium containing 10% horse serum. These cells have a doubling time of about 12 hours.

The human promyelocytic leukemia **HL60 cell** line, obtained from ATCC, is derived from a single patient with acute promyelocytic leukemia. It provides a unique <u>in vitro</u> model system for studying the cellular and molecular events involved in the proliferation and differentiation of leukemic cells of the granulocyte/monocyte/macrophage lineage (48). HL60 cells continuously proliferate in suspension culture (in RPMI-1640 medium supplemented with 10% fetal bovine serum and containing the antibiotics penicillin, streptomycin and gentamicin) with a doubling time of about 36 hours.

Human lymphoblastoid leukemia **CCRF-CEM cells**, obtained from ATCC, are also grown in suspension culture in RPMI-1640 medium supplemented with 10% fetal bovine serum. These cells have a doubling time of about 20 hours.

2. Development of drug-resistant cell sublines - HL60 cells were grown in increasing concentrations of gallium nitrate over a period of months. Increments in the concentration of gallium nitrate in the medium were made only when the growth of the resistant cells were equivalent to that of the control cells. The resistant cells were routinely subcultured in medium containing 84 μM gallium nitrate. The gallium-resistant HL60 cells were approximately 29 times more resistant to growth inhibition by gallium nitrate than the control HL60 cells.

L1210 cells were made resistant to hydroxyurea by growing the cells in the presence of increasing concentrations of hydroxyurea in the growth medium. The resistant cells were then routinely maintained in medium containing 250 μM hydroxyurea. The hydroxyurea-resistant cells were approximately 15 fold more resistant to growth inhibition by hydroxyurea as compared to control L1210 cells.

B. Preparation of cell-free extracts

Cells were plated in 500 ml spinner flasks in the absence (control) or presence of 400μg/ml gallium nitrate. After an 18 hr incubation, cells (about 5×10^8/flask) were harvested and washed twice with ice cold PBS. The final cell pellet was resuspended in 1 ml of Tris-DTT buffer (0.02 M Tris-Cl, pH 7.4, containing 1 mM DTT) and allowed to sit on ice for 5 min.

Cells were then disrupted using a 15 ml Dounce homogenizer (20 strokes) equipped with a motor driven pestle. Disruption of cells was confirmed by light microscopy. The samples were centrifuged at 100,000 × g for 1 h in a Sorval RC80 ultracentrifuge (and the supernatant containing the cellular cytosolic fraction was concentrated using a centricon 30 microconcentrator (Amicon, Danvers, MA) for iron titration studies), and the supernatant was passed through a Dowex acetate column (1 cm × 1 cm) to remove the endogenous nucleotides. 1 ml of the buffer (Tris-DTT) was also eluted through the column and collected along with the supernatant. Solid ammonium sulfate (corresponding to 80% saturation) was added in small amounts to the cold supernatant, while stirring it gently, in order to precipitate most of the ribonucleotide reductase. The precipitate obtained by centrifugation, at 40,000 × g for 30 min, was then resuspended in 0.5 ml of Tris-DTT. It was then dialyzed against the same buffer for 3 h (3 × 1 liter) with a change in buffer every hour. After dialysis the sample was concentrated in a centricon 30 microconcentrator.

C. Measurement of protein content

Samples were assayed for total protein content using a BCA protein assay kit from Pierce (Rockford, IL). The Pierce BCA protein assay reagent system combines the well known

biuret reaction of protein with Cu^{2+} in an alkaline medium (yielding Cu^{1+})- with a highly sensitive detection reagent for Cu^{1+}, namely bicinchoninic acid (BCA). The purple reaction product, formed by the interaction of two molecules of BCA with one cuprous ion, is water soluble and exhibits a strong absorbance at 562 nm. Bovine serum albumin is used as the protein standard to generate a standard curve, from which the protein concentration of unknown samples are determined.

D. ESR spectroscopy

ESR studies of the tyrosyl free radical of ribonucleotide reductase were performed at the National Biomedical ESR Center of the Medical College of Wisconsin. X-band EPR spectra were obtained by using a standard Century series Varian E-109 spectrometer operating at X-band (9 to 9.5 GHz) with 100 kHz field modulation. ESR measurements were made on frozen cytosolic preparations (4 mm diameter × 3 cm long icicles) at -196°C in quartz finger dewars. Each of the EPR spectra were recorded nine (or sixteen) times and averaged with a computer program called Viking. The baseline background spectra was obtained using water icicle as the sample (same number of scans were averaged) under the same spectrometer conditions. The background was then subtracted from the sample ESR signal using a computer program called Sumspec. Absolute

concentration of the tyrosyl radical was determined by comparison of the areas under the double integral of the ESR signal to a 1 mM copper perchlorate standard (generously provided by Dr. Helmut Beinert). The ratios of the spectrometer gains and the square root of the microwave powers were also taken into account for the calculation of concentrations.

The Q-band spectra were taken using a Varian E-110 Q-band spectrometer wherin the Varian Q-band bridge was extensively modified (49). The additions were a low-phase noise Gunn diode oscillator, a low-noise GaAs field-effect transistor microwave signal amplifier, and a balance mixer requiring high input power (10 mW) at the local oscillator port. It was shown that the microwave amplifier and the mixer improved the overall sensitivity by a factor of seventeen (49).

Some of the experimental ESR spectra were filtered for high frequency noise and occasionally pseudomodulated using the computer program "Sumspc90". Pseudomodulation algorithm transforms the digitized spectra and can also filter noise, resulting in resolution enhancement (50,51). Resolution enhancement is obtained by adding or subtracting the even harmonics of the digitized spectrum to or from the original spectrum. The second harmonic of the original experimental spectra was used in cases where pseudomodulation was applied. Representative spectra on which noise filter and pseudomodulation routines were applied are shown in figure

II.1.

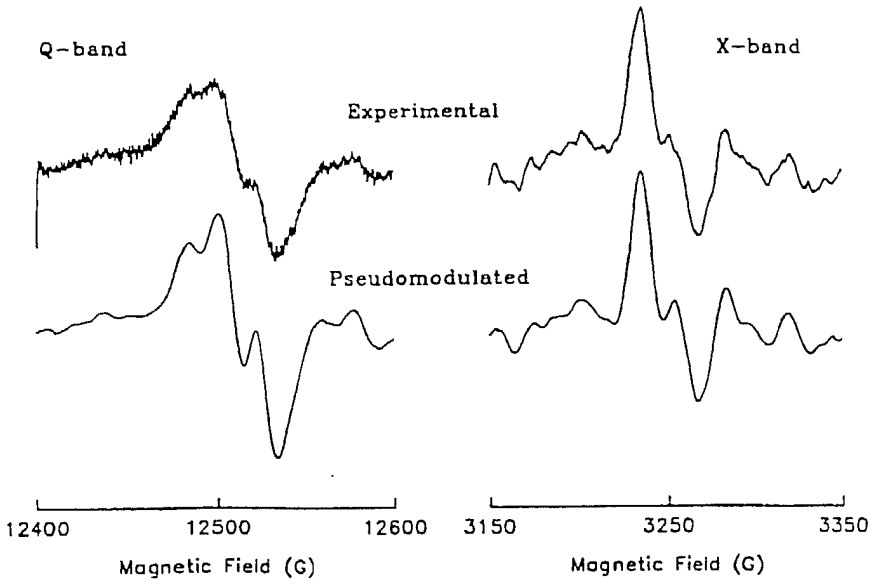

Fig II.1. Tyrosyl free radical ESR spectra obtained from hydroxyurea-resistant L1210 cells at Q-band, and from HL60 cells at X-band. Experimental spectra are the top ones, and the noise filtered, pseudomodulated spectra are shown in the bottom spectra.

E. Assay for the activity of ribonucleotide reductase

1. CDP reductase assay - CDP reductase activity in the cell-free preparation was assayed using a modification of a previously described method (52,53). The assay mixture (total volume, 150 μl) contained 1.0 μmol sodium phosphate buffer pH 7.0, 0.6 μmol magnesium acetate, 0.9 μmol DTT, 0.15 μmol AMP-

p-nitrophenyl phosphate, 10 μl of the protein, 0.07 nmol [U-^{14}C] CDP, and 1.8 nmol CDP. After the mixture was incubated at 37°C for 30 minutes, the reaction was stopped by heating in a boiling water bath for 4 min. The samples were cooled and incubated for 2 h with snake venom phosphodiesterase mixture [1.2 μmol Tris pH 8.7, 3.0 μmol $MgCl_2$, 20 nmol dCMP, and 1 mg/ml snake venom phosphodiesterase]. Deoxycytidine was separated from cytidine using 1 ml Dowex 1-borate columns (52,53). Dowex borate has a high capacity for binding low molecular weight compounds with coplanar cis-diol groups. Thus, the[^{14}C]-cytidine derived from the substrate adheres to the column, whereas the product, deoxy[^{14}C]cytidine, does not.

2. ADP Reductase assay: ADP reductase activity was assayed as previously described (54). The assay mixture (total volume, 150 μl) contained 0.15 μmol dGTP, 0.9 μmol DTT, 1 μmol sodium phosphate buffer pH 7.0, 0.6 μmol magnesium acetate, 10 μl protein preparation, 0.013 nmol [2,8-^{3}H]ADP, 6.0 nmol ADP. After the mixture was incubated at 37°C for 30 minutes, the reaction was stopped by heating in a boiling water bath for 4 min. The samples were cooled and incubated for 2 h with snake venom phosphodiesterase mixture [1.2 μmol Tris pH 8.7, 3.0 μmol $MgCl_2$, 20 nmol dAMP, and 1 mg/ml snake venom phosphodiesterase]. Deoxyadenosine was separated from adenosine using 1 ml Dowex 1-borate columns (54). The radiolabeled adenosine derived from the substrate adheres to the column,

whereas the product, radiolabeled deoxyadenosine does not bind to the column.

F. Procedure for preparing dATP-Sepharose column for the affinity purification of ribonucleotide reductase

Affinity chromatography has found wide application in the purification of a variety of enzymes. Enzymes regulated by allosteric effectors might be selectively adsorbed to columns where the effector is linked to sepharose by a suitable linkage group. In the purification of ribonucleotide reductase, sepharose substituted with p-aminophenyl esters of ATP and dATP, two effectors of the enzyme, have been used. The scheme given below is a representation of dATP bound to sepharose via the linker molecule.

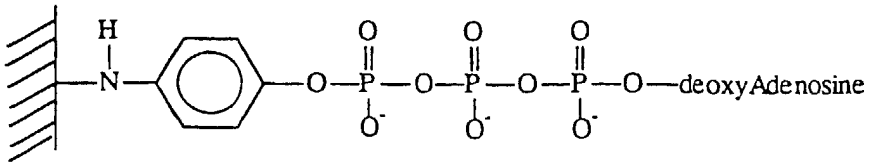

1. Synthesis of p-aminophenyl ester of dATP - The synthesis of p-aminophenyl ester of dATP was carried out according to the literature methods with some modifications (55,56). The acid catalyzed activation of dATP with dicyclohexyl carbodiimide resulting in the formation of adenosine-5′-trimetaphosphate is the first step. The p-nitrophenyl ester of dATP is formed by the reaction of trimetaphosphate with 4-

nitrophenol, which is then hydrogenated (at atmospheric pressure in the presence of palladium) to the p-aminophenyl ester.

The starting material, namely, triethylammonium (TEA) salt of dATP had to synthesized from the disodium salt of dATP. To do this, an ion exchange resin, Dowex 50H (1 cm X 5 cm), was first washed with 20% triethylamine followed by wash with water to bring the pH of the washing to about 9. 25 mg dATP disodium salt (from Sigma) was dissolved in 1 ml deionized water and poured over the column at 4°C. 40 drop fractions were collected by eluting with deionized water. The absorbance of the fractions at 259 nm is measured. The peak fractions containing the di-triethylammonium salt of dATP are pooled (about 8 ml) and lyophilized over night in a preweighed 30 ml Corex tube.

The dry TEA salt of dATP was weighed and dissolved in DMSO (0.15 mmole in 1.5 ml) and (0.5 mmole) solid DCC (dicyclohexylcarbodiimide) was added while on the balance. DMSO will absorb moisture, and DCC will not work efficiently in the presence of water: therefore the above reaction was carried out quickly. The mixture was allowed to react for 2 hours in a covered tube. The mixture was then dried by evaporation with pyridine (0.1 ml). Since the above reaction supposedly yields 100% of the product, namely, deoxyadenosine-5′-trimetaphosphate, it is assumed that 0.15 mmole of the product was formed. 0.15 mmole of the trimetaphosphate was

dissolved in 1.7 ml of DMF and 2.8 mmole each of triethylamine and 4-nitrophenol were added (added TEA first) and the mixture allowed to react for 24 hours at room temperature in a fume hood. Both TEA and 4-nitrophenol were added while the sample is on the balance. To the product formed in the above reaction, p-nitrophenyl ester of dATP, 5 ml of distilled water was added and hydrogenated at atmospheric pressure in the presence of palladium on charcoal (50 mg) at room temperature for 3 hours. The product formed in this step is the p-aminophenyl ester of dATP. This product has to be separated from the p-aminophenol (formed by the reduction of the excess p-nitrophenol) and other substances in the reaction mixture. Part of the palladium was removed by filtration with a Whatman No. 1 filter. The filtrate was then subjected to chromatography on a column of DEAE-Sephadex A-25 (1 cm X 15 cm) with a gradient of triethylammonium bicarbonate pH 7.6 (0.1-0.5 M, total volume of 1 l).

The triethylammonium bicarbonate buffer was made fresh before use, and kept cold. To prepare 0.5 M triethylammonium bicarbonate buffer at pH 7.6, the appropriate amount of TEA (50.6 g/l) was weighed into a beaker and added to the water (Prepared under a fume hood). The pH is around 12 to begin with. Small pellets of dry ice (solid CO_2) were added to lower the pH. The solution was kept on ice and the pH monitored constantly. Also, CO_2 gas was bubbled into the solution slowly. The final adjustment of pH was made with

gaseous CO_2 alone.

The DEAE Sephadex A-25 (1 X 15 cm) column was washed with 0.1 M triethylammonium bicarbonate buffer. The p-aminophenyl ester of dATP (after filtering) is then loaded on the DEAE column, and subjected to a gradient of triethylammonium bicarbonate buffer at pH 7.6. 500 ml each of 0.1 M and 0.5 M buffer was used. The absorbance of the fractions at 259 nm were read. p-aminophenyl ester of dATP eluted between 0.3 and 0.35 M. The peak fractions at this concentration were pooled and lyophilized overnight in preweighed centrifuge tubes.

2. Preparation of dATP Sepharose affinity column - The cyanogen bromide activated sepharose-4B (sigma) was soaked for 15 min in 1 mM HCl. 1 g powdered gel gives about 3.5 ml gel volume. The p-aminophenyl ester of dATP was dissolved in 0.1 M $NaHCO_3$ buffer pH 8.3, containing 0.5 M NaCl (coupling buffer). The concentration of dATP in the buffer should be between 0.7 and 3.0 μmole per ml. The dATP solution in buffer was mixed with the gel suspension in an end over end mixer overnight at 4°C. The gel was allowed to settle and the coupling buffer was discarded. The gel was mixed with the blocking agent, 0.2 M glycine pH 8.0, and allowed to settle; after which the blocking buffer was discarded, and fresh blocking buffer was added. The gel was poured in a 1 cm i.d. column and washed with coupling buffer, followed by acetate buffer (0.1 M acetate pH 4.0, containing 0.5 M NaCl). The

column was washed again with coupling buffer followed by acetate buffer and then followed by coupling buffer again. The column is stored with 0.02% sodium azide. The dATP-sepharose thus prepared was ready to be used for the purification of ribonucleotide reductase.

L1210 cell free extracts, prepared as mentioned before, were loaded on the affinity column at room temperature to allow the binding of ribonucleotide reductase in the extracts to the dATP-sepharose column. The column was then washed extensively with 0.1 M potassium phosphate pH 7.0, until the absorbance at 280 nm of the wash was negligible. The enzyme ribonucleotide reductase was then eluted either (1) in one step with 0.1 M potassium phosphate buffer pH 7.0 containing 0.5 mM dATP, or (2) in multiple steps with differential concentrations of ATP in the potassium phosphate elution buffer (57). In the multiple step elution method of ribonucleotide reductase (57), a loosely bound fraction is first eluted with the elution buffer containing 3 mM ATP. The moderately bound fraction is then removed by washing with buffer containing 300 mM sodium chloride. The tightly bound fraction containing ribonucleotide reductase is then eluted with the elution buffer containing 100 mM ATP, pH 7.6.

The second method of elution for the purification of ribonucleotide reductase from L1210 cells resulted in the dissociation of the two subunits of the enzyme and the loss of the smaller M2 subunit in the process. Use of glycerol in the

elution step may prevent the dissociation of the subunits.

Moreover, the amount of intact enzyme isolated from 1 to 2 X 10^9 L1210 cells (accounting for losses over the duration of the purification process) is very small, and hence the lower stability of the enzyme at these low concentrations may be a set back in the purification of the enzyme. Small amount of the enzyme isolated using the first method of elution showed two bands (corresponding to M1 and M2) on gel electrophoresis followed by silver staining of the gel. The enzyme thus obtained was not very stable. Purification of the enzyme from a cell line that overexpresses the enzyme (like the hydroxyurea-resistant subline of L1210 cells) will help eliminate this problem. In the supplementary section, the development of the hydroxyurea-resistant cell line and their ribonucleotide reductase content relative to control are discussed.

III. TYROSINE RADICALS IN BIOLOGICAL SYSTEMS

A. Introduction

The amino acid residues most likely to be involved in catalysis proceeding via radical intermediates are those that are most easily oxidized; namely, tryptophan, tyrosine, cysteine, histidine, and perhaps, phenylalanine and methionine. The redox potentials for tyrosine and tryptophan residues at pH 7 are 0.93 and 1.015 V (vs normal hydrogen electrode) respectively (58). The relative magnitude of the redox potentials for these residues show a marked pH dependence. The radicals generated are either stabilized by the resting protein (intrinsic radicals) or generated transiently prior to catalysis (transient radicals). There is tremendous diversity in the modes of generation of the protein radicals, and most of the enzymes that involve protein radicals during catalysis have metal ion requirements. A mention will be made of the different enzymes that involve tyrosine radicals during their catalytic action and their EPR properties.

Ribonucleotide reductase, as mentioned earlier, contains an intrinsic stable tyrosyl free radical, required for the catalytic activity, in its smaller non-heme iron containing

subunit. The tyrosyl radical from ribonucleotide reductase exhibits a doublet on EPR spectroscopy due to coupling (20 G) of one of the β-methylene protons. The isotropic hyperfine coupling of the 3,5 ring protons of about 7 G is apparent at low temperatures.

Prostaglandin H synthetase (PGHS) catalyzes the first two steps in the biosynthesis of prostaglandins, prostacyclins and thromboxanes: oxidation of arachidonic acid to produce 9,11 endoperoxide C-15 peroxide, PGG_2, and its subsequent reduction to the C-15 alcohol (59). The enzyme is a dimer of 72 kD that contains a single protoporphyrin IX prosthetic group required for both the cyclooxygenase and peroxidase activities. Stopped flow kinetic studies and low temperature EPR studies have indicated that incubation of PGHS with PGG_2 results in rapid production of compound I, the spectral properties of which are consistent with Fe(IV)=O (60). Spectroscopically, the rapid conversion of compound I to compound II is detected. Compound II has a doublet EPR signal, at g = 2.005 with a splitting of about 19 G. The signal has been assigned to a tyrosyl radical; and it is very similar to the tyrosyl radical in ribonucleotide reductase, although in this system the tyrosyl radical is produced transiently (60). Examination of the kinetics of radical formation with ethyl hydroperoxide demonstrated the generation of a tyrosyl free radical within 5 seconds at 259 K (61). The doublet signal was shown to convert to a singlet with a similar peak to trough width; the

doublet to singlet transition was complete in 60 seconds (61). A similar effect was demonstrated upon addition of arachidonic acid or 5-phenyl-4-pentenyl-1-hydroperoxide to prostaglandin H synthase (62). It was suggested that the protein-derived radicals are not catalytically competent intermediates in cyclooxygenase catalysis (62).

In plants and algae, Photosystem II couples light induced charge separation to the oxidation of H_2O to O_2 and reduction of plastoquinone. This is a complex system composed of a minimum of seven polypeptides and multiple cofactors including chlorophyll, quinones, manganese, and two organic radical species (59). Two radical species have been shown to be located on the redox active tyrosine residues, Y_D and Y_Z (63). The doublet coupling in the $Y_D^{\bullet}$ species, which gives rise to a stable EPR signal, is 10.5 G; the second β-methylene proton is calculated to have a coupling of 4 G (63). The function of the $Y_D^{\bullet}$ is not clearly defined yet. The second tyrosine radical, $Y_Z^{\bullet}$, is only observed transiently and is involved in the electron transfer events that link reaction center photochemistry to water oxidation. Despite the difference in function, the EPR spectra of the $Y_D^{\bullet}$ and $Y_Z^{\bullet}$ radicals are identical. Thus, the conformation of the side chain must be identical for both these residues. The EPR properties of the tyrosine radicals in Photosystem II are different from those of the tyrosyl radical in ribonucleotide reductase, mainly due to the variations in the conformation of the β-methylene group

with respect to the phenol head group (63).

Galactose oxidase is a copper metalloenzyme (from the fungus Dactylium dendroides) that catalyzes the two electron oxidation of alcohols at a mononuclear copper active site (59). In its oxidized form the enzyme exhibits intense visible and near-IR absorption features and is ESR silent (59). One electron reduction of the native protein results in catalytic inactivation and an increase in the Cu^{2+} fraction of the protein that is ESR accessible. One electron oxidation of the native protein results in high specific activity for this protein, but the copper is ESR inactive (59). One electron oxidation of the copper-free apoprotein with ferricyanide leads to the formation of a stable free radical, which was located on a tyrosine residue (64). The triplet hyperfine structure is shown to arise from the coupling of the two β-methylene protons to the unpaired spin (64). The EPR saturation characteristics of the tyrosine radical are different from that found in ribonucleotide reductase. The tyrosyl radical signal obtained from the one electron oxidation of apogalactose oxidase is easily saturated at low microwave power levels (approximately 20 microwatts) even at elevated temperatures (130 K) (64).

In aromatic radicals the odd electron is delocalized, so that the average unpaired spin population of a particular carbon 2p orbital is considerably smaller than unity. The extent to which the C-H σ electrons are polarized is given by

McConnell's relation $a_H = Q\rho_\pi$, where ρ_π is the π electron spin density on the carbon atom, and Q is the proportionality constant with a value of -22.5 gauss. The mechanism of β-proton coupling involves hyperconjugation rather than exchange interactions. The methylene (β) group is normally free to rotate, and an isotropic splitting (an average splitting) is observed in the liquid phase. In the case of single crystal spectra, the methylene group is not freely rotating and the EPR spectrum reveals the presence of unequal interactions with the β-protons. Hyperfine coupling to β-hydrogens is usually related to the spin density at the α-carbon and to the dihedral angle between the α-carbon 2p orbital and the plane containing the β-proton C-H bond through an expression $a_\beta = B\cos^2\theta$. The dihedral angles (θ) formed by the β-hydrogens in the tyrosyl radical in ribonucleotide reductase are about 27° (the large β-hydrogen coupling of about 19 G) and near 90° (the very small β-hydrogen coupling of << 1 G) (9). The tertiary structure of the protein constrains the phenyl ring to certain fixed orientation(s) relative to the peptide backbone, leading to limited rotations about the C_α-C_β bond resulting in inequivalent methylene protons.

B. Results

1. Tyrosyl free radical ESR signal from ribonucleotide reductase in various cell lines - The electron spin resonance signal from the tyrosyl free radical in ribonucleotide reductase from different cell lines has been obtained. The intensities of the ESR signals of the tyrosyl radical in several cell lines are compared in figure III.1. Different cells, namely, human promyelocytic leukemia HL60 cells, murine lymphocytic leukemia L1210 cells, human lymphoblastoid leukemia CCRF cells, hydroxyurea resistant L1210 cells, gallium nitrate resistant HL60 and L1210 cells grown in suspension culture, were harvested during log phase of their growth. Approximately, the same number of cells were harvested from each cell type; washed with PBS and the cell pellet frozen into an icicle (4 mm diameter X 3 cm height) in liquid nitrogen. ESR measurements were made at liquid nitrogen temperatures. Corneal stromal cells in culture infected with Herpes simplex virus-1 were examined under both liquid nitrogen and helium temperatures at X-band microwave frequency (Figure III.2). The spectra obtained at lower temperatures show a better resolution of the hyperfine structure in the tyrosyl radical signal. A difference in the hyperfine structure of the tyrosyl radical spectra at 20 K between the viral and the mammalian source is evident from

figure III.2. Moreover, the tyrosyl radical in viral reductase saturates at lower microwave powers than the mammalian one.

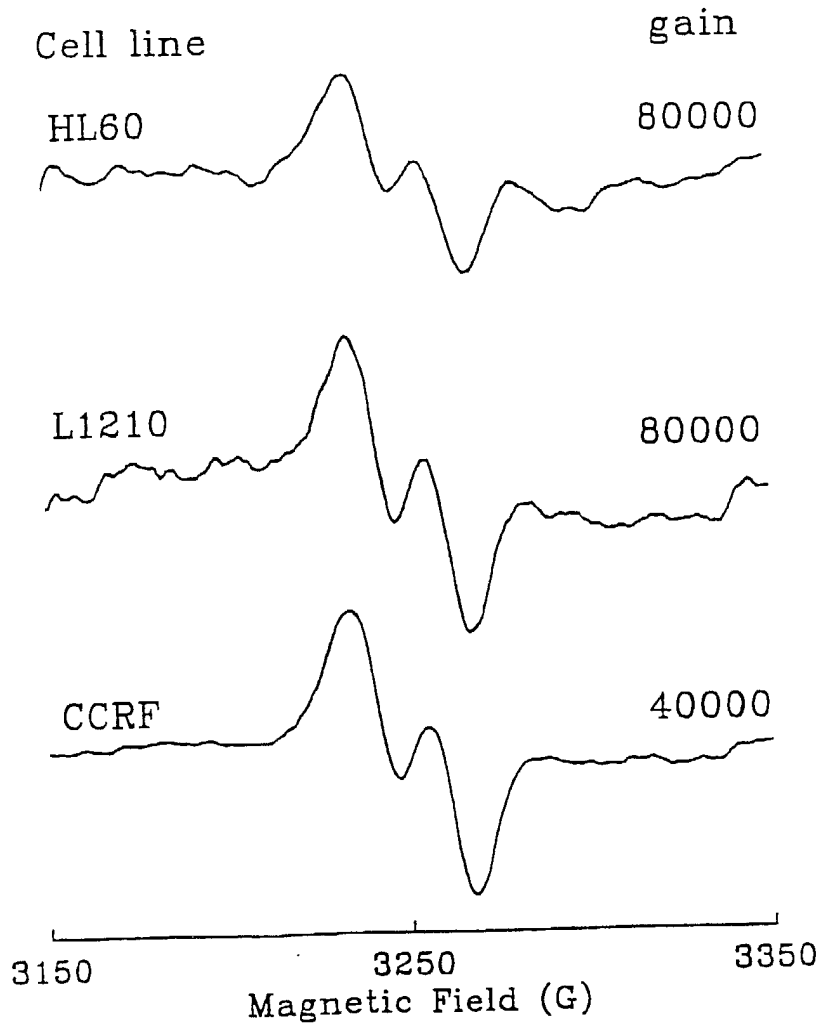

Fig. III.1. X-band ESR signal of the tyrosyl free radical in ribonucleotide reductase from different cell lines (approximately the same number of cells in each case). The names of the cell lines are written on the corresponding spectra, along with the spectrometer gains used in the measurement of the signal. The spectrometer conditions are: center field 3250 G, scan range 200 G, modulation amplitude 10 G, modulation frequency 100 kHz, time constant 0.5 sec, scan time 2 min, microwave power 100 mW.

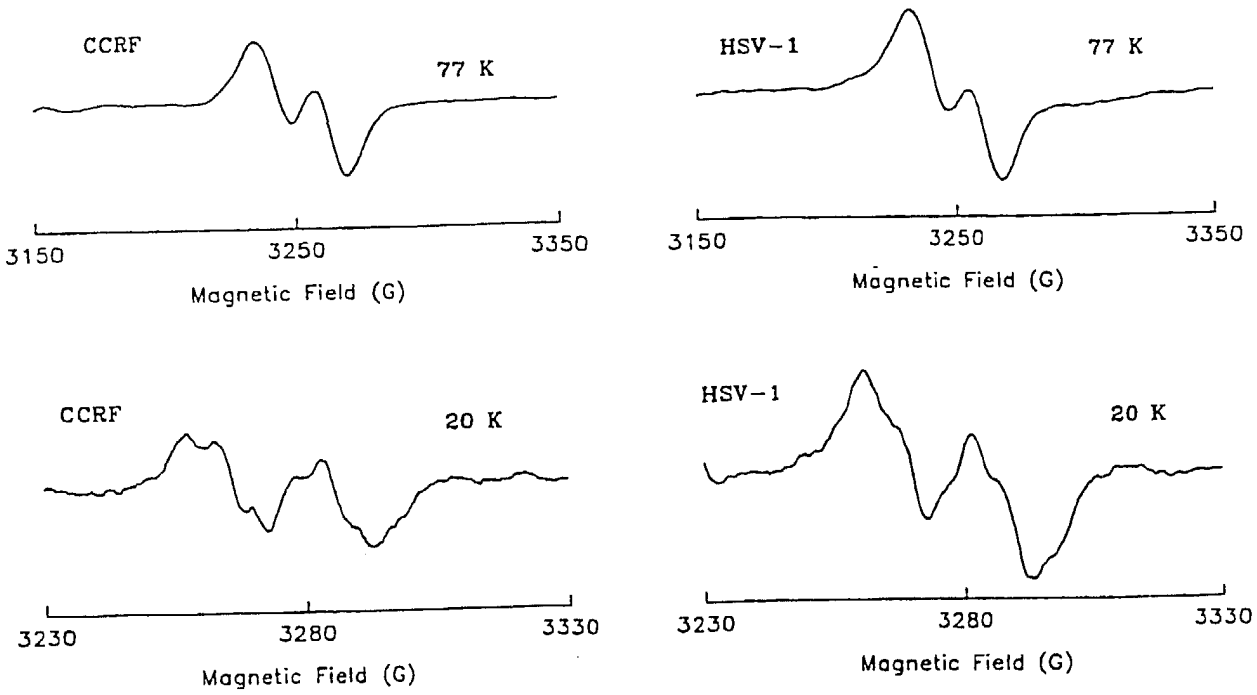

Fig. III.2. Tyrosyl free radical ESR signal of HSV-1 ribonucleotide reductase in infected corneal stromal cells (viral), and CCRF-CEM reductase (mammalian) at 77 K and 20 K. The spectrometer conditions at 77 K are the same as that indicated in figure 1 for both mammalian and viral reductase. The spectrometer gains used are 40000 and 32000 for CCRF and HSV-1 respectively. The spectrometer conditions at 20 K are: microwave power 12.5 mW for CCRF and 0.05 mW for HSV-1, modulation amplitude 5 G for CCRF and 2.5 G for HSV-1, spectrometer gain 400,000 for CCRF and 630,000 for HSV-1. The number of CCRF cells used was about 5×10^8, whereas the number of corneal stromal cells infected with HSV-1 was an order of magnitude lower.

2. Apo, reduced, and active forms of M2 subunit in ribonucleotide reductase - Addition of exogenous Fe^{2+} to apo-M2 subunit in the presence of oxygen results in an increase in the tyrosyl radical signal. Using cell free extracts, the intrinsic EPR signal of the tyrosyl radical, the signal after exposure to air, and the signal after exposure to ferrous iron in the presence of air, have been observed. This phenomenon is illustrated in (figure III.3) for cell free extracts from L1210 cells. The intrinsic tyrosyl radical signal is attributed to the active M2 subunit; the signal after exposure to air to the sum of active and reduced forms of the M2 protein; the signal after the addition of ferrous iron in the presence of air to the sum of active, reduced and apo forms of M2. Using these criteria, when compared to HL60 cells, the L1210 cells have 1.5 fold more active M2, two fold more active plus reduced M2, three fold more active plus reduced plus apo M2 subunit. HL60 cells have very little reduced or apo form of M2 as compared to the active form. CCRF-CEM cells have two times more active M2 subunit than the L1210 cells.

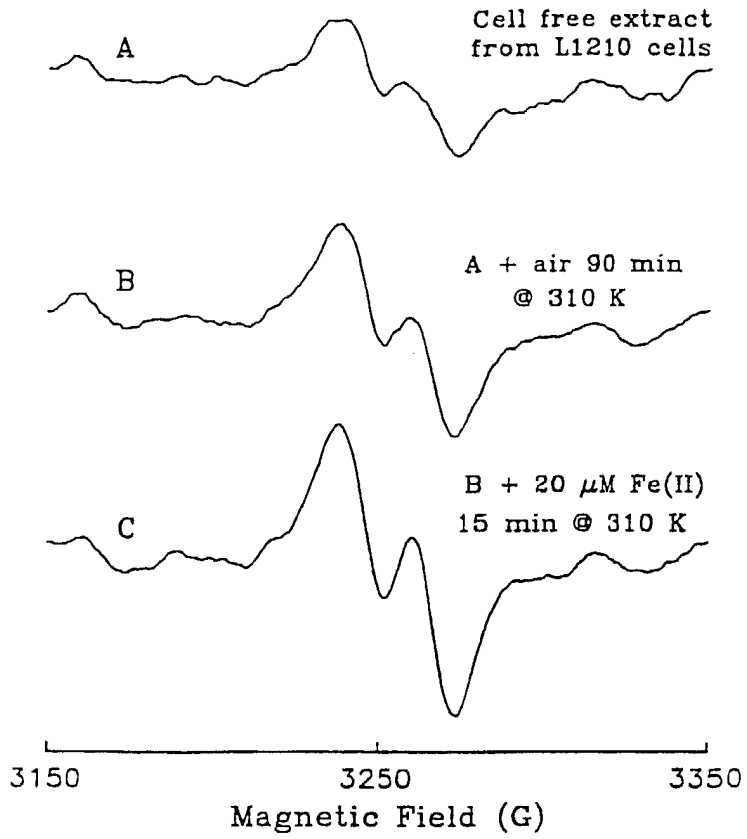

Fig. III.3. Effect of oxygen and ferrous ion (ferrous ammonium sulfate) on the tyrosyl free radical ESR signal from ribonucleotide reductase of L1210 cells. The cell free extracts were frozen in liquid nitrogen in precision bore tubing. The ESR spectrum (A) was obtained using the same spectrometer conditions as in figure 1. The same sample is then thawed and incubated in a 37°C water bath for 90 minutes, after which it is frozen in the precision bore tubing for ESR measurement (B). The same sample is thawed once again and incubated with 20 μM ferrous ammonium sulfate at 37°C for 15 minutes. It is then frozen in liquid nitrogen for obtaining ESR spectrum (C). Each of the spectra indicated represent the signal average of 16 spectra. The spectra also have been filtered for noise (using gaussian filter) using "Sumspc90".

3. Measurement of tyrosyl radical ESR signal from ribonucleotide reductase at X- and Q-band frequencies - Feher discusses the dependence of the minimum detectable number of spins on the microwave frequency (65). For a given volume of sample, V_s, the minimum number of electrons per unit volume is proportional to $V_c.V_s^{-1}.Q_o^{-1}.\omega^{-1}.P_o^{-0.5}$, where V_c is the volume of the cavity, Q_o is the quality factor of the empty cavity and P_o is the microwave power. Q_o is assumed to be inversely proportional to the square root of frequency (65). Using this relationship, the sensitivity at Q-band frequency using a cylindrical TE 110 cavity was compared to that at X-band with a rectangular TE 102 cavity. The sensitivity of Q-band was calculated to be a factor of two more than X-band when the sample is not limiting (i.e., sample volume at X-band is almost an order of magnitude greater than at Q-band). On the other hand, when sample is limiting (sample volumes are similar for X- and Q-band frequencies), the Q-band was calculated to be more sensitive than X-band by a factor of about 16.

Q-band spectra of the tyrosyl free radical signal were obtained from the cytosolic preparations of CCRF and hydroxyurea resistant L1210 cells. The volume of the sample used at Q-band was 32 μl for CCRF cytosol, as compared to the 320 μl sample used at X-band. The signal to noise obtained at the two different frequencies from the CCRF cytosol were comparable (Figure III.4). ESR signal from the manganese

impurities on the wall of the cavity is seen as a shoulder on the low field side of the tyrosyl radical signal at Q-band.

Comparing the tyrosyl radical signals from cytosol of HU-R L1210 cells at Q- and X-band, using the same sample tube (0.15 cm i.d, sample volumes of 18 μl at Q-band and 44 μl at X-band), a factor of 15 was gained in the signal to noise ratio at Q-band as compared to X-band (Figure III.5). These results are in agreement with the calculated values (discussed earlier) of sensitivity comparisons between X- and Q-band frequencies.

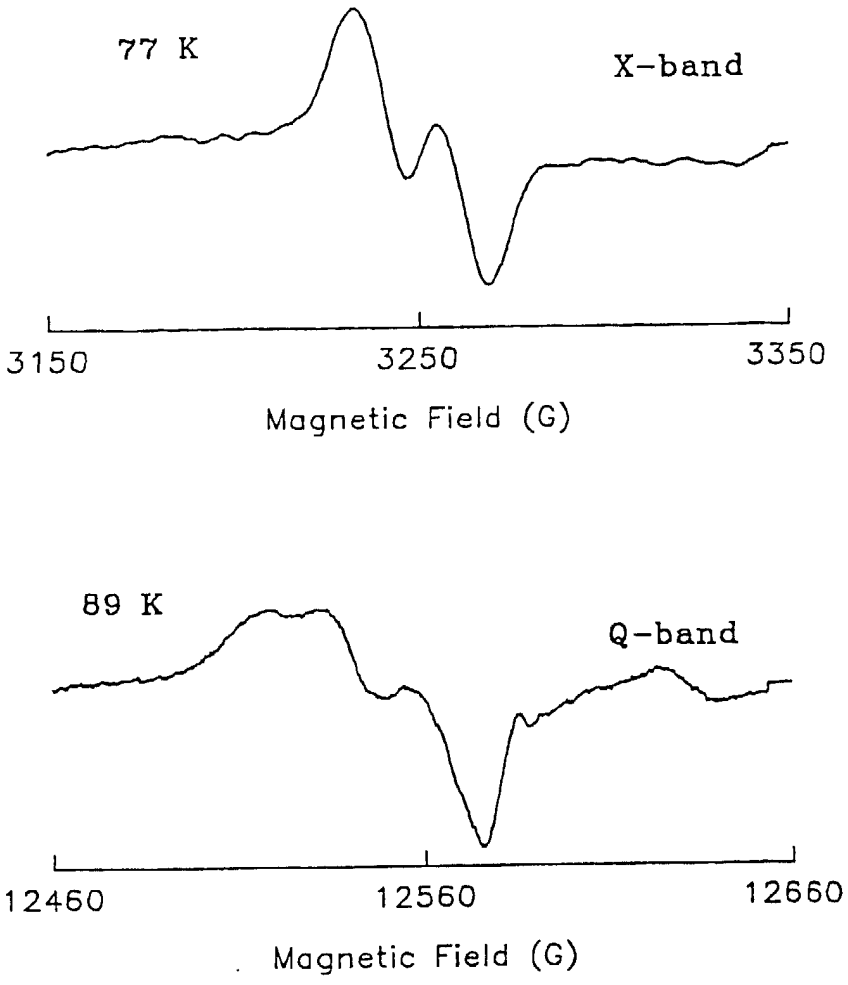

Fig. III.4. Tyrosyl free radical ESR signal from CCRF cytosol at X- and Q-band frequencies. The spectrometer conditions at X-band were the same as that in figure 1. The sample volumes were about 320 μl and 32 μl for X-band and Q-band respectively. The spectrometer conditions at Q-band were: Modulation amplitude 10 G, center field 12560 G, scan range 200 G, microwave frequency 35.164 GHz, microwave power 3 dB, spectrometer gain 1250. The temperature was 89 K for Q-band measurements and 77 K for X-band measurements. The background signal (at Q-band) using water sample was subtracted from the tyrosyl radical spectrum to subtract out the radical signal that was seen on the high field side of the tyrosyl radical signal.

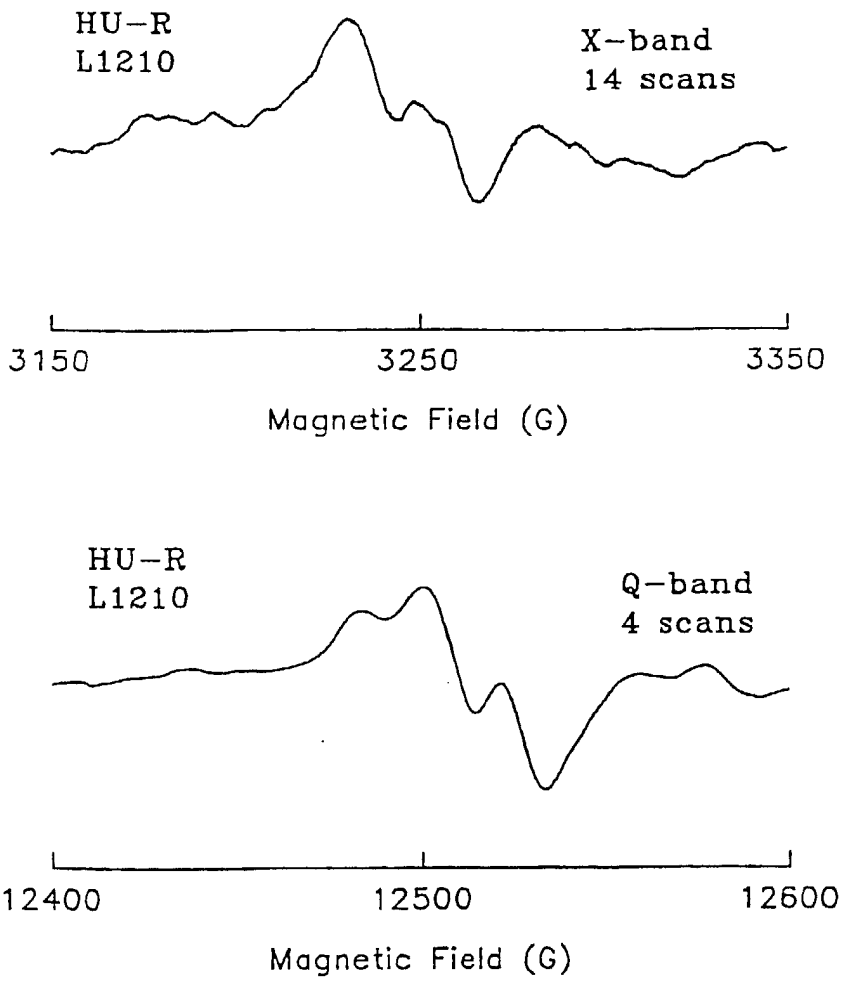

Fig. III.5. Tyrosyl free radical signal from hydroxyurea-resistant L1210 cells measured at X- and Q-band frequencies. A quartz sample tube (i.d. 0.15 cm, sample volume of about 18 μl for 1 cm height [q-band] and 44 μl for 2.5 cm height [x-band]) was used at both frequencies. The spectrometer conditions at X-band were the same as that mentioned for figure 1. The spectrometer conditions at Q-band were: microwave frequency 35.063 GHz, microwave power 10 dB, modulation amplitude 5 G, time constant 1 sec, gain 10 mV, center field 12500 G, scan range 200 G. The number of scans averaged is given along with the spectra. The Q-band spectrum has been filtered for noise and pseudomodulated as mentioned in the 'ESR spectroscopy' section of the "General methodology" chapter.

C. Discussion

Tyrosine radicals play an impotant role in various biological systems as indicated in the introductory section. The tyrosyl radical is essential for the activity of the key enzyme in cellular proliferation, namely, ribonucleotide reductase. A comparison of the tyrosyl radical signal from different cell lines indicates the differences in the amount of active, reduced and apo M2 present. The human leukemic cell lines (both CCRF and HL60 cells) have very little apo and reduced forms of the M2 subunit as compared to the mouse cell line (L1210). The hyperfine structure in the tyrosyl radical signal is seen more clearly at 20 K than at 77 K. The differences in the hyperfine structure of the tyrosyl radical signal between the mammalian and the viral ribonucleotide reductase is evident in figure 2. This is probably due to the difference in the tertiary structure of the protein (between the two species) that constrains the phenyl ring.

The ability to use Q-band for routine measurement of the tyrosyl radical signal would be time and cost effective. An order of magnitude less sample volume is required at Q-band than at X-band, thus enabling 10 experiments (at Q-band) in place of one (at X-band). Moreover, Q-band would be ideal for the measurement of the tyrosyl radical signal from clinical samples.

IV. STUDIES USING COPPER COMPLEXES

Abstract: The EPR signal of the tyrosyl radical attributed to ribonucleotide reductase decreases after treatment of promyelocytic leukemic HL60 cells with 2-formylpyridine mono-thiosemicarbazonato copper(II). EPR studies indicate that CuL forms adducts with both histidine and cysteine-like Lewis bases associated with isolated membranes from HL60 cells. After the addition of CuL, the EPR signal for the cysteine-like adduct decreases substantially over a 15 minute period. The reduction of signal is consistent with oxidation of thiols as shown by analysis of sulfhydryl content. It is hypothesized that receptor-mediated transferrin internalization is inhibited by oxidation of critical thiols. Since the uptake of ^{59}Fe-transferrin is greatly inhibited by the treatment of HL60 cells with CuL, the reduced uptake of iron by cells, in the presence of CuL, may lead to decreased iron availability for the activity of the M2 subunit of ribonucleotide reductase and a subsequent decrease in the tyrosyl radical signal of the enzyme. Moreover, the intact subunit M2 is no longer detected by EPR, even after the addition of excess iron.

A. Introduction

Copper is a biologically essential transition metal for

a variety of metalloproteins in different organisms. The biotransformations of copper is considered to be a series of metal transfer reactions in which copper moves from one ligand (amino acids in proteins) to another as it enters the organism or cell, reaches its sites of functional activity and then is released during biodegradation processes (66). To the extent that copper escapes its normal paths of reaction, it can become toxic to the biological system. The lipid soluble copper complexes used in this study are expected to bypass the normal metabolic pathway to produce its cytotoxic effect. The structures of the copper complexes used in the study, namely, 2-formylpyridine monothiosemicarbazonato copper(II), CuL, and 3-ethoxy-2-oxobutyraldehyde bis(thiosemicarbazonato) copper (II), CuKTS, are shown below. The uncharged CuKTS, [3-ethoxy-2-oxobutyraldehyde bis (thiosemicarbazonato) copper(II)], is more soluble in lipids [octanol:water ratio of 20:1] than the positively charged CuL [octanol to water ratio of 1:1]. CuKTS is a tetradentate complex while CuL is a tridentate complex,

and hence CuKTS, unlike CuL, is not expected to form adducts.

CuL

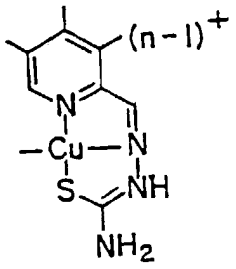

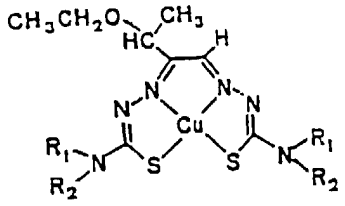

	R_1	R_2
CuKTS	H	H
CuKTSM	CH_3	H
$CuKTSM_2$	CH_3	CH_3

It is generally thought that endogenous redox active metals such as iron or copper participate in oxidation-reduction reactions in cells and lead to DNA damage and lipid peroxidation (67). Alternatively, oxidative reactions can be initiated by the introduction of metal complexes into cells, which catalyze the electron transfer between cellular reductants such as thiols and molecular oxygen. One group of compounds, α-N-heterocyclic-carboxaldehyde thiosemicarbazonato Cu(II) complexes, are effective agents of oxidative stress. Pyridoxal thiosemicarbazonato Cu(II) reacts in cells to cause thiol oxidation and DNA strand scission by a mechanism that involves the reduction of O_2 probably to hydroxyl radicals (68). A related structure, 2-formylpyridine thiosemicarbazonato Cu(II), CuL, has been studied in Ehrlich ascites and red blood cells and is similarly active (69,70).

In addition, both this copper complex and parent ligand inhibit the activity of partially purified ribonucleoside diphosphate reductase (RDR) (71). The ligand is also known to inhibit this enzyme in cells (71). However, the possible relationship between oxidative chemistry of CuL and its effect on RDR has not been investigated.

In past studies, it has been shown that CuL readily forms ternary complexes in biological media. Such adducts with thiols, including glutathione and cysteine residues of cat hemoglobin, and with nitrogen donor atoms from amino acid residues of normal human hemoglobin, histidine, and plasma have been described by EPR spectroscopy (69,72,73). With cells, CuL forms an adduct that is characterized by an EPR spectrum at room temperature indicative of its near rigid limit motion. Its loss of rotational motion might be due to binding to macromolecules or to intercalation into the plasma membrane phospholipid structure as shown with 3-ethoxy-2-oxobutyraldehyde bis(N^4-dimethylthiosemicarbazonato) Cu(II) (74). Little attention has been directed toward reactions of CuL that may occur in membranes.

Hydroxyurea, guanazole, and various thiosemicarbazones are relatively specific inhibitors of RDR (75,76). Combinations of the iron chelating agent, desferrioxamine, and hydroxyurea, guanazole, or thiosemicarbazones produce greater inhibition of DNA synthesis than these latter compounds alone (77). Moreover, endogenous iron reversed at least in part the

effects of these inhibitors (77). These results suggest that their reactions with RDR involve the iron containing subunit of the enzyme (77). Cory et al., have suggested that the inhibitors of the non-heme iron containing subunit of mammalian ribonucleotide reductase can be subclassified based on their response to the presence of iron chelating agents (36). Although the non-heme iron subunit of RDR is inhibited by IMPY (pyrazolo-imidazole), hydroxyurea, and MAIQ (4-methyl-5-amino isoquinoline thiosemicarbazone), the mechanism of inhibition by hydroxyurea and IMPY is distinct from that of MAIQ (35). Further, studies with hydroxyurea resistant cells have shown that the HU-7-S7 cells exhibit cross resistance to IMPY/desferal, but remain sensitive to the thiosemicarbazones (78).

The present experiments are undertaken to examine features of the cellular oxidative chemistry of CuL, particularly its reactions with membrane associated thiols, that may explain how it suppresses the tyrosyl radical signal of ribonucleotide reductase. A hypothesis is set forth that CuL affects RDR and cell growth by preventing the uptake of iron into HL60 cells, thereby limiting the synthesis of iron-containing M2 subunit of ribonucleotide reductase. Most of the CuL work has been published (79). A comparison is also made between the toxicity caused by a mono and a bis thiosemicarbazone copper complex.

B. Materials and methods

1. Reagents and materials - 2-Formylpyridine monothiosemicarbazonato copper(II), CuL, was prepared as previously described (80). Standard solutions of CuL in 25% DMSO or 100% DMSO were added either to isolated membranes or cells. Cells were grown at an atmosphere of 7% CO_2 in RPMI 1640 supplemented with 10% fetal calf serum. Human leukemic HL60 cells, Chinese hamster ovary cells, and Ehrlich ascites cells were maintained as previously described (71,81,82). All cell membranes were prepared by the method of Deziel and Girotti (83) without resealing the membranes. Membranes were washed with lysing buffer (5 mM $NaPO_4$, 5 mM NaCl, pH 8) three or four times.

2. Physical measurements - The trypan blue dye exclusion method was used to test the membrane integrity of the cells. Total thiol content in cells or membranes was determined colorimetrically using Ellman's reagent (84). Cells were sonicated and after incubation at 0-4° C for 1 hr, centrifuged at 27000 x g . To 200 μl of the cell lysate or the cell membranes, 150 μl of 10% SDS (sodium dodecyl sulfate), 300 μl of 0.1 M phosphate buffer at pH 7.5, and 150 μl of 0.01 M DTNB were added and the volume brought to 1500 μl with deionized water. The reaction mixture was incubated in the dark, at 25°

C for 30 min, after which the absorbance at 412 nm was measured against a blank of water. The extinction coefficient for the product 5-thio-2-nitrobenzoate was taken to be 1.36 x 10^4 $M^{-1}cm^{-1}$.

3. **^{59}Fe Uptake** - ^{59}Fe-transferrin (1.2 μg Tf, 13000 ^{59}Fe cpm/ml) was added to HL60 cells in 1 mL multi-well plates in the presence or absence (control) of CuL. The concentration of CuL used (10 μL) was the same as that which inhibited the tyrosyl free radical EPR signal. After incubation for 30 min to 24 h, the cells were harvested by centrifugation at 1000 rpm for 15 min. The supernatant was removed and the cell pellet counted for radioactivity using a Compugamma gamma counter.

4. **EPR spectroscopy** - ESR spectra were obtained at the National Biomedical ESR Center in Milwaukee, Wisconsin, on a Varian Century Series spectrometer. The magnetic field was measured with a Radiopan magnetometer and the microwave frequency with a Dana EIP Autohet microwave counter. Spectra from frozen samples were obtained by supporting frozen icicles (3 cm long and 4 mm in diameter) in a finger dewar containing liquid nitrogen.

5. **Measurement of cellular ferritin content** - HL60 cells were harvested, washed twice with PBS containing 0.1% bovine

serum albumin and were resuspended in the same buffer containing 0.1% Triton X-100. After disruption of cells by sonication, cellular debris was removed by centrifugation (10,000 x g for 30 min) and the cytoplasmic supernatant was assayed for ferritin using a radioimmunoassay kit from Bio-Rad (Richmond, CA). This assay is based on the general principles of two-site immunoradiometric assays or "sandwich assays" wherein the antigen (ferritin) becomes sandwiched between the labeled and immobilized antibodies. This assay uses purified ^{125}I-labeled antibody to ferritin as the tracer, and ferritin antibodies immobilized on polyacrylamide beads as the solid phase. A standard curve is generated by using the ferritin standards provided.

C. Results

1. Inhibition of cell growth by CuL and CuKTS - The cytotoxicity of these two copper complexes on human promyelocytic leukemia HL60 cells in culture is shown in figure IV.1. CuKTS seems to be more cytotoxic for a shorter incubation period even at lower concentrations than CuL, probably because of its high lipid solubility compared to CuL; thus enabling direct damage to the membranes even before entering the cell. The control cell populations increased almost four fold during three days, while those treated with CuL decreased and had 20% dye permeable cells at 24 h and 30% at 72 h. Cell **viability** as measured by trypan blue exclusion also indicates that much less CuKTS (0.2 μM) is needed compared to CuL (10 μM) to compromise the cell membrane to a similar degree. The cytotoxicity of these copper complexes on murine leukemic L1210 cells was also studied. Figure IV.2 shows the L1210 cell growth inhibition caused by CuKTS over a period of 24 and 72 hours. Since the doubling time for L1210 cells is about 12 hours, higher number of cells were plated for 24 hr incubation (1 X 10^6 cells/ml) than for the 72 hour incubation (5 X 10^4 cells/ml) with CuKTS. For HL60 cells, cell densities of 0.5 X 10^6 cells/ml and 1 x 10^6 cells/ml were used for 72 and 24 hour incubations respectively. The concentration of CuKTS (Fig IV.2) is normalized for 5 X 10^4 cells.

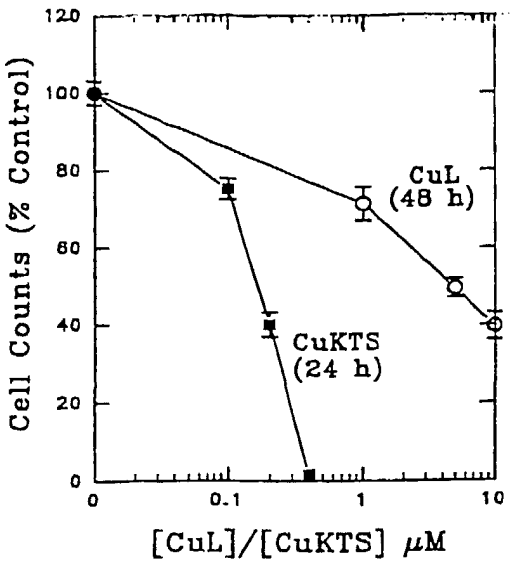

Fig IV.1. A plot of CuL and CuKTS concentration vs HL60 cell count. Error bars represent standard deviation of triplicate values.

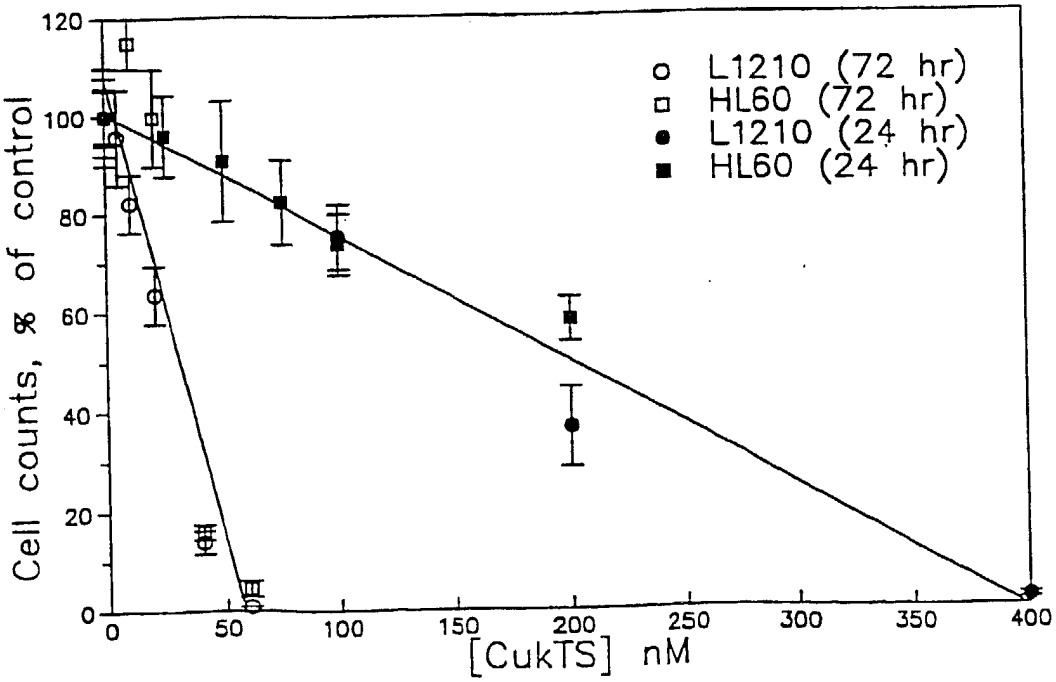

Fig IV.2. A plot of CuKTS concentration vs HL60 and L1210 cell count after 24 and 72 hours of incubation with CuKTS.

2. ^{59}Fe uptake studies - The studies on iron uptake carried out by monitoring the radiolabel ^{59}Fe indicated that both CuL and CuKTS were inhibitory to the process of transferrin mediated iron uptake over a period 6 to 24 hours (figures IV.3 and IV.4). The concentrations of CuL and CuKTS chosen for the iron uptake studies determination were 10 μM and 200 nM respectively. These concentrations were chosen because it inhibited cell proliferation (Fig. IV.1) over a 72 h period with only modest effects on cell membrane integrity. Complete inhibition of iron uptake was achieved with 10 μM CuL after about 6 hours, while 200 nM CuKTS brought about a 40% decrease in the uptake of radiolabeled Fe-Tf over 24 hours. Complete inhibition of the iron uptake with CuKTS was not achieved because of the decrease in viability upon addition of higher concentrations of CuKTS. 100 nM CuKTS also inhibited ^{59}Fe uptake in L1210 cells, the curve (not shown) was in between control and that of 200 nM CuKTS.

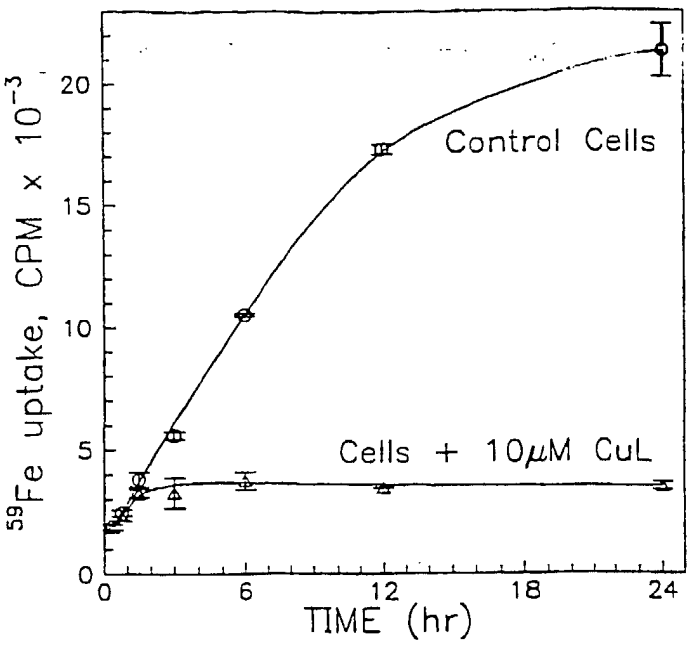

Fig IV.3. ^{59}Fe-Tf uptake by HL60 cells in the absence (control) and presence of 10 μM CuL for various lengths of time. The data represent an average of triplicate values, the error bars being ± 1 standard deviation.

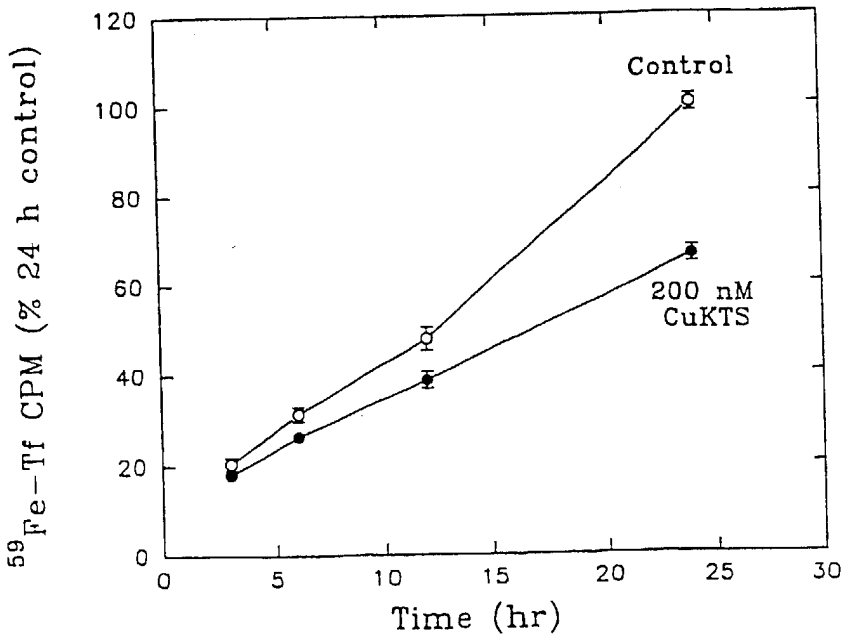

Fig IV.4. ^{59}Fe-Tf uptake by HL60 cells in the absence (control) and presence of 200 nM CuKTS for various lengths of time.

3. ESR study of adduct formation between CuL and cell membranes - Copper catalyzed oxidation of sulfhydryl groups by molecular oxygen was shown to involve adduct species of CuL, which were detected by EPR spectroscopy (73). According to past work, cysteine- and histidine-like adducts were formed when CuL was added to hemoglobin, plasma, or Ehrlich cells (Table 1). Similarly, the rigid limit spectrum and EPR parameters obtained after freezing the membranes from cells confirmed a shift from almost equal amounts of histidine-like and thiol-like adducts to predominantly histidine-like adducts (Fig IV.5 and Table 1). EPR signals obtained after addition of CuL to isolated membranes from either HL60 (Fig IV.5,A), red blood, Ehrlich ascites (Fig IV.5,B), or CHO cells (data not shown) were similar. Thus, the adduct formation between CuL and donor atoms from histidine and cysteine-like ligands associated with membranes appears to be a general phenomenon in a variety of cell lines. For these experiments, the isolated membranes were frozen within 1 to 2 minutes after addition of CuL. When isolated membranes were frozen more than 15 minutes after addition of CuL, the cysteine-like adduct was diminished (Fig IV.5, A' and B'). It is presumed that this resulted from CuL-catalyzed depletion of thiols and the formation of disulfides. Approximately 30 minutes after the addition of CuL, a third signal from a cupric complex was evident by the increase in intensity at the low field side of the $g_{\parallel}$ lines for the Cu-histidine like adducts (Fig IV.5, A'

and B'). Presumably, a nitrogen donor atom(s) was replaced by an oxygen donor atom (85). The pool of histidine-like donor atoms in the membrane fraction was more extensive than the pool of cysteine-like donor atoms as indicated by the increase of the CuL-histidine-like complex with respect to the CuL-cysteine-like species as the concentration of CuL was increased from 50 μM to 400 μM in packed isolated membranes (Fig IV.6).

4. Thiol concentration in cells and membranes in the absence and presence of CuL - The decrease in thiol content of HL60 cells and isolated membranes suggested by the EPR results was quantitated with the Ellman assay (Table 2). For short incubation periods, the thiol concentration was higher in the absence than in the presence of 100 μM CuL (Table 2(a),(b) and (c)). The increased thiol concentration of HL60 cells after treatment with 10 μM CuL for 24 h (Table 2(d)) suggests that cells may have overcome the inhibition of 10 μM CuL by increasing the GSH content after the initial CuL stress. After the addition of 100 μM CuL to membranes, the thiol concentration decreased by about 50 μM (Table 2(e) and (f)). After 30 min incubation with CuL, the decrease in thiol was about 90 μM (Table 2(e) and (g)). From these results it was evident that some of the redox activity of CuL occurred in the membrane fraction of these cells.

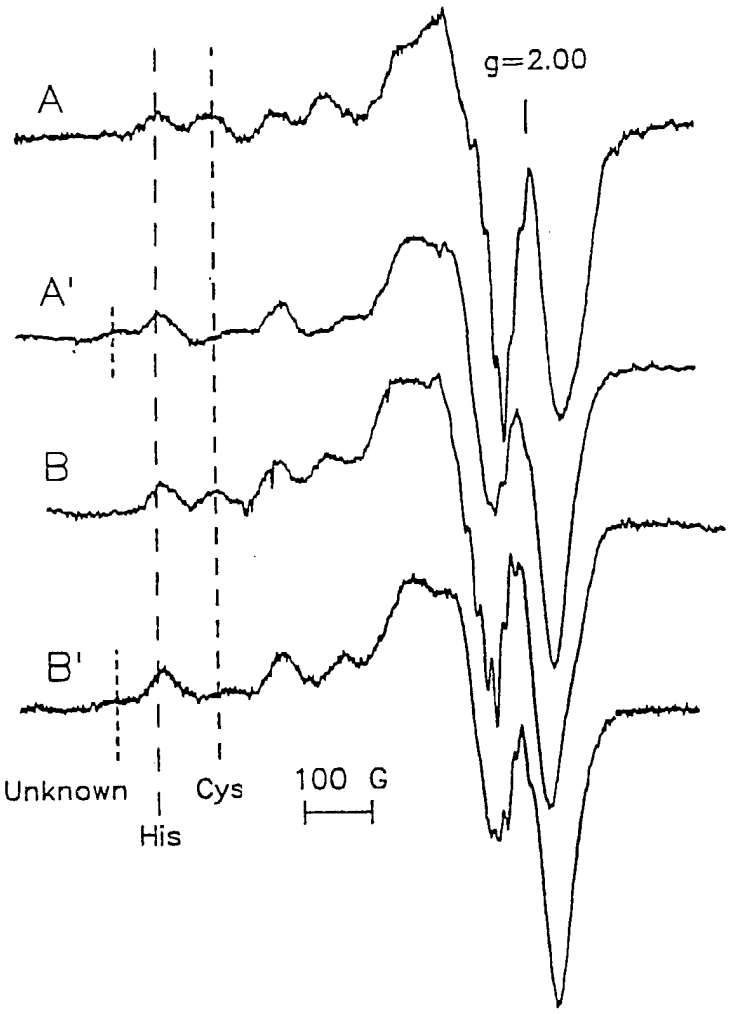

Fig IV.5. EPR spectra at 77 K of HL60 membranes after addition of 200 μM CuL and (A) frozen within 45 sec; (A') incubated at room temperature for 30 min before freezing. (B) and (B') are similar to (A) and (A') respectively, but with Ehrlich ascites cell membranes. The low field line in the $g_{\parallel}$ region for each adduct is indicated by dashed lines. Spectrometer settings: Scan time 4 min, modulation frequency 100 kHz, modulation amplitude 5 G, microwave power 5 mW; (A) gain 1.25×10^4, time constant 0.5 sec, microwave frequency 9.00 GHz; (A') gain 1.6×10^4, time constant 0.5 sec, microwave frequency 9.111 GHz; (B) gain 2×10^4, time constant 0.5 sec; (B') gain 1.6×10^4, time constant 0.25 sec.

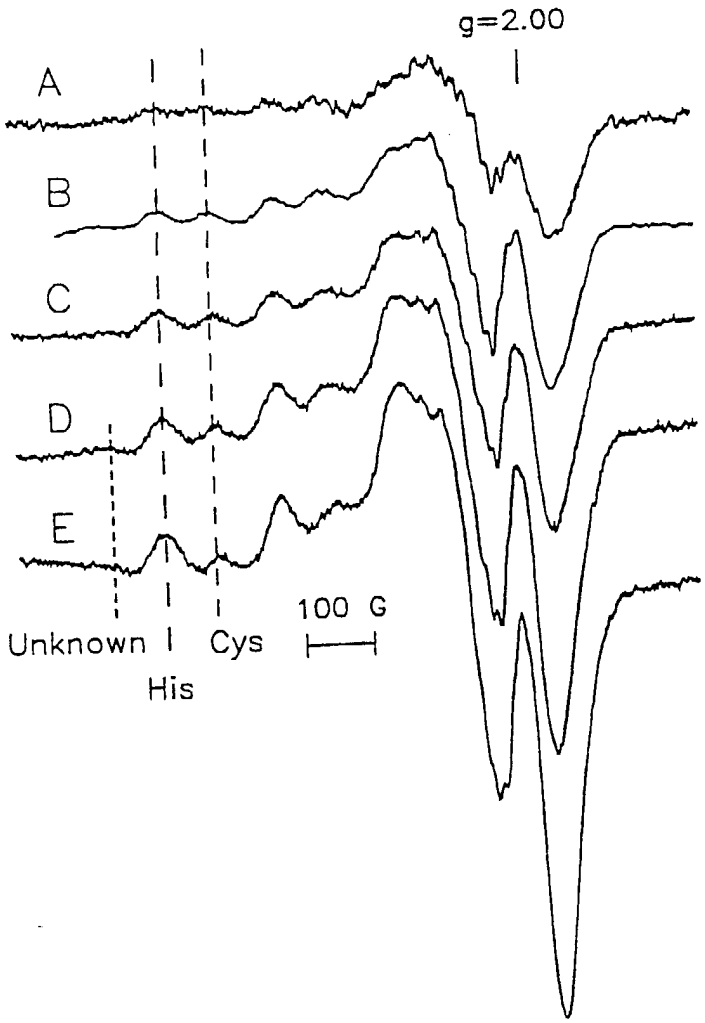

Fig IV.6. EPR spectra at 77 K of RBC membranes with increasing concentrations of CuL: (A) 50 μM CuL, (B) 100 μM CuL, (C) 200 μM CuL, (D) 300 μM CuL, (E) 400 μM CuL. Spectrometer conditions: scan time 4 min, modulation amplitude 5 G, modulation frequency 100 kHz, microwave power 5 mW; (A) gain 5 x 10^4; (B) gain 4 x 10^4; (A) and (B) time constant 1 sec; (A-E) microwave frequency 9.095 GHz; (C-E) time constant 0.5 sec and gain 1.6 x 10^4.

Table 1. EPR Parameters for CuL in Frozen Solutions

Species	$g_\parallel$ Adduct			$A_\parallel$ G Adduct		Ref
	H_2O-like	His-like	Thiol-like	H_2O-like	His-like	Thiol-like	
CuL	2.206			185			(86)
CuL+His		2.188			183		
CuL+Plasma		2.181	2.152		188	167	
		2.187	2.160		184	170	
CuL+HbA		2.19			172		(72)
CuL+CatHb		2.19	2.12		187	176	
CuL+GSH			2.14			178	
Membranes[a] of							Current work
CuL+RBC		2.19	2.14		170	165	
CuL+CHO		2.19			180		
CuL+HL60		2.189	2.139		175	169	

[a] RBC, Red blood cells; CHO, Chinese hamster ovary cells; HL60, Human leukemic cells.

Table 2. Thiol Values* as Determined by the DTNB Assay

Cells/Membranes	Thiol Content in mM per 10^8 cells**	Conditions
a) HL60 cells	3.2 ± 0.02	Stock cells cultured for 24 hrs
b) HL60 cells + 100 μM CuL	2.0 ± 0.1	Cells were incubated with 100 μM CuL for 5 min prior to assay.
c) HL60 cells + 100 μM CuL	2.7 ± 0.1	Cells were incubated with 100 μM CuL for 30 min prior to assay.
d) HL60 cells + 10 μM CuL	5.9 ± 0.4	Cells were cultured with 10 μM CuL for 24 hrs.
e) HL60 membranes	0.12 ± 0.02	Membrane was prepared according to Ref. (83).
f) HL60 membranes + 100 μM CuL	0.07 ± 0.01	Membrane was incubated with 100 μM CuL for 5 min prior to assay.
g) HL60 membranes + 100 μM CuL	0.03 ± 0.01	Membrane incubated with 100 μM CuL for 30 min prior to assay

* The thiol values represent an average of triplicate measurements ± one standard deviation.
** Thiol content for 10^7 cells and membranes from 10^7 cells are measured and corrected to 10^8 cells.

5. Effect of CuL on ribonucleotide reductase - Twenty-four hours after the addition of CuL, cells packed to 5×10^8 cells/ml and frozen into an icicle (4 mm diameter and 3 cm long) had little or no detectable EPR signal from the tyrosyl free radical attributed to RDR (Fig IV.7, A vs B). In the absence of CuL, the peak-to-peak height of the free radical signal in packed HL60 cells was at least four times greater than that seen in the presence of CuL. Sometimes a sharp single line from a second radical was superimposed on the tyrosyl radical signal (data not shown). The g-value for the radical is 2.004 and the coupling of the doublet is about 18 G. These values are consistent with the parameters for the RDR radical (8,22,29). The activity of RDR has been shown to be directly related to the intensity of the tyrosyl radical of RDR (87). Thus, it is inferred that, in these cells, ribonucleotide reductase activity is greatly reduced. Since the tyrosyl radical is only linked to the concentration of the active M2 unit, the concentration of the M1 unit is not known, but without active M2, the enzyme activity is lost. The reduction in the ribonucleotide reductase tyrosyl radical signal after the addition of CuKTS to HL60 cells was not recorded due to the large number of cells needed to record the EPR spectra; the decrease in the viability of cells in the presence of CuKTS made it very difficult to collect such large number of cells.

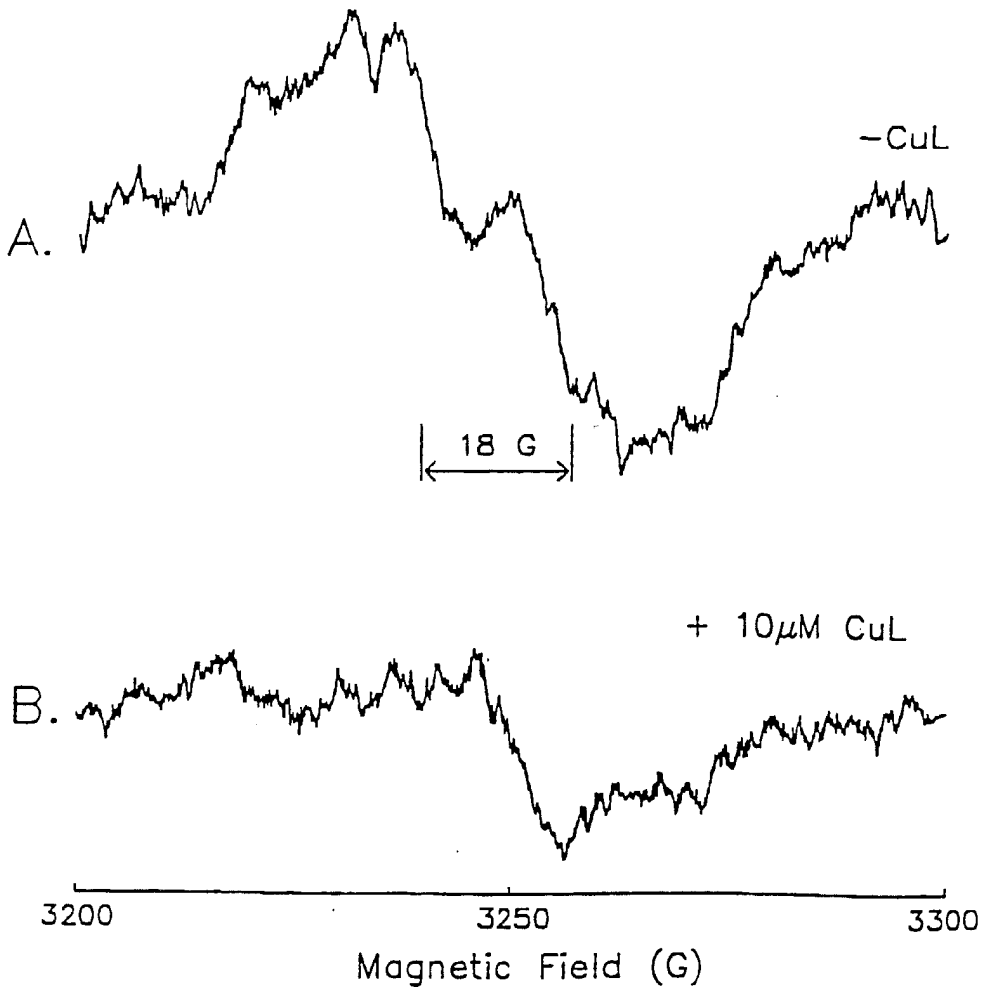

Fig IV.7. EPR spectra of the tyrosyl free radical signal from packed HL60 cells (5×10^8 cells/ml) at 77 K in the absence (A), and presence (B) of 10 μM CuL for 24 hrs. A second unidentified free radical signal is sometimes superimposed on the tyrosyl radical signal (B and data not shown). The center of the tyrosyl doublet is 2.004. Spectrometer conditions: field set 3250 G, scan range 100 G, time constant 0.25 sec, modulation amplitude 5 G, modulation frequency 100 kHz, gain 5×10^4, microwave power 90 mW; microwave frequency 9.107 GHz.

A direct inhibitory effect of CuL on the tyrosyl radical in ribonucleotide reductase is seen when CuL is incubated with cell free extracts from HL60 cells for 30 min at 37°C. No copper EPR signals are detected. Upon allowing the same sample to incubate overnight at room temperature, a copper signal is found (Fig IV.8) which is indicative of the redox chemistry of copper. A predominant (unknown) species with an $A_{\parallel}$ value of 185 G and a $g_{\parallel}$ value of 2.24 was obtained. A second species which has an $A_{\parallel}$ value of 172 G and a $g_{\parallel}$ value of 2.19, presumably is a histidine-like adduct of CuL.

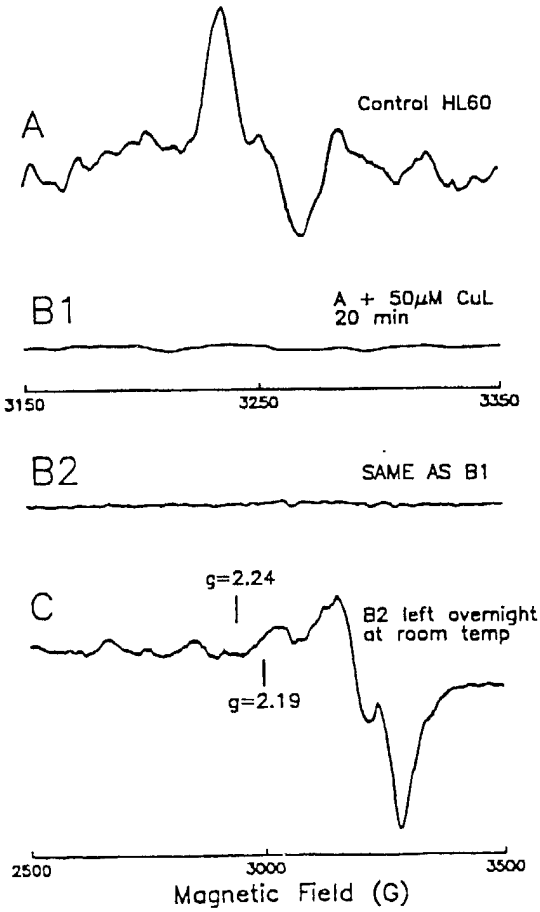

Fig IV.8. The tyrosyl free radical ESR spectrum from the cytosol of HL60 cells is seen in (A), and the inhibition of the signal upon incubation with 50 μM CuL is seen in (B1). The spectrometer conditions for A and B1 are: modulation amplitude 10 G, microwave power 100 mW, gain 80,000, time constant 0.5 sec. 16 scans were averaged. The spectrum in B2 is a 1000 G scan of the CuL treated sample. The spectrum in C was collected after allowing the CuL treated sample to incubate overnight at room temperature. The spectrometer conditions for B2 and C are: modulation amplitude 10 G, microwave power 5 mW, gain 80,000, microwave frequency 9.0875 GHz,time constant 0.5 sec. The temperature was 77 K for all the measurements.

D. Discussion

Although CuL is a strong, direct inhibitor of ribonucleotide reductase, it is of interest to know if its more general reactivity in cellular redox reactions might also have a role to play in the cellular inhibition of the enzyme, which further leads to arrest of cell growth. Prior studies have documented the loss of cellular thiols that occurs after exposure of Ehrlich cells to CuL (69). At least two possible origins exist for the CuL-SR adduct. First, CuL may be bound to cysteine residues of high molecular weight proteins associated with the membrane. Second, CuL could form an adduct with GSH, i.e., CuL-SG. The sulfhydryl group should neutralize the charge of CuL and help facilitate its uptake into the membrane, but the two carboxylic acid groups, an amino group, and two amides from GSH may not favor incorporation of the adduct into the membrane.

After CuL stressed the pool of GSH, it seems that the cells responded to the stress through the over production of GSH. This is seen most clearly in Table 2 (d), the thiol content for the cells that were grown in a medium containing 10 μM CuL for 24 hours.

In an experiment to relate the oxidation chemistry of CuL with its effects on RDR, the uptake of ^{59}Fe from ^{59}Fe-transferrin into HL60 cells was examined in the absence and

presence of CuL. According to Fig IV.3, using the concentration of CuL that reduced the tyrosyl radical signal and cell growth, there was an almost complete inhibition of cellular uptake of ^{59}Fe from ^{59}Fe-transferrin. The ^{59}Fe uptake was shut down after about three hours. Only 40% of the ^{59}Fe-Tf measured was internalized (both in the presence and absence of CuL) and 60% can be removed by acid wash, but, in absolute amounts, there was a 6-fold decrease in the uptake of ^{59}Fe-Tf in the presence of CuL after 24 hrs. From these results, it appeared that CuL may affect both plasma membrane binding of Fe-Tf and/or the mechanism of release of iron from transferrin in endosomes. Because there was no direct effect of CuL on the elution profile of ^{59}Fe-Tf when it was passed through a G-150 column (Fig IV.9), it appears that inhibition of cellular iron is a membrane effect and not a result of alteration of the iron in Fe-transferrin. Since 60% of the ^{59}Fe-Tf is associated with the cell but is not internalized, transferrin binding to its receptor probably occurred. This experiment suggests that CuL may indirectly inhibit the activity of RDR by preventing cellular iron uptake needed for the synthesis of the enzyme. Nevertheless, it is not known whether CuL affected internalization of the receptor-transferrin complex, endosomal pumps, etc. It is hypothesized that cells contain a reactive sulfhydryl that can be oxidized by CuL such that Tf can bind but not internalize Fe. Treatment of cells with a sulfhydryl reagent was shown to prevent receptor-mediated

internalization of Tf (88).

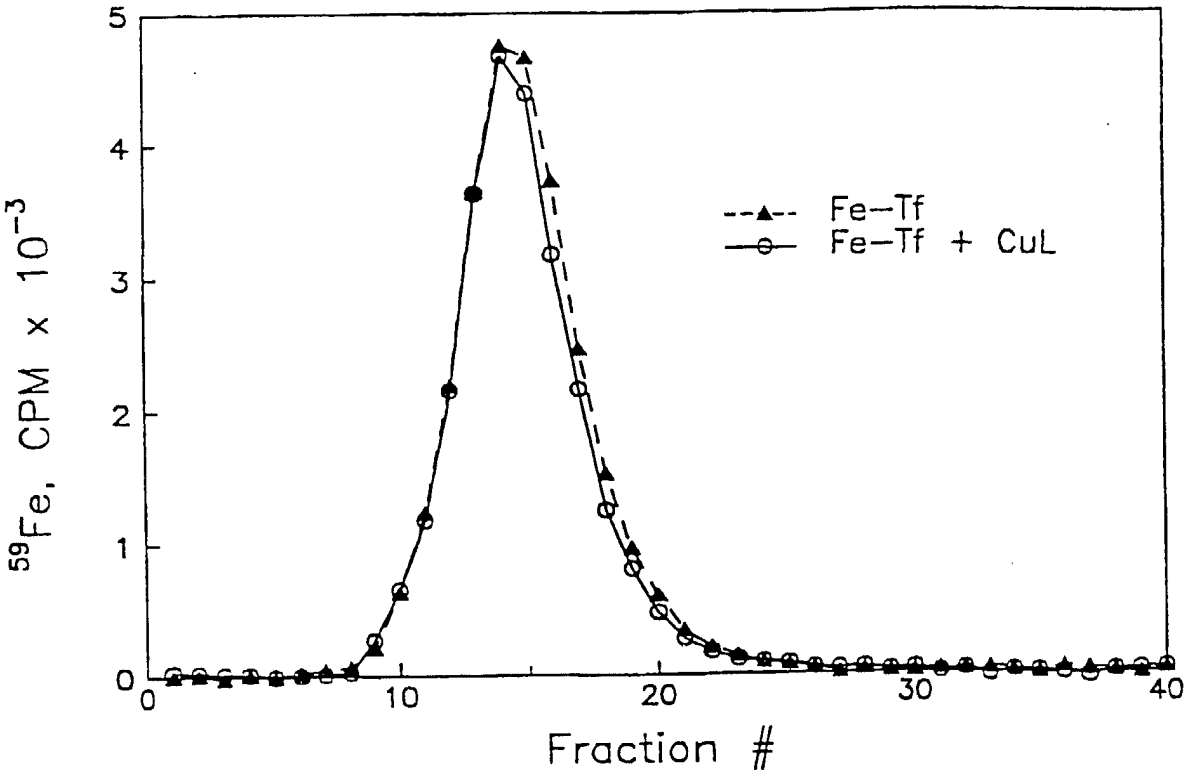

Fig IV.9. Elution profile of ^{59}Fe-Tf, in the absence and presence of CuL incubation, when passed through a G-150 column.

Addition of excess Fe^{2+} and O_2 to a cytosol preparation of CuL treated cells did not give a tyrosyl radical signal. Lack of signal indicates minimal quantities of apo M2 in the cytosol. The cytosol of control cells (i.e., cells not treated with CuL) also did not show an increase in the tyrosyl radical signal. Other cell lines, i.e., murine leukemia (L1210) cells, had 1.5-fold more tyrosyl radical in 5×10^8 cells, 2-fold more tyrosyl radical after a 90 min exposure to

air, and 3-fold more tyrosyl radical after addition of excess Fe^{2+}. It is presumed that the intrinsic tyrosyl radical signal correlates with active M2 (87), the signal after exposure to air to the sum of active and reduced forms of the M2 subunit, and the signal after exposure to excess Fe^{2+} in the presence of oxygen to the sum of active, reduced, and apo forms of the M2 subunit. This suggested that little unmodified apo RDR exists in HL60 cells and CuL may have inhibited the synthesis of the M2 subunit of RDR. It follows that iron from depleted RDR was released inside the cell. Ferritin measurements were consistent with a significant increase in cellular ferritin in CuL treated cells. The ferritin content was found to be 7.3 μg / mg of protein in control cells as compared to 39.7 μg / mg protein in CuL treated cells.

Previously, it was shown that inactivation of M2 or RDR by hydroxyurea resulted in the release of iron (89). The release of iron may control regulation of the expression of genetic information and biosynthesis and/or post-translational stability of transferrin receptor, RDR, and/or ferritin (90,91). Whether the mechanism of action of copper complexes involves an alteration in the free iron pool, which may regulate the expression of genetic material, needs further investigation.

Bleomycin (50 μM) was incubated with cytosol from CCRF cells (30 min at 37°C) to see if iron from the M2 subunit

could form a complex with bleomycin. In that study, it was noted that bleomycin did not reduce the tyrosyl radical from ribonucleotide reductase, and ESR detectable iron-bleomycin signal was not seen. A similar experiment was conducted with 50 μM IQ (1-formyl isoquinoline thiosemicarbazone). Under the experimental conditions used, the tyrosyl radical from ribonucleotide reductase was reduced upon incubation of CCRF cytosol with IQ, but the iron-IQ complex was not detected through ESR spectroscopy.

In summary, experiments reported here support the model that CuL initially reacts with cellular membranes as it is taken up into cells. It forms adducts with thiols, oxidizes them to disulfides, and, by analogy with model studies (69), generates oxy radicals in membranes as well as in the cytosol. In model studies with CuL and GSH in air, both $O_2^{\cdot}$ and $^{\cdot}OH$ were trapped by 5,5 dimethyl-1-pyrroline-N-oxide (DMPO), and GSH oxidized to GSSG (69). CuL was shown to be involved in multiple reactions, primarily oxidation of thiols and generation of oxy radicals before the release of radicals (66). The oxidation of critical sulfhydryls from both receptors (88) and RDR (46,66) after addition of CuL are consistent with affinity of CuL for thiols. The formation of small amounts of histidine-like adduct (seen in figure IV.8; overnight incubation of cytosol with CuL at room temperature) suggests the availability of intact CuL. The predominant species in figure IV.8c is probably the copper bound to

nitrogen atoms from histidine residues of denatured proteins in the cytosol. Thiol-like adduct is clearly not observed (Fig IV.8), suggesting the oxidation of thiols by CuL during the incubation period.

Effects of the inhibition of iron uptake and protein synthesis of other iron containing enzymes including cytochromes and iron-sulfur centers need to be examined. Detoxifying agents such as metallothionein may prevent extensive damage in the cytosol from small concentrations of the copper complex (92,93). Membranes, on the other hand, may be more sensitive to metal catalyzed oxidative damage. The nature of the membrane damage that inhibits the cellular uptake of iron from transferrin needs further study. After the onset of inhibition of this process, the tyrosyl radical signal decreases. That one event is related to the other is suggested by the fact that iron is depleted within 3 hrs, RDR turns over in about 3 hrs in cells (22), the tyrosyl radical signal is diminished, and the previous finding that the decrease in the radical signal correlated with the decrease in the activity of RDR (87). This study expands the understanding of the effects that metal-catalyzed reactions may cause in cells. Generalized oxidation of membranes and soluble thiol compounds may secondarily lead to the generation of toxic oxy-radicals. In addition, thiol oxidation, itself, may specifically result in the inhibition of iron uptake, leading to the loss of RDR activity.

V. STUDIES USING GALLIUM COMPOUNDS

Abstract: Gallium, as a nitrate or a citrate, inhibits the growth of murine leukemic L1210 cells and quenches the tyrosyl free radical signal from cell free extracts containing the M2 subunit of ribonucleotide reductase (RR). Micromolar quantities of iron(II) reversed the effect of gallium in cells. The cell free extracts, from 5×10^8 L1210 cells that were incubated with 400 μg/ml (960 μM) gallium in the culture medium for 18 hours, showed a negligible tyrosyl radical signal from RR, when compared to the extracts from (5×10^8) control L1210 cells. Upon incubation of the extracts with 10 μM ferrous ammonium sulfate in the presence of air, there was a larger increase in the intensity of the tyrosyl radical signal from the extract of gallium treated cells than the control. Incubation of the cell free extracts with millimolar concentrations of gallium citrate for 30 minutes diminished the intensity of the tyrosyl radical signal. The tyrosyl radical signal was regenerated to its original intensity upon addition of millimolar concentrations of exogenous iron. This suggests that one of the inhibitory effects of gallium on the enzyme, is a direct one, at the level of the bridged iron in the ribonucleotide reductase. Moreover, immunoprecipitation of the ^{59}Fe labeled M2 subunit of ribonucleotide reductase with the antibody against the M2 subunit shows a release of the

iron from the M2 protein in the presence of gallium. This is in strong support to the ESR data indicating the direct effect of gallium on the M2 subunit of ribonucleotide reductase.

A. Introduction

Gallium, a group IIIA metal, has recently gained clinical importance as a pharmacologic agent for the treatment of hypercalcemia and certain malignancies (94,95). Although gallium is not a transition element, many aspects of its chemistry resemble those of iron. The ionization potentials, ionic radii, and the coordination number of the aqueous +3 cations are similar for both metals. The remarkable similarity between gallium and iron allows for the interaction of gallium with various iron-containing proteins. It is known that gallium binds to the iron transport protein transferrin, resulting in stable transferrin-gallium complexes (96), which can be incorporated into cells via transferrin receptor-mediated endocytosis (81,97). The cytotoxicity of gallium can be enhanced significantly when cells are exposed to gallium as transferrin-gallium rather than gallium nitrate (98). In addition, exposure of cells to transferrin-gallium results in a decrease in iron uptake, an increase in cellular transferrin receptors and a decrease in ferritin content, findings consistent with cellular iron deprivation (98).

The redox reactivity of gallium is different from that of iron. The oxidation potential for Ga^{2+} to Ga^{3+} is 0.65 V (99). The +2 oxidation state for gallium exists but the most stable aqueous oxidation state is the +3 state.

The importance of iron in DNA synthesis is related in part to the activity of the enzyme ribonucleotide reductase, which catalyzes the conversion of ribonucleotides to deoxyribonucleotides. Mammalian ribonucleotide reductase consists of two non-identical subunits termed M1 and M2 (24). The M1 subunit contains the substrate and the effector binding sites while the M2 subunit contains non-heme bridged iron atoms and a tyrosyl free radical, which gives a characteristic signal on ESR spectroscopy (8). The activity of ribonucleotide reductase is closely linked to the tyrosyl radical and the presence of iron. Removal of this iron results in the loss of both the tyrosyl radical ESR signal and enzyme activity (6,8).

In prior studies, it has been shown that exposure of HL60 cells to transferrin-gallium results in a decrease in deoxyribonucleotide pools and a loss of the tyrosyl radical ESR signal. This inhibited ESR signal can be restored by co-incubation of cells with hemin (100). To obtain a better insight into the mechanism of action of gallium, we have extended our earlier investigations to examine the direct effect of gallium on the tyrosyl radical in cell-free preparations and show that this effect can be modulated by the addition of exogenous iron. Furthermore, immunoprecipitation

studies of ^{59}Fe-labeled M2 protein from a hydroxyurea-resistant, ribonucleotide reductase over-expressing cell line suggest that gallium inhibits the M2 subunit of ribonucleotide reductase by displacing iron from the subunit.

B. Materials and methods

1. Materials - Gallium nitrate was obtained from Alfa products (Danvers, MA). Human transferrin, dithiothreitol (DTT), ferrous ammonium sulfate, thiocarbohydrazide and goat anti-rat IgG alkaline phosphatase conjugate were purchased from Sigma Chemical Co. (St.Louis, MO). Standard gallium (1010 μg/ml), sodium thiosulfate, potassium hydrogen phthalate and salicylaldehyde were obtained from Aldrich Chemical Company (Milwaukee, WI). Sodium fluoride, and sodium phosphate (mono and dibasic) were purchased from Fisher Scientific Co. (Fair Lawn, NJ). Tachisorb Rat IgG immunoadsorbent (goat antibody to rat IgG conjugated to Pansorbin Staphylococcus aureus cells) was obtained from Calbiochem (La Jolla, CA). Rat monoclonal antibody (MoAb) JB4 against the M2 subunit of mouse ribonucleotide reductase (32) was generously provided by Dr. Lars Thelander (University of Umeå, Sweden). $^{59}FeCl_3$ was obtained from New England Nuclear (Boston, MA), and ^{59}Fe-Tf was prepared as previously described

(98).

2. Cell culture and preparation of cell extracts - Murine leukemic L1210 cells were obtained from American Type Culture Collection (Rockville, MD) and were maintained in an atmosphere of 6% CO_2 at 37°C in RPMI 1640 medium containing 10% horse serum. Cell growth studies were performed in 1 ml multi-well plates in the presence of increasing concentrations of gallium nitrate or gallium citrate. Cell growth was determined after 72 hours of incubation. For ESR studies, large volumes of cells were required and cells were plated in 500 ml spinner flasks in the absence (control) or presence of 960 μM gallium nitrate. After an 18 hr incubation, cells (5×10^8/flask) were harvested, washed twice with ice-cold phosphate-buffered saline and cell homogenates were prepared as previously described for assay of ribonucleotide reductase enzyme activity in cell-free extracts (101). The final cytosolic sample containing ribonucleotide reductase was dialyzed against Tris-DTT buffer (0.02 M Tris-Cl, pH 7.4, containing 1 mM DTT) and concentrated using a Centricon 30 microconcentrator (Amicon Corporation, Danvers, MA). For immunoprecipitation studies (described below), a hydroxyurea-resistant subline of L1210 cells was developed by incubating cells step-wise in increasing concentrations of hydroxyurea. These cells were routinely maintained in medium containing 250 μM hydroxyurea and displayed growth kinetics equivalent to the

parental cell line. Consistent with reports by others (78,102), ribonucleotide reductase activity is increased in these cells.

3. **ESR spectroscopy** - After obtaining the initial ESR spectra of the tyrosyl free radical (in ribonucleotide reductase) of cytosolic preparations from control and gallium-treated cells, the samples were thawed and ferrous ammonium sulfate / gallium citrate was added to each sample. Following a 15 minute incubation at 37°C in air (30 min incubation for gallium citrate), the samples were frozen again and a second series of ESR measurements were made.

4. **Measurement of Gallium content in cells** - Gallium content in cells was determined using a modification of a previously described fluorometric method (103), which is based on the reaction of gallium with salicylaldehyde thiocarbohydrazone (SATCH). The reagent SATCH was synthesized by the condensation of salicylaldehyde with thiocarbohydrazide and a 1 mM SATCH solution was prepared in 100% ethanol (104). Following incubation with gallium nitrate, cells (1×10^8 cells) were washed with ice-cold PBS (10 mM sodium phosphate, pH 7.5, 150 mM NaCl) and centrifuged at 1000 rpm for 10 min. 5 ml of concentrated HNO_3 was added to the pellet and the sample digested in a round bottom flask in a reflux apparatus for 45 minutes with drop-wise addition of 5 ml of 30% H_2O_2.

After digestion, the samples were evaporated to a small volume (< 0.5 ml), cooled, neutralized with sodium hydroxide, and diluted to 10 ml with deionized water.

For determination of gallium content, varying concentrations of gallium standard (atomic absorption grade, 10 μg/ml) and cell digests were used. 0.3 ml of 0.1% sodium thiosulfate and 25 μl of 0.1% sodium fluoride were added to 250 μl sample (cell digest or gallium standard) and the mixture was incubated for 5 minutes at room temperature. The following reagents were then added: 1.6 ml 0.1 M potassium hydrogen phthalate buffer pH 2.3, 4 ml 100% ethanol, 1.2 ml of SATCH and deionized water to yield a final volume of 10 ml in each assay tube. The reaction mixture was incubated at room temperature for 30 minutes. The fluorescent intensity of each sample was then measured with a SPF-500 ratio spectrofluorometer (American Instrument Co., Silver Spring, MD) using an excitation wavelength of 395 nm and an emission wavelength of 445 nm. A standard curve was generated from the fluorescent intensities of samples containing known concentrations of gallium, and the gallium content in cell samples was determined from this curve. Cell digests from control cells (grown without gallium) were used as background blanks. A representative standard curve, fluorescent intensity vs gallium concentration is shown below. An R-squared value of 0.997 was obtained.

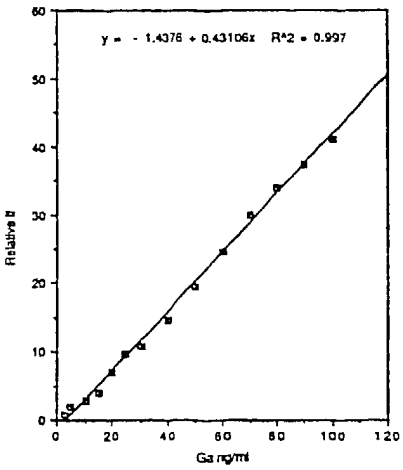

5. Detection of M2 protein by immunoblotting - Cytosolic extracts from cells incubated without or with 960 μM gallium were analyzed for M2 protein content by immunoblotting using a commercially available chromogenic immunoblotting assay (Immun-Blot Assay kit, Bio-RAD, Richmond, CA). Previous studies have established the use of MoAb JB-4 for detection of M2 protein by this method (105). 15 and 30 μg of total protein from the extracts were loaded onto BA83 nitrocellulose membrane using a 96-well Minifold apparatus (Schleicher and Schuell Inc., Keene, N.H.). After incubation of the membrane in blocking buffer (3% gelatin in 50 mM Tris, 100 mM NaCl, pH 7.5), M2 protein was detected by probing the membrane with buffer (1% gelatin, 50 mM Tris, 100 mM NaCl, pH 7.5) containing JB4 MoAb against the M2 protein, followed by incubation in buffer containing goat anti-rat IgG alkaline phosphatase conjugate. The membrane was then incubated in color development reagent according to the manufacturer's recommendations and the intensity of the color of the dots was compared. No color reaction was detected in control dots loaded with 50 μg bovine serum albumin.

6. Immunoprecipitation of ^{59}Fe-labeled M2 protein - To determine the interaction of gallium with the iron center of the M2 subunit of ribonucleotide reductase, cells or cell lysates were labeled with ^{59}Fe. In order to obtain sufficient ^{59}Fe cpm incorporation into the M2 protein, a hydroxyurea-resistant subline of L1210 cells possessing increased ribonucleotide reductase activity was used for these studies. Cells were labeled with ^{59}Fe under two conditions- a) Hydroxyurea-resistant L1210 cells were incubated for 18 h with ^{59}Fe-Tf in growth medium containing 1% horse serum. Cells were washed, homogenized, and the soluble cytosolic fraction containing ^{59}Fe-labeled proteins was used for immuno-precipitation; b) Unlabeled lysates from control cells were incubated with $^{59}FeCl_3$ for 15 minutes at 37°C in air, after which immunoprecipitation was carried out. Immunoprecipitation of the ^{59}Fe-labeled M2 protein was performed using a double antibody method. Samples were incubated without (control) or with 5 μg JB4 MoAb to mouse M2 protein for 90 minutes at 37°C. 1.1 volumes of Tachisorb (goat antibody to rat IgG) was then added and the incubation continued for an additional 45 min at room temperature. Following this, the tubes were centrifuged and the radioactivity in the pellet (representing ^{59}Fe-labeled M2 protein) was counted. Specific incorporation of ^{59}Fe into M2 was calculated by subtracting the ^{59}Fe cpm precipitated in control samples from the cpm immunoprecipitated by anti-M2 antibody. To examine the effect of gallium on ^{59}Fe bound to M2

protein, samples were incubated with 1 - 3 mM gallium citrate for 30 minutes at 37°C prior to immunoprecipitation. In separate experiments, it was determined that 3 mM gallium citrate did not interfere with the binding of the antibody to the M2 protein.

C. Results

1. Inhibition of cell growth by gallium - In prior studies, the growth-inhibitory effects of gallium were examined using either gallium nitrate or transferrin-gallium incubated with cells in culture medium. However, in initial studies examining the effect of gallium nitrate on the M2 tyrosyl radical ESR signal in cell-free extracts it was noted that the addition of millimolar concentrations of gallium nitrate resulted in the formation of precipitates in the sample. To avoid this problem, gallium citrate was used in the ESR studies involving direct addition of gallium salts to samples. To establish that gallium nitrate and gallium citrate were equivalent with respect to growth inhibitory effects, L1210 cells were incubated with increasing concentrations of both agents. Figure V.1 shows that both forms of gallium inhibited cellular proliferation in a similar manner. While marked inhibition was seen with low concentrations of gallium, cells retained a viability equal to control cells (95 -98% viability

as tested by trypan blue exclusion). At 100 μM gallium, there was a decrease in viability by 20% after 72 h of incubation.

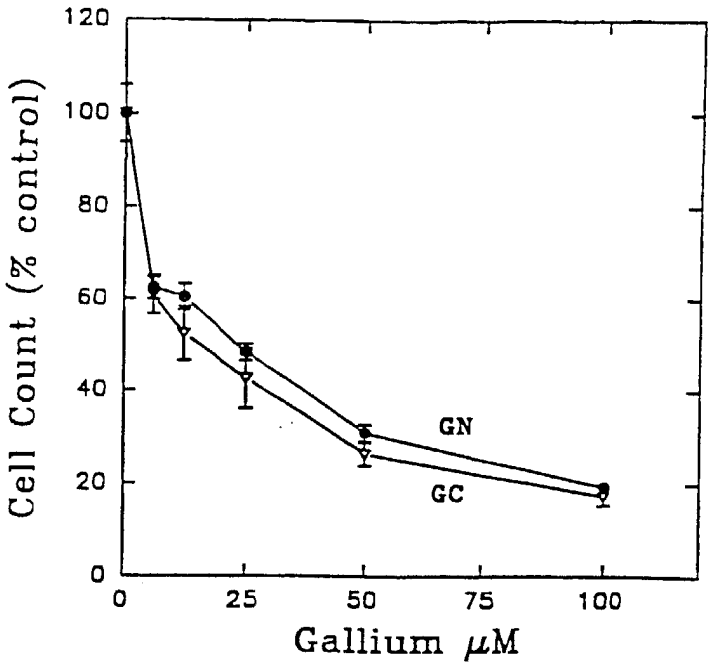

Fig V.1. Effect of gallium nitrate and gallium citrate on the growth of L1210 cells. Cell counts were performed after 72 h of incubation.

2. ESR studies on cytoplasmic extracts of cells incubated with gallium nitrate - For ESR studies, L1210 cells were incubated with 960 μM gallium nitrate for 18 hours and then analyzed. Cells exposed to this concentration of gallium for this duration retained a viability equal to control cells. Following an 18 hour incubation of cells with 960 μM gallium nitrate cytosolic extracts were analyzed by ESR spectroscopy. Figure V.2 shows that the M2 subunit tyrosyl radical signal in

the cytosol from cells incubated with gallium nitrate was decreased by >60%. Upon incubation of cytosols with increasing concentrations of ferrous ammonium sulfate for 15 minutes at 37°C, there was a progressive increase in the ESR signals from control and gallium-treated samples.

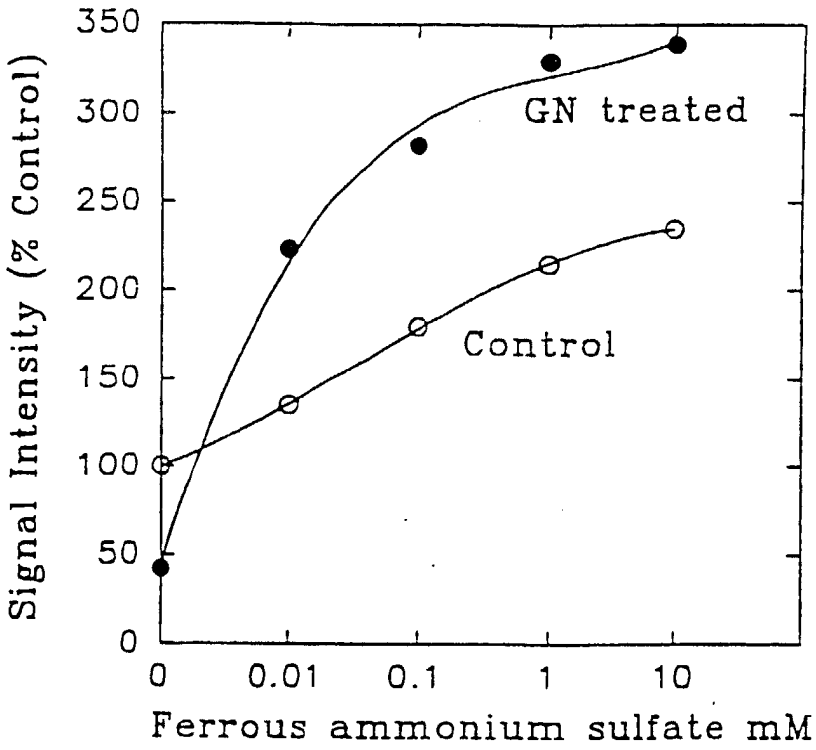

Fig V.2. Effect of iron on the relative intensity of the M2 tyrosyl radical ESR signal from cytoplasmic extracts of control and gallium-treated cells. After obtaining initial ESR spectra, samples were thawed and incubated with ferrous ammonium sulfate for 15 min at 37°C in air. Data shown represent ESR spectra obtained on the same samples following the consecutive addition of increasing concentrations of ferrous ammonium sulfate. The amplitude of the ESR spectrum of control cells prior to the addition of iron is expressed as 100% and all other values shown are relative to this.

Interestingly, the addition of FAS resulted in a larger increase in the intensity of the tyrosyl radical signal in the cytosolic extract from gallium-treated cells than in the control. A bi-phasic charateristic is evident for the titration curve of the gallium treated sample (Fig V.2). This could probably be due to two subpopulations of the protein, the first being independent M2 subunits, and the second being M1-M2 together as a unit. Under the experimental conditions used, the binding of added iron to M2 may be different for the two subpopulations present. The amount of the different subpopulations may then affect the rate of binding of iron to the M2 subunit in ribonucleotide reductase.

Figure V.3 shows the changes in the tyrosyl radical ESR spectra in cytosolic extracts following the addition of FAS and/or gallium citrate. The addition of 10 μM FAS to cytosolic extracts from gallium-treated cells resulted in recovery of the tyrosyl radical ESR signal (compare spectra A with B in Figure V.3). The addition of gallium citrate to the same sample resulted in a decrease in the amplitude of the signal (spectra C and D, Figure V.3); however, the ESR signal could again be restored to its prior level with further addition of FAS (spectrum E).

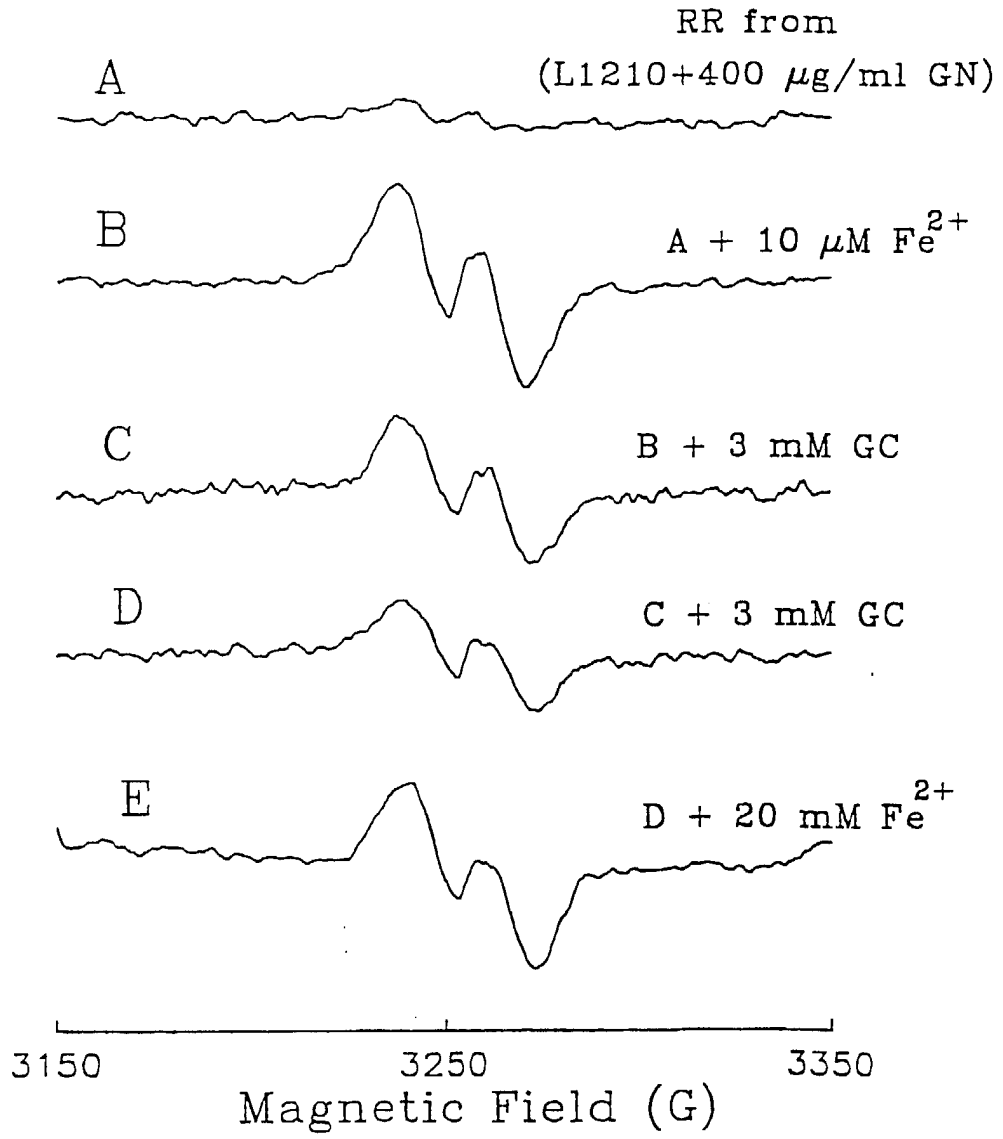

Fig V.3. Effect of sequential addition of iron and gallium on the M2 tyrosyl radical ESR signal: Cytoplasmic extracts were prepared from cells incubated for 18 hours with 960 μM gallium nitrate. A, B, C, D and E represent spectra obtained from the same sample. A, initial spectrum; B following the addition of ferrous ammonium sulfate; C and D, following the addition of gallium citrate; and E, following the addition ferrous ammonium sulfate. Note that the spectrum shown in A represents a signal which has been markedly inhibited by incubation of cells with gallium nitrate.

3. M2 protein content following incubation of cells with gallium nitrate - To verify that the decrease in the tyrosyl radical signal after the 18-hour incubation of cells with gallium did not result from a decrease in M2 protein content, cytosolic extracts from cells were analyzed for M2 protein by immunoblotting. As shown in Figure V.4, although incubation of cells with gallium nitrate resulted in a marked decrease in the M2 tyrosyl radical ESR signal, the M2 protein content of these cells remained comparable to that of controls.

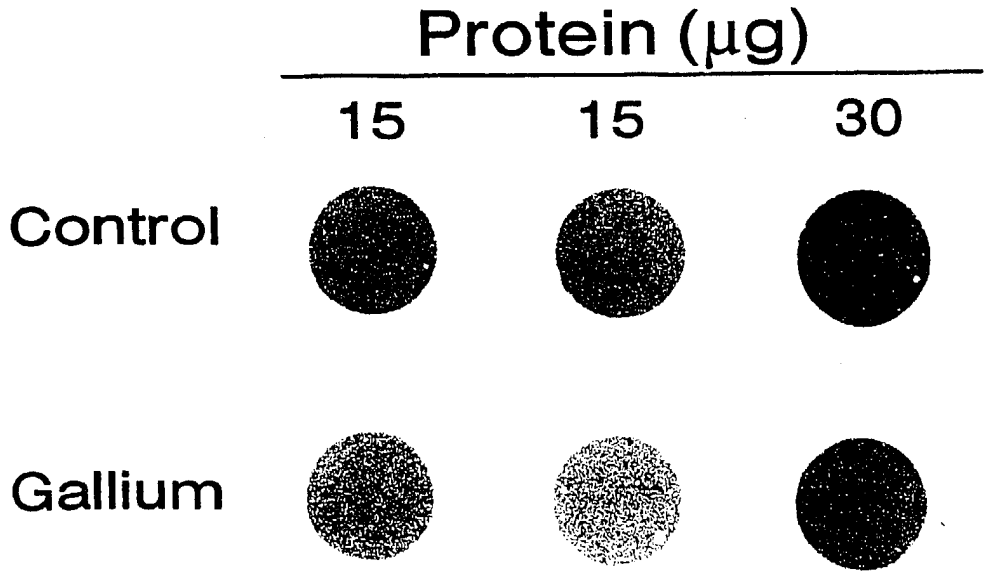

Fig V.4. Comparison of M2 protein content of control and gallium-treated cells: Cytoplasmic extracts prepared from cells incubated for 18 hours without or with 960 µM gallium nitrate were loaded onto nitrocellulose filter and were analyzed for M2 protein by immunoblotting using an anti-M2 MoAb as the probe.

4. ESR studies on cell-free extracts from control cells - The studies described above were performed on cytosolic extracts from cells that had been incubated with gallium nitrate for 18 hours and displayed a baseline decrease in the ESR signal. To examine the effect of gallium on the tyrosyl radical signal from cells not previously exposed to gallium, increasing concentrations of gallium citrate were added sequentially to the cytosolic extract of L1210 cells. As shown in Figure V.5, a progressive diminution in the intensity of the M2 tyrosyl radical signal was seen with the addition of gallium citrate. A 60% inhibition of the ESR signal was seen with 16 mM gallium citrate (not shown). Figure V.5 also shows that the inhibitory effect of 9 mM gallium on the tyrosyl radical was reversed with the addition of 20 mM ferrous ammonium sulfate to the sample. These studies, utilizing cytosolic extracts from both gallium-treated and control cells, suggest that the inhibitory effect of gallium on the M2 subunit tyrosyl radical involves interaction with the iron center of the M2 protein.

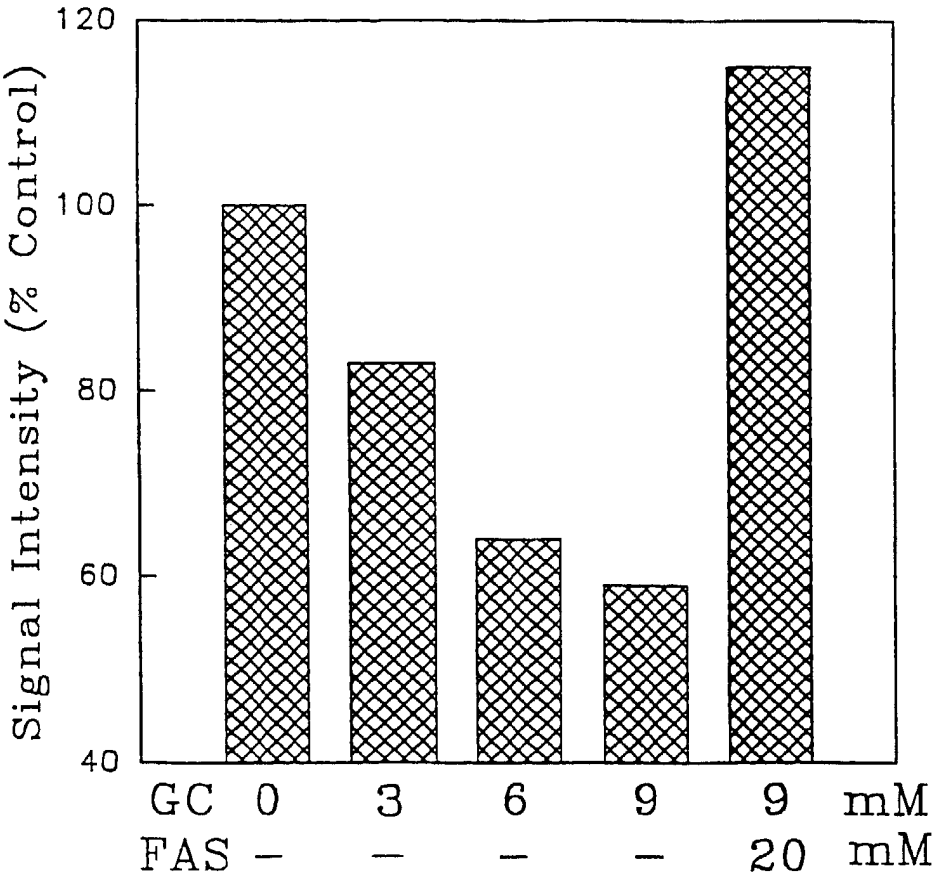

Fig V.5. Effect of gallium on the M2 tyrosyl radical ESR signal from cytoplasmic extracts of L1210 cells: Cytoplasmic extracts were prepared from cells grown in the absence of gallium nitrate. As in the previous experiments, increasing concentrations of gallium citrate were added to the same sample. Note that 100% signal intensity (control) represents the amplitude of the tyrosyl radical signal from cytoplasmic extracts of control L1210 cells grown without iron or gallium added to the medium.

5. Cellular concentration of gallium - From the above studies it can be seen that millimolar amounts of exogenous gallium citrate were required for inhibition of the ribonucleotide reductase M2 tyrosyl radical signal. Since the ESR studies were performed on concentrated cytosolic extracts representing ribonucleotide reductase from 5 x 10^8 cells, it was important to determine whether the amount of gallium used in these studies correlated with the amount of gallium actually incorporated into cells. Gallium citrate is more stable than gallium nitrate [log K_i=10.02 for the reaction Ga^{3+} + Cit^{2-} giving Ga-Cit^- (106)]. Therefore, the Ga^{3+} ion available for the inactivation of the M2 subunit (during the 30 minute incubations of cytosol) would be less with gallium citrate than with gallium nitrate (but gallium citrate was used instead of the nitrate to avoid precipitation of gallium as $Ga(OH)_3$). Measurement of the gallium content of packed cells (5 x 10^8 cells/ml) after 18 hours of incubation with 960 μM gallium nitrate revealed a gallium concentration of 2.1 ± 0.45 mM (mean ± S.E.). Hence the amount of gallium incorporated into cells is sufficient to inhibit the tyrosyl radical signal.

A comparison of the intracellular concentrations of gallium of different cell lines upon incubation of the cells with the same amount of gallium in the medium was found to be different. Incubation of HL60 cells in medium containing 960 μM gallium nitrate for 18 hours showed a gallium concentration

of 219.9 ± 13.9 mM (Mean ± 1 S.D) for 5 X 10^8 cells per milliliter; incubation of cells with 480 μM gallium in the medium gave 42.2 ± 1.5 mM gallium for packed cells; incubation with 240 μM gallium in the medium gave 0.3 ± 0.05 mM gallium for 5 X 10^8 cells/ml. Similar measurements using CCRF-CEM cells, showed a gallium concentration of 4.4 ± 1.1 mM (for 5 X 10^8 cells/ml) when these cells were incubated in a medium containing 240 μM gallium. For 480 μM and 960 μM gallium in the medium, CCRF cells took up 50.7 ± 9.5 mM and 184 ± 30.5 mM gallium (for 5 X 10^8 cells/ml) respectively.

6. Effect of gallium on ^{59}Fe-labeled M2 subunit of ribonucleotide reductase - To examine the effect of gallium on the iron center of the M2 protein, ^{59}Fe-labeled M2 protein was immunoprecipitated using a specific MoAb. M2 protein was labeled with ^{59}Fe by pulsing cytosolic extracts with ^{59}Fe in air at 37°c for 30 min (thus allowing for ^{59}Fe incorporation into the M2 subunit) or by incubating ^{59}Fe with cells for 18 hours. Figure V.6 shows that the amount of immunoprecipitable ^{59}Fe cpm (representing ^{59}Fe-bound to M2 protein) was decreased by gallium. 55% of the ^{59}Fe, which had been incorporated into M2 protein over an 18 hour incubation, was displaced from the M2 protein by 1 mM gallium citrate. 60% of the ^{59}Fe which had been incorporated into M2 protein during incubation with cellular cytosolic extracts was displaced by 3 mM gallium citrate. It is known that removal of iron from the M2 protein

results in loss of the tyrosyl radical and subsequent inactivation of ribonucleotide reductase (6,8). These immunoprecipitation studies therefore suggest that gallium inhibits the tyrosyl radical by displacing iron from the M2 protein.

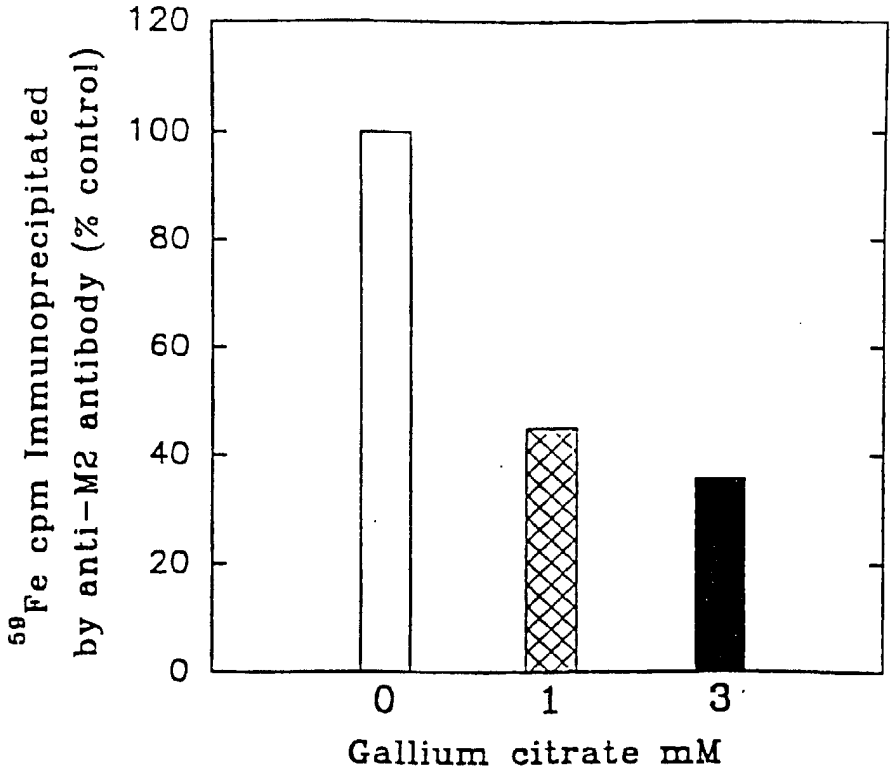

Fig V.6. Effect of gallium on the binding of ^{59}Fe to M2 protein: M2 protein in cell extracts or intact cells was labeled with ^{59}Fe as described in Methods. ^{59}Fe-M2 was immunoprecipitated with JB4 MoAb against the M2 subunit in the absence (control) or presence of gallium citrate. Open bar, 100% control, represents the specific ^{59}Fe cpm immunoprecipitated by antibody in the absence of gallium. Hatched bar, immunoprecipitation of ^{59}Fe-M2 labeled by incubation of ^{59}Fe with intact cells. Solid bar, immunoprecipitation of ^{59}Fe-M2 labeled by incubation of cell extracts with ^{59}Fe. A representative experiment is shown.

D. Discussion

Because of its important role in the synthesis of DNA precursors, ribonucleotide reductase is considered to be an attractive target enzyme for anti-neoplastic and anti-viral drugs. Intense investigation by a number of different groups has resulted in considerable advances in the understanding of this enzyme in mammalian and non-mammalian systems. Functionally active ribonucleotide reductase is composed of a large and a small dimeric subunit felt to exist in 1:1 stoichiometry. Studies of the enzyme in E. coli have shown that each monomer of the smaller subunit (termed B2 in bacteria) contains an iron center which is made up of 2 iron atoms linked by a μ-oxo bridge. The tyrosyl free radical is located at Tyr 122, 5.3 Å from the nearest iron (18). Full activity of the B2 subunit requires an intact iron center and an active tyrosyl radical. Loss of iron from this subunit results in loss of the tyrosyl radical and enzyme activity. Titration experiments under anaerobic conditions have suggested that the B2 subunit can exist as apoB2 which lacks the iron center and contains a nonradical tyrosine 122. With the addition of ferrous iron, apoB2 is converted to reduced B2 which, in the presence of oxygen, is converted to the fully active B2 containing ferric iron and an ESR detectable tyrosyl radical. Reduction of active B2 results in the formation of

metB2 which contains ferric iron but lacks the tyrosyl radical. MetB2 in turn, may either be further reduced or may lose its iron to yield reduced B2 or apoB2 respectively (87). It is felt that a similar situation may exist in mammalian systems with regard to the M2 subunit. Hence, the iron center of the B2/M2 subunit plays a critical role in the overall activity of the enzyme.

Studies of the M2 subunit of ribonucleotide reductase during the cell cycle have shown that the activity of this subunit increases several-fold as mouse mammary tumor cells enter S phase (22). Since iron is an essential component of the M2 subunit, it is important that sufficient intracellular iron be available to support its activity. The uptake of iron occurs through cell surface transferrin receptor-mediated endocytosis of transferrin-iron; and transferrin receptor expression increases during early S phase to ensure adequate delivery of iron for DNA synthesis (107). Chelation of iron by desferrioxamine results in inhibition of deoxyribonucleotide synthesis (108), while blockade of cellular iron uptake by certain anti-transferrin receptor monoclonal antibodies also inhibits cell growth (109), presumably through the same mechanism of decreased iron availability to the cell.

In earlier studies, we have shown that gallium inhibits the cellular uptake of iron (98,110) and the synthesis of dCDP and dADP in a direct assay of ribonucleotide reductase activity (101). Because gallium resembles iron in many

respects, the present study was undertaken to specifically examine the interaction of gallium with the iron-dependent M2 subunit of ribonucleotide reductase. Our studies show that the activity of the M2 tyrosyl radical is inhibited after exposure to gallium. Although maximum inhibition was seen after an 18 hour incubation of cells with gallium, direct addition of gallium to cytoplasmic extracts also led to inhibition of the tyrosyl radical ESR signal. In both situations, the radical signal could be restored by the addition of exogenous ferrous iron in the presence of air. Immunoblotting of cytoplasmic extracts after the 18 hour incubation of cells with gallium nitrate showed that both control and gallium-treated cells contained comparable amounts of M2 protein. Hence, the decrease in the tyrosyl radical signal following incubation with gallium was not the result of a decrease in M2 protein in cells.

When gallium citrate was added directly to cytoplasmic extracts containing an active tyrosyl radical, a reduction in the intensity of the radical ESR signal was seen. With the addition of iron, the tyrosyl radical signal was restored to its previous level thus indicating that the inhibitory effect of gallium involved an interaction with the iron center of M2. This conclusion was further confirmed by the immunoprecipitation studies which demonstrated that gallium was able to displace ^{59}Fe from radiolabeled M2. These studies, taken together, suggest strongly that the M2 protein present

in cells after incubation with gallium exists mainly as inactive apoM2 or as an inactive form containing gallium in place of iron (or a combination or both). Either situation would result in a loss of the tyrosyl radical ESR signal and an inhibition of overall enzyme activity. It still remains to be conclusively shown that gallium directly takes the place of iron in the M2 subunit.

In conclusion, our studies have further elucidated the mechanism of inhibition of ribonucleotide reductase by gallium and have underscored the importance of iron in DNA synthesis. Others have shown synergistic inhibition of cell growth with combinations of agents directed against both subunits of ribonucleotide reductase (111). Similarly, we have shown that gallium acts synergistically with other inhibitors of ribonucleotide reductase to block the growth of leukemic cells in vitro (100,112). The development of optimal chemotherapeutic strategies to inhibit ribonucleotide reductase may result in better control of malignant cell growth and may lead to further advances in the treatment of patients with cancer.

VI. STUDIES USING COMBINATION OF AGENTS

A. Introduction

The ultimate goal of cancer chemotherapy is to achieve selective killing of tumor cells which results in the cure of malignant diseases. Due to the heterogeneity within the tumor cell population, complete cure with a single chemotherapeutic agent is very rare. Moreover, development of resistance to an agent is a major problem encountered with single-drug therapy. Hence, combination chemotherapy is widely accepted for the treatment of certain malignancies. The drugs used in combination can be selected based on specificity for different metabolic targets and different phases of the cell cycle. Drug combinations which include a ribonucleotide reductase inhibitor (IMPY/desferal) and a DNA polymerase inhibitor (aphidicolin) have been used to show synergistic inhibition of leukemic cell growth (34). Ribonucleotide reductase-specific inhibitors (such as hydroxyurea, IMPY and MAIQ) in combination with cytosine arabinoside (araC) or fluoropyrimidines have also been shown to inhibit synergistically the growth of certain tumor cells (34).

Ribonucleotide reductase catalyzes the critical step which is required for DNA synthesis and hence cellular proliferation. Due to its critical role in DNA replication,

ribonucleotide reductase makes an excellent target for chemotherapy. Several different classes of compounds have been shown to be relatively specific inhibitors of ribonucleotide reductase. Certain combination of agents [such as IMPY (M2 effector) plus dGTP (M1 effector); or IMPY plus dATP] have been used to inhibit the activity of ribonucleotide reductase more efficiently than a single inhibitor. Cory et al. have performed such studies using various combinations (such as IMPY/EDTA; IMPY/desferal; MAIQ/desferal) of ribonucleotide reductase inhibitors directed at the individual subunits of the enzyme (34,35).

Iron chelating agents have also been used in combination with the specific inhibitors of ribonucleotide reductase. Desferal has been shown to potentiate the inhibitory effect caused by hydroxyurea and IMPY on isolated ribonucleotide reductase. These combinations were shown to result in synergistic inhibition of tumor cell growth, by specific action on the M2 subunit of ribonucleotide reductase (113).

Deoxyadenosine in combination with EHNA [erythro-9-(2-hydroxy-3-nonyl)adenine] resulted in synergistic inhibition of L1210 cell growth (113). The specific inhibition of adenosine deaminase (an enzyme that deaminates deoxyadenosine to deoxyinosine) activity by EHNA results in the accumulation deoxyadenosine, which in turn leads to the accumulation of sufficient levels of dATP necessary for the feedback inhibition of ribonucleotide reductase (113). The combination

deoxyguanosine/8-aminoguanosine results in inhibition of cell growth via accumulation of dGTP which results in the feedback inhibition of ribonucleotide reductase (113) (8-Amino-guanosine is a specific inhibitor of purine nucleoside phosphorylase, an enzyme which degrades deoxyguanosine to guanine and deoxyribose-1-phosphate). The above mentioned combination is targeted at the effector binding M1 subunit of ribonucleotide reductase. The set of M1 subunit effectors (deoxyadenosine/EHNA) when combined with the agents targeted at M2 (hydroxyurea / desferal), was shown to inhibit tumor cell growth in a synergistic manner (114). The concentration of the individual drugs used in a combination scheme was much less than that used when administered independently. Thiosemicarbazones (also inhibitors of the enzyme via M2 subunit), in combination with dATP, dGTP or dTTP (M1 effectors) was shown to inhibit the enzyme in an additive fashion (114).

Fludarabine phosphate (2-fluoro-ara AMP), an inhibitor of DNA synthesis through the action on the M1 subunit of ribonucleotide reductase and on DNA polymerase, was shown to potentiate the growth-inhibitory effects of gallium nitrate (112). Studies using transferrin-gallium and hydroxyurea showed synergistic inhibition of HL60 cell growth when the two agents were used in combination (100). In the present study, the direct effect of combination of gallium and hydroxyurea on the tyrosyl free radical signal intensity was examined.

A combination of CuL and radiation (with X-rays) was tested on the survival of synchronous and asynchronous Chinese hamster ovary (CHO) cells, which suggested an additive interaction (82).

B. Results

1. Effect of gallium in combination with hydroxyurea on the tyrosyl free radical signal from ribonucleotide reductase - In order to study the direct effect of the combination Gallium/hydroxyurea on ribonucleotide reductase, the tyrosyl free radical signal obtained from cell free extracts (from CCRF-CEM cells) was monitored as a function of concentration of gallium nitrate, hydroxyurea and of the combination. It is seen from figure VI.1 that a combination of the agents gives rise to an additive effect of inhibition of the tyrosyl radical than either one alone, especially at lower concentrations of both the agents. In this experiment, after obtaining the intrinsic tyrosyl radical ESR signal at 77 K, the cytosols (prepared as mentioned in the METHODS section from CCRF-CEM cells) were incubated with gallium nitrate, hydroxyurea or a combination of the two agents for 30 min at 37°C. The samples were frozen (in precision bore tubes) to measure the tyrosyl radical signal. It is evident from this figure that gallium nitrate is more effective than gallium citrate (compare with Fig V.5.) in reducing the tyrosyl radical of ribonucleotide reductase from cell free extracts. This is due to the stability of gallium citrate (explained earlier) as compared to that of gallium nitrate.

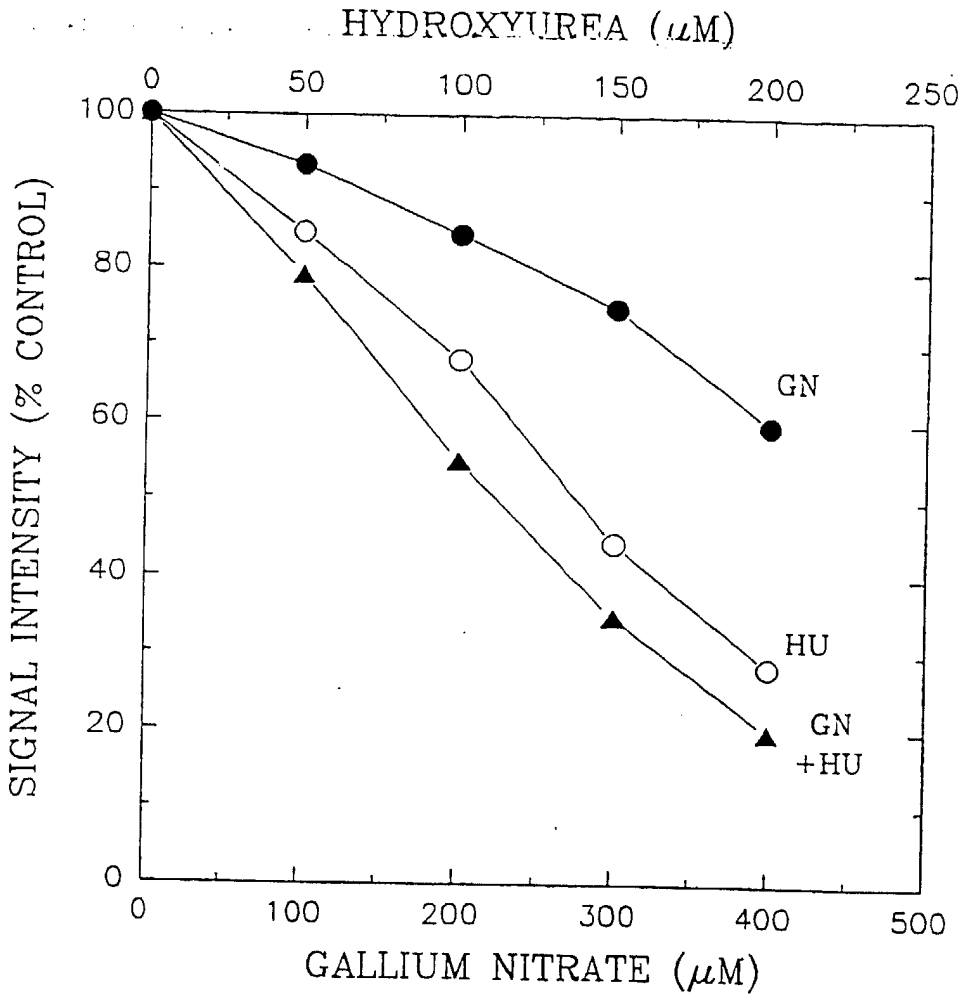

Fig VI.1. Effect of combination of gallium and hydroxyurea on the tyrosyl free radical ESR signal intensity from CCRF cytosol. The peak to trough height of the signal from the control sample is taken to be 100%. The concentrations of gallium nitrate and hydroxyurea are indicated on the bottom and top abscissa respectively. Three samples from the same preparation were used in this study. The samples were incubated at 37°C for 30 minutes in a water bath with gallium nitrate or hydroxyurea or a combination of the two agents, and then frozen in precision bore tubing for ESR measurements. The spectrometer conditions used for obtaining the spectra and the number of scans averaged was the same in each case. The changes in the sample volume during freezing and thawing were taken into account.

2. The effect of combination of gallium and hydroxyurea on ribonucleotide reductase enzyme activity - The functional assay for the enzyme showed inhibition of the enzyme activity in the presence of gallium alone. In combination with hydroxyurea (at concentrations that did not inhibit the enzyme activity when used independently), gallium showed a greater inhibition of the enzyme than when used alone (Fig VI.2).

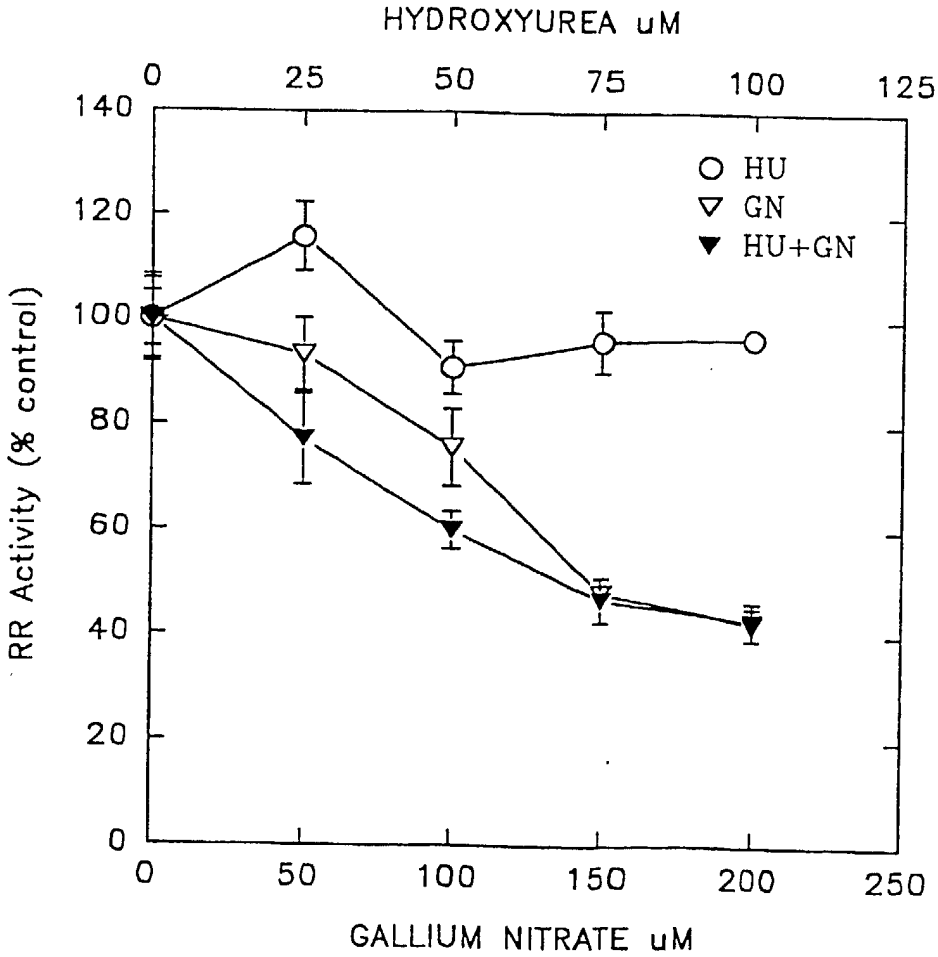

Fig VI.2. Ribonucleotide reductase activity as a function of concentration of gallium nitrate and hydroxyurea. The error bars represent standard deviation of triplicate values. Gallium and hydroxyurea were added to the assay mixtures before the addition of substrate which initiates the reaction.

3. Effect of hydroxyurea and deferoxamine on the tyrosyl free radical from ribonucleotide reductase - A reduction in the ESR signal intensity of the tyrosyl radical was seen upon incubation of cell lysates (from CCRF-CEM cells) with deferoxamine for 30 min at 37°C. In combination with hydroxyurea, the reduction in the signal was more than that caused by either reagents alone, as seen in figure VI.3. An additive effect was seen for 20 μM DFX plus 200 μM HU.

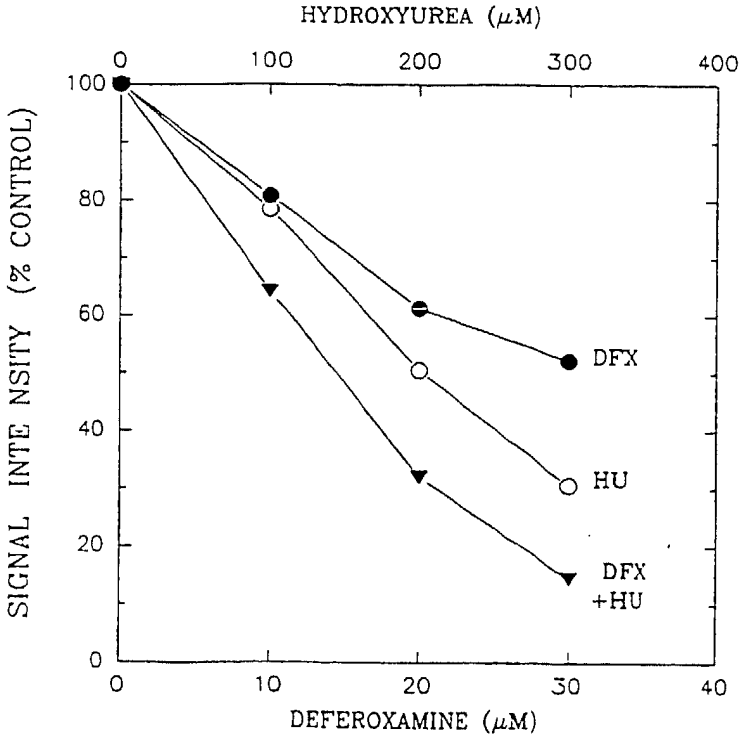

Fig VI.3. Tyrosyl free radical signal intensity vs concentrations of hydroxyurea and deferoxamine. The intrinsic tyrosyl radical of ribonucleotide reductase from cytosolic preparations of CCRF-CEM cells were first measured at 77 K; the samples were thawed and incubated with the reagents for 30 minutes and then frozen for ESR measurements. The peak to trough height of the signal from the control sample (before addition of agents) was taken as 100%.

C. Discussion

The effect of combining two or more agents directed at ribonucleotide reductase has previously been shown to be more effective than the use of a single agent. The synergistic inhibitory effect of a combination of gallium nitrate and hydroxyurea on HL60 cell growth has already been demonstrated (100). In this study, potentiation of the inhibitory effect at the level of the M2 subunit of ribonucleotide reductase is seen upon combination of these agents by monitoring the reduction in the tyrosyl free radical signal. Gallium was shown to displace the iron from the M2 subunit of ribonucleotide reductase using immunoprecipitation studies of the ^{59}Fe labeled protein. A reduction or the removal of the iron in the iron center of the M2 subunit would lead to a loss of the tyrosyl radical located in its vicinity. Previously published work has shown that hydroxyurea treatment leads to the formation of the met form of the M2 subunit (115) wherein the iron center is intact but the tyrosyl radical is lost. Thus, by combining gallium with hydroxyurea, both the iron center and the tyrosyl radical of the M2 subunit are targeted simultaneously to give a greater inhibition of ribonucleotide reductase. This effect is observed in figure VI.1, where a combination of gallium and hydroxyurea leads to greater reduction in the tyrosyl radical signal than with either

reagent alone. The synergistic inhibitory effect on cell growth (100) is then explained by the inhibition of cellular iron uptake by gallium (110), and the direct action of gallium and hydroxyurea on the M2 subunit of ribonucleotide reductase.

The growth inhibitory effect of gallium nitrate on HL60 cells was shown to be reversed by coincubating the cells with deferoxamine (112). This was shown to be due to the inhibition of cellular uptake of gallium caused by the iron chelating agent. However, sequential incubation of cells with gallium nitrate and the iron chelators indicated a potentiation of the growth inhibitory effects of gallium (112). A study of the direct effect of gallium and deferoxamine on the tyrosyl free radical from cell lysates would require the removal of gallium from the samples before incubation with deferoxamine. Gallium may chelate to deferoxamine resulting in complex formation, thereby reducing the effective concentration of deferoxamine available to chelate the iron from the M2 subunit of ribonucleotide reductase.

In the presence of desferal, the concentration of hydroxyurea required to completely inhibit cell growth was shown to be markedly reduced (114). In the experiment depicted in figure VI.3, it is seen that a combination of deferoxamine and hydroxyurea produced an additive effect on the inhibition of the tyrosyl radical from cell free extracts than either reagent alone; indicating the direct effect on the

iron center and the tyrosyl radical in the M2 subunit in ribonucleotide reductase. The binding constant for iron to the met form of M2 (formed upon treatment of M2 with hydroxyurea) is probably less than that for deferoxamine.

A number of iron chelators (such as desferal, EDTA) can act as potent inhibitors of cellular proliferation. The treatment using a combination of agents, which leads to a perturbation of cellular iron metabolism and ribonucleotide reductase, is an important strategy in the control of tumor cell growth.

VII. SUPPLEMENTARY MATERIAL

A. Resistance to hydroxyurea

Hydroxyurea is a clinically useful drug for the treatment of malignancies (116). It inhibits ribonucleotide reductase by reducing the tyrosyl radical in the M2 subunit (11,38). Kinetic studies of inactivation of the tyrosine radical in B2 subunit using UV-Vis spectrophotometry indicated that hydroxyurea reduced the tyrosine radical (410 nm peak) with a second-order rate constant of 0.44 $M^{-1}s^{-1}$ (38).

The development of drug resistance to hydroxyurea is complex and varied. It has been shown that there is first an amplification of the M2 gene followed by an increase in M2 mRNA (115,117). With resistance to increasing concentrations of hydroxyurea, there is an increase in the M2 synthesis and the accumulation of higher concentrations of M2 protein. M1 protein is either unchanged or only modestly increased (115).

1. Description of hydroxyurea-resistant L1210 cells - The L1210 cells were grown in increasing concentrations of hydroxyurea (50, 100, 250 μM) in (1 ml) 24 well plates. They were then transferred to tissue culture flasks (10 ml), where they were constantly maintained in RPMI-1640 media (supplemented with 10% donor horse serum) containing 250 μM

hydroxyurea. After these cells reached growth levels equivalent to that of control L1210 cells, they were tested for resistance to growth inhibition by hydroxyurea. The control and hydroxyurea-resistant L1210 cells were plated in 24 well plates at a cell density of 5 X 10^4 cells/ml in the absence or presence of different concentrations of hydroxyurea. The cell counts were taken after incubation for 72 hours in a 37°C incubator. A plot of the cell count as a function of hydroxyurea concentration for control and resistant L1210 cells is shown in figure VII.1.

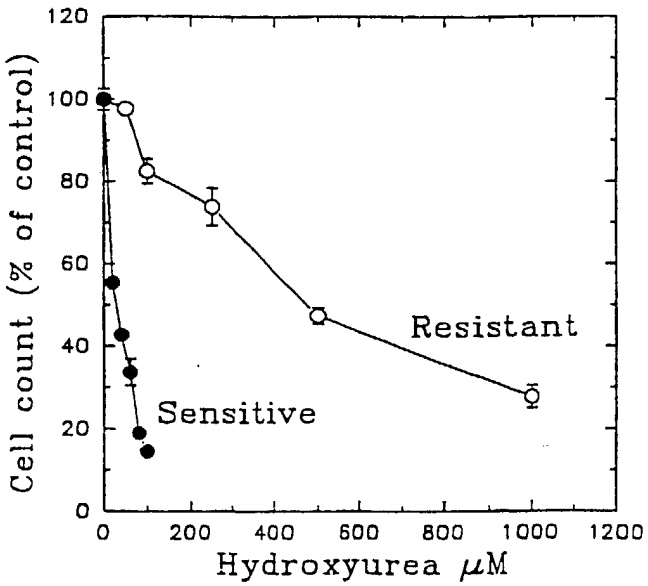

Fig VII.1. Growth of hydroxyurea-sensitive (control) and resistant L1210 cells in the presence of hydroxyurea.

It is seen from this plot that the hydroxyurea-resistant cells are about 16 times more resistant to the growth inhibition by hydroxyurea than the control cells. The concentration of hydroxyurea that brought about a 50% inhibition of cell growth

was found to be 29 μM for the control cells and 474 μM for the resistant cells. The viability (as detected by trypan blue exclusion) of both the cell lines was found to be greater than 90% even in the presence of the highest concentrations of hydroxyurea used in each case for the 72 hour incubation.

2. Ribonucleotide reductase in hydroxyurea-sensitive and resistant L1210 cells - The ESR signal from the tyrosyl radical of the M2 subunit of ribonucleotide reductase is markedly increased in hydroxyurea-resistant L1210 cells, as shown in figure VII.2.

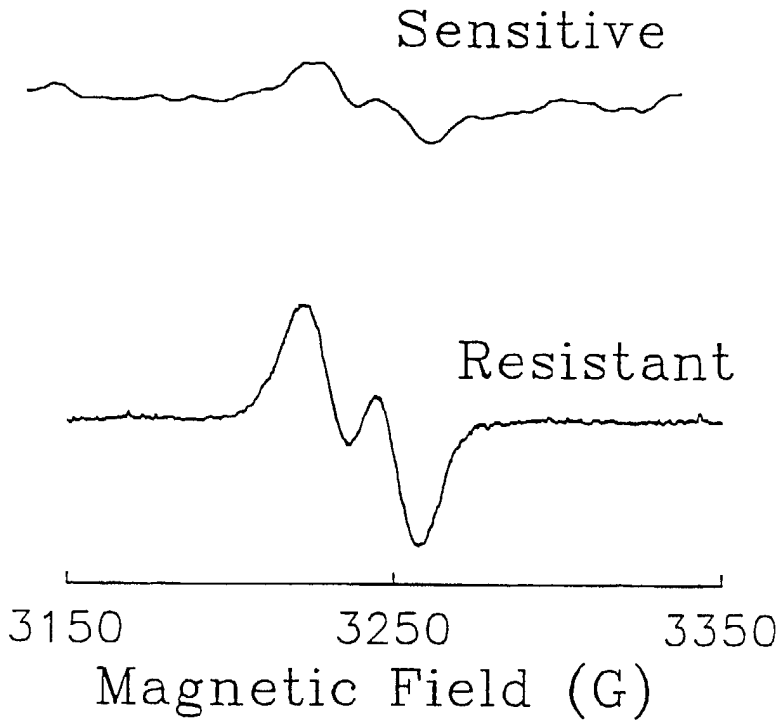

Fig VII.2. Tyrosyl free radical ESR signal in hydroxyurea-sensitive and resistant L1210 cells.

Cell free extracts prepared from hydroxyurea-sensitive and

resistant L1210 cells were used for the ESR measurement. Under conditions of equal cell growth, the ribonucleotide reductase activity (measured by the conversion of the radiolabeled ^{14}C-CDP to deoxyCDP) is approximately six-fold higher in hydroxyurea-resistant cells as compared to that in sensitive cells.

3. Comparison of the effect of gallium nitrate on hydroxyurea-sensitive and resistant L1210 cells - Since both gallium and hydroxyurea targeted the M2 subunit of ribonucleotide reductase, it was interesting to see if gallium exhibited any cross resistance with hydroxyurea. The growth inhibitory effect of gallium nitrate on hydroxyurea-sensitive and resistant L1210 cells was examined (Fig VII.3). There was no marked difference in the inhibition of cell growth by gallium nitrate between control and hydroxyurea-resistant cells, except at high concentrations of gallium nitrate. This indicates that the mechanism of resistance to cell growth inhibition by gallium is probably different from that by hydroxyurea. The initial effect of inhibition of cellular iron uptake by gallium may play an important role in cellular growth inhibition at lower concentrations of gallium (< 20 μM). A combination of the inhibition of iron uptake and the direct action on the M2 subunit of ribonucleotide reductase could probably be the mode of action at higher concentrations of gallium (> 40 μM). This could then explain the differences

in the growth inhibitory effect at higher concentrations of gallium nitrate between the hydroxyurea-sensitive and resistant cells. Hydroxyurea-resistant cells, which express five to six-fold more ribonucleotide reductase activity than control cells, are therefore more resistant to gallium nitrate than hydroxyurea-sensitive cells at higher concentrations of gallium.

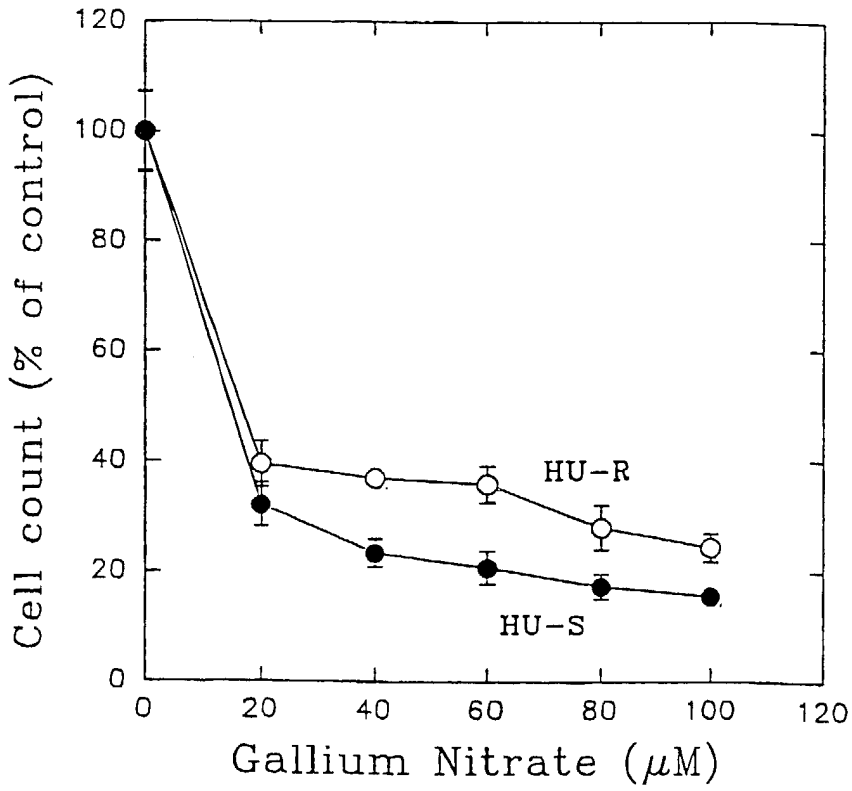

Fig VII.3. Effect of gallium nitrate on the growth of hydroxyurea-sensitive and resistant L1210 cells. 1 X 10^5 cells per milliliter were plated in 1 ml multi-well plates in the absence and presence of varying concentrations of gallium nitrate. After incubation at 37°C for 72 hours, the cells were counted using a hemocytometer. Their viability, checked using trypan blue exclusion, was greater than 90% even at high concentrations of gallium nitrate. The error bars represent the standard deviation of triplicate values.

The inhibition of the ribonucleotide reductase activity in the hydroxyurea-resistant cells by gallium nitrate was tested in a cell-free assay using ^{14}C-CDP and about 80% inhibition was observed at a concentration of 100 μM gallium nitrate (Fig VII.4). A comparison (has not been made per mg protein) with similar titration of gallium on ribonucleotide reductase activity from control L1210 cells would indicate the requirement of higher concentrations of gallium to inhibit the activity in the hydroxyurea-resistant cells. This would then be a reflection on the higher concentrations of the enzyme in the hydroxyurea-resistant cells as compared to that in control L1210 cells.

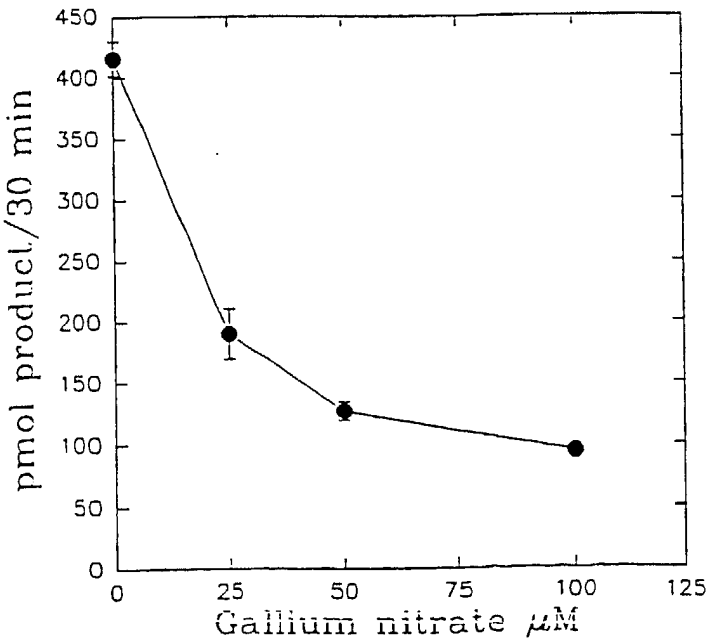

Fig VII.4. Effect of gallium nitrate on the enzymatic activity of ribonucleotide reductase.

B. Resistance to gallium nitrate

1. Studies on gallium nitrate-resistant cells - A subline of gallium nitrate-resistant HL60 cells was developed in Dr. Chitambar's laboratory to examine the mechanism of drug resistance to gallium. The gallium-resistant subline of HL60 cells was found to be about 29-fold more resistant to the growth inhibition by gallium nitrate than the sensitive parent line. An ESR study of the comparison of the tyrosyl free radical signal from the parent HL60 cells and the gallium-resistant subline showed that the active M2 subunit (containing an intact iron center and the tyrosyl radical) did not decrease upon treatment of the resistant cells with increasing concentrations of gallium nitrate, whereas a decrease in the signal was seen in the case of the parent cells (Fig. VII.5) (118).

Despite the increase in the cellular iron uptake by the gallium-resistant HL60 cells (118), the ferritin content was shown to be lower in the resistant cells as compared to the sensitive cells (118). The resistance to gallium nitrate in this subline of HL60 cells was mainly due to the ability to overcome the block in iron incorporation (through an increase in the number of transferrin receptors), and by trafficking the iron preferentially to a non-ferritin compartment, most likely to ribonucleotide reductase where it is needed for DNA

synthesis to maintain cellular proliferation.

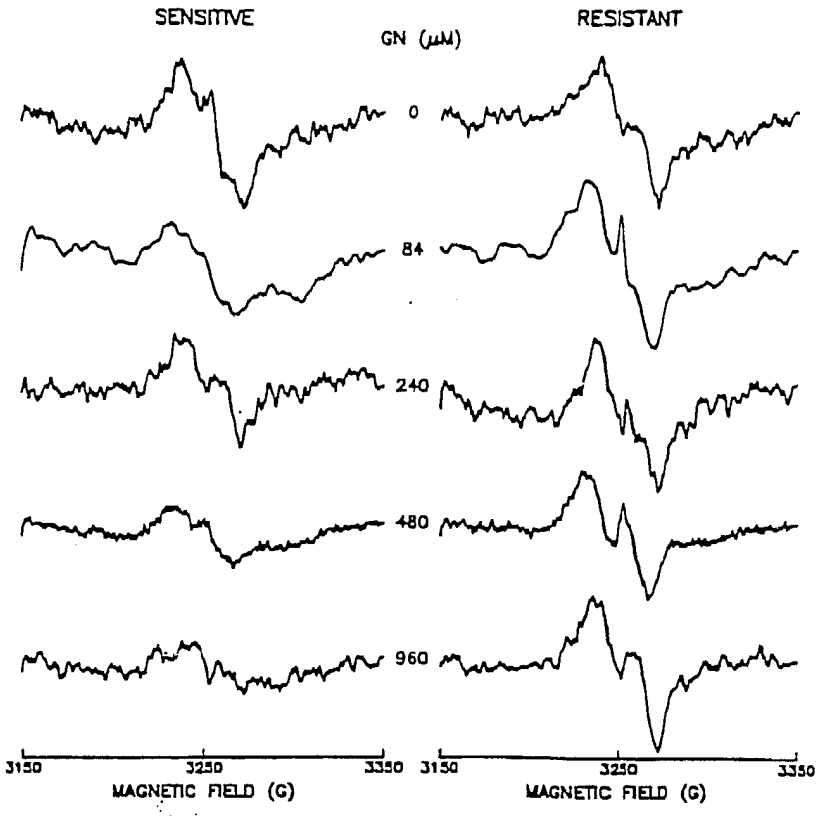

Fig VII.5. ESR spectra of the tyrosyl free radical of ribonucleotide reductase. Gallium nitrate-sensitive and resistant HL60 cells were harvested after 24 hours of exposure to 0-960 μM gallium nitrate. The gallium nitrate concentrations (GN) are indicated in the middle column. ESR measurements were performed at 77 K on frozen samples containing 5 X 10^8 cells. Spectrometer conditions: microwave frequency, 9.098 GHz; modulation amplitude, 5 Gauss; modulation frequency, 100 kHz; incident microwave power, 100 mW; gain, 8 X 10^4. Data represent the signal average of nine scans for each spectrum.

Comparison of the iron signals in gallium-sensitive and resistant HL60 cells by ESR measurements at 10 K indicated

differences in the distribution of iron among them (Fig. VII.6). The iron signals at very low fields (g=6.7 and 5.2) obtained from control HL60 cells resemble those from the high-spin ferric heme in, for example, the native PGH synthase (60). Upon fractionation of HL60 cells, the high-spin ferric heme signals were seen in the microsomal fractions (data not shown). The gallium-resistant cells showed the presence of other low field iron signals (g=6.0 and g=4.3), the source of which has not yet been identified. This in itself is evidence for the mobilization of (EPR detectable) iron by gallium in the gallium nitrate-resistant cells (maintained in growth medium containing gallium).

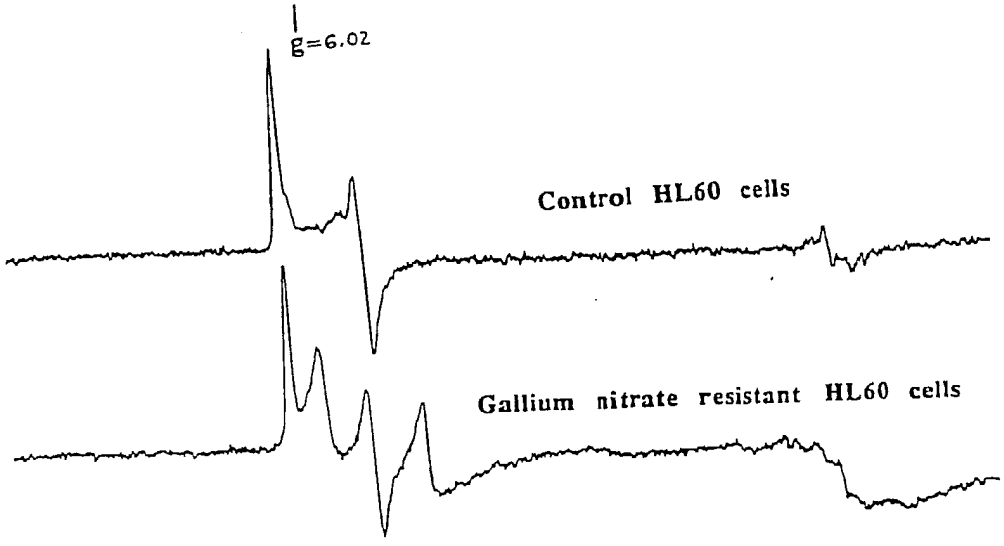

Fig VII.6. ESR detectable iron signals from the gallium-sensitive (control HL60 cells) and resistant HL60 cells at 11 K. Spectrometer conditions are: microwave power 100 mW, modulation amplitude 5 G, center field 2000 G, scan range 4000 G, time constant 0.128 sec, receiver gain 25,000, microwave frequency 9.188 GHz.

VIII. SUMMARY AND FUTURE WORK

Ribonucleotide reductase is a important enzyme which is absolutely essential for cellular proliferation. It is responsible for the conversion of ribonucleoside diphosphates to deoxyribonucleoside diphosphates, which are the substrates for DNA synthesis catalyzed by polymerase. The reaction catalyzed by ribonucleotide reductase is the rate limiting step in the process of DNA synthesis. Due to the absolute essentiality of this enzyme for cell proliferation, it has been a prime target for cancer chemotherapy by various chemical agents. The basis for cancer chemotherapy is to preferentially kill tumor cell growth over the normal cells. Combination chemotherapy has gained clinical importance due to the problem of development of resistance in single-drug therapy. Moreover, the heterogeneity within a tumor cell population favors the use of combination chemotherapy. The mammalian ribonucleotide reductase is comprised of two components (M1, the substrate and effector binding component; and M2, the non-heme and tyrosyl radical containing subunit) both of which have been shown to be required for catalysis in Navikoff hepatoma, rabbit bone marrow, Ehrlich tumor cells, human lymphoblasts and calf thymus (21). Proliferating cells (such as those mentioned above) found in embryonic tissues, transplantable hepatomas, and acute or chronic myelocytic

leukemias (119) contain elevated levels of ribonucleotide reductase activity relative to (control) normal tissues. The differences in the levels of ribonucleotide reductase activity between lymphocytes from normal and myelocytic leukemia patients (119) is the basis for targeting this enzyme in chemotherapy.

The effect of gallium and copper complexes on ribonucleotide reductase from human and murine leukemic cells was studied. The copper complex, CuL, showed redox reactivity in the cell membrane by formation of histidine-like and thiol-like adducts, followed by oxidation of thiols in the membranes, which then manifested in the inhibition of the iron uptake into cells. Following iron deprivation, CuL affects the key enzyme for cellular proliferation, ribonucleotide reductase (which requires intact iron center and tyrosyl free radical in its M2 subunit), by reducing M2 in ribonucleotide reductase, culminating in the inhibition of cell growth.

The gallium compounds, both gallium nitrate and gallium citrate, showed inhibition of growth of L1210 cells. A direct effect of gallium on the M2 subunit was shown by the reduction in the tyrosyl free radical signal upon incubation of cell-free extracts with gallium nitrate or citrate. This effect was then reversed by the addition of ferrous ion, suggesting the accumulation of apo-M2 in the presence of gallium. Immunoprecipitation of the ^{59}Fe labeled M2 protein showed the displacement of iron in the M2 by gallium, which would lead to

the loss of the tyrosyl radical in the vicinity of iron.

The combination of agents (gallium nitrate /hydroxyurea and deferoxamine/hydroxyurea), at certain concentrations, showed an additive inhibitory effect at the level of the reduction in tyrosyl radical from ribonucleotide reductase. The fact that these combinations exert a synergistic inhibitory effect on the cell growth (100), indicates that blockade of iron uptake in cells brought about by gallium and deferoxamine (chelation of iron by deferoxamine before it enters the cell) also plays an important role (along with the effect on ribonucleotide reductase) in the inhibition of cell growth.

The tyrosyl radical in ribonucleotide reductase can be used as an indicator of tumor response to various drugs, since the tyrosyl radical is related to the activity of the enzyme in proliferating cells. Lymphocytes from leukemic patients can be monitored for ribonucleotide reductase activity via the tyrosyl radical signal, and their response to different drugs can be studied. Comparison of the tyrosyl radical signal from lymphocytes of leukemic patients with that in normal subjects will be clinically useful. The proliferative capacity of the lymphocytes may well differ from one leukemic patient to another (cell proliferation of a given tumor may differ between patients). The measurement of the tyrosyl radical signal from these patients (lymphocytes or tumor tissue) as a function of time before and after treatment with drugs will

prove to be very useful, since one can predict the direction of progression of the disease (for better or for worse) and treat accordingly. An inhibition of the tyrosyl radical signal by drug treatment would translate to a much greater inhibition of DNA synthesis (in the population of cells being studied).

In order to look at the tyrosyl radical ESR signal from normal lymphocytes, about 50 ml of blood was drawn from a normal volunteer and ficoll separated to obtain the lymphocytes. It was then activated with a mitogen (PHA-phytohemagglutinin), after plating the lymphocytes in tissue culture flasks, for 72 hours. The cells were then washed in PBS and the cell pellet frozen in EPR tubes. Even at Q-band, (where an order of magnitude was gained in the signal to noise ratio) the tyrosyl radical signal from normal lymphocytes was not observed. This in itself is an indication of the low levels of active enzyme in the normal lymphocytes relative to leukemic ones. The use of Q-band (15-30 μl samples) to monitor the tyrosyl radical in ribonucleotide reductase (which correlates to the amount of active (M2) enzyme present) from normal and leukemic lymphocytes would enable the studies of development of single or multi-drug therapy at the preclinical level.

IX. REFERENCES

1. Weber, G. Biochemical strategy of cancer cells and the design of chemotherapy: G. H. A. Clowes memorial lecture. Cancer Res., *43*: 3466-3492, 1983.

2. Takeda, E. and Weber, G. Role of ribonucleotide reductase in expression of the neoplastic program. Life Sci., *28*: 1007-1014, 1981.

3. Elford, H.L., Freese, M., Passamani, E., and Morris, H.P. Ribonucleotide reductase and cell proliferation - Variations of ribonucleotide reductase activity with tumor growth rate in a series of rat hepatomas. J. Biol. Chem., *245*: 5228-5233, 1970.

4. Hogenkamp, H.P.C. and McFarlan, S.C. Nature and properties of bacterial ribonucleoside reductases. In: J.G. Cory and A.H. Cory (eds.), Inhibitors of ribonucleoside diphosphate reductase activity, pp. 17-36, New York: Pergamon Press. 1989.

5. Thelander, L. Reaction mechanism of ribonucleoside diphosphate reductase from Escherichia coli. Oxidation-reduction-active disulfides and the B1 subunit. J. Biol. Chem., *249*: 4858-4862, 1974.

6. Atkin, C.L., Thelander, L., Reichard, P., and Lang, G. Iron and free radical in ribonucleotide reductase. Exchange of iron and mossbauer spectroscopy of the protein B2 subunit of the Escherichia coli enzyme. J. Biol. Chem., *248*: 7464-7472, 1973.

7. Sjöberg, B-M., Reichard, P., Graslund, A., and Ehrenberg, A. Nature of the free radical in ribonucleotide reductase from Escherichia coli. J. Biol. Chem., *252*: 536-541, 1977.

8. Graslund, A., Sahlin, M., and Sjoberg, B-M. The tyrosyl free radical in ribonucleotide reductase. Environ. Health Perspect., *64*: 139-149, 1985.

9. Sealy, R.C., Harman, L., West, P.R., and Mason, R.P. The electron spin resonance spectrum of the tyrosyl radical. J. A. Chem. Soc., *107*: 3401-3406, 1985.

10. Bender, C.J., Sahlin, M., Babcock, G.T., Barry, B.A., Chandrashekar, T.K., Salowe, S.P., Stubbe, J., Lindstrom, B., Petersson, L., Ehrenberg, A., and Sjöberg, B-M. An ENDOR study of the tyrosyl free radical

in ribonucleotide reductase from Escherichia coli. J. Am. Chem. Soc., *111*: 8076-8083, 1989.

11. Petersson, L., Graslund, A., Ehrenberg, A., Sjöberg, B-M., and Reichard, P. The iron center in ribonucleotide reductase from Escherichia coli. J. Biol. Chem., *255*: 6706-6712, 1980.

12. Sahlin, M., Graslund, A., Petersson, L., Ehrenberg, A., and Sjoberg, B-M. Reduced forms of the iron-containing small subunit of ribonucleotide reductase from Escherichia coli. Biochemistry, *28*: 2618-2625, 1989.

13. Hendrich, M.P., Elgren, T.E., and Que, L.Jr. A mixed valence form of the iron cluster in the B2 protein of ribonucleotide reductase from Escherichia coli. Biochem. Biophys. Res. Commun., *176*: 705-710, 1991.

14. Sjöberg, B-M., Loehr, T.M., and Loehr, J.S. Raman spectral evidence for a μ-oxo bridge in the binuclear iron center of ribonucleotide reductase. Biochemistry, *21*: 96-102, 1982.

15. Sjoberg, B-M., Loehr, J.S., and Loehr, T.M. Identification of a hydroxide ligand at the iron center of ribonucleotide reductase by resonance raman spectroscopy. Biochemistry, *26*: 4242-4247, 1987.

16. Beck, W.F., Innes, J.B., Lynch, J.B., and Brudvig, G.W. Electron spin-lattice relaxation and spectral diffusion measurements on tyrosine radicals in proteins. J. Magn. Reson., *91*: 12-29, 1991.

17. Lynch, J.B., Garcia, C.J., Münck, E., and Que, L.Jr. Mössbauer and EPR studies of the binuclear iron center in ribonucleotide reductase from Escherichia coli- A new iron to protein stoichiometry. J. Biol. Chem., *264*: 8091-8096, 1989.

18. Nordlund, P., Sjöberg, B-M., and Eklund, H. Three-dimensional structure of the free radical protein of ribonucleotide reductase. Nature, *345*: 593-598, 1990.

19. Bollinger, J.Jr., Edmondson, D.E., Huynh, B.H., Filley, J., Norton, J.R., and Stubbe, J. Mechanism of assembly of the tyrosyl radical-dinuclear iron cluster cofactor of ribonucleotide reductase. Science, *253*: 292-298, 1991.

20. Elgren, T.E., Lynch, J.B., Garcia, C.J., Münck, E., Sjöberg, B-M., and Que, L.Jr. Electron transfer associated with oxygen activation in the B2 protein of

ribonucleotide reductase from Escherichia coli. J. Biol. Chem., *266*: 19265-19268, 1991.

21. Nutter, L.M. and Cheng, Y-C. Nature and properties of mammalian ribonucleoside diphosphate reductase. In: J.G. Cory and A.H. Cory (eds.), Inhibitors of Ribonucleoside Diphosphate Reductase Activity, pp. 37-54, New York: Pergamon Press. 1989.

22. Eriksson, S., Graslund, A., Skog, S., Thelander, L., and Tribukait, B. Cell cycle-dependent regulation of mammalian ribonucleotide reductase. J. Biol. Chem., *259*: 11695-11700, 1984.

23. Turner, M.K., Abrams, R., and Lieberman, I. Levels of ribonucleotide reductase activity during the division cycle of the L cell. J. Biol. Chem., *243*: 3725-3728, 1968.

24. Thelander, L. and Reichard, P. Reduction of ribonucleotides. Ann. Rev. Biochem., *48*: 133-158, 1979.

25. Luthman, M. and Holmgren, A. Glutaredoxin from calf thymus. Purification and properties. J. Biol. Chem., *257*: 6686-6690, 1982.

26. Moore, E.C. and Hurlbert, R.B. Regulation of mammalian deoxyribonucleotide biosynthesis by nucleotides as activators and inhibitors. J. Biol. Chem., *241*: 2802-2809, 1966.

27. Sahlin, M., Petersson, L., Graslund, A., Ehrenberg, A., Sjöberg, B-M., and Thelander, L. Magnetic interaction between the tyrosyl free radical and the antiferromagnetically coupled iron center in ribonucleotide reductase. Biochemistry, *26*: 5541-5548, 1987.

28. Aakerblom, L., Ehrenberg, A., Graslund, A., Lankinen, H., Reichard, P., and Thelander, L. Overproduction of the free radical of ribonucleotide reductase in hydroxyurea-resistant mouse fibroblast 3T6 cells. Proc. Natl. Acad. Sci. USA, *78*: 2159-2163, 1981.

29. Graslund, A., Ehrenberg, A., and Thelander, L. Characterization of the free radical of mammalian ribonucleotide reductase. J. Biol. Chem., *257*: 5711-5715, 1982.

30. Ochiai, E-I., Mann, G.J., Graslund, A., and Thelander, L. Tyrosyl free radical formation in the small subunit of mouse ribonucleotide reductase. J. Biol. Chem., *265*:

15758-15761, 1990.

31. Engstrom, Y., Rozell, B., Hansson, H.A., Stemme, S., and Thelander, L. Localization of ribonucleotide reductase in mammalian cells. EMBO J., *3*: 863-867, 1984.

32. Engstrom, Y. and Rozell, B. Immunocytochemical evidence for the cytoplasmic localization and differential expression during the cell cycle of the M1 and M2 subunits of mammalian ribonucleotide reductase. EMBO J., *7*: 1615-1620, 1988.

33. Sikorska, M., Brewer, L.M., Youdale, T., Richards, R., Whitfield, J.F., Houghten, R.A., and Walker, P.R. Evidence that mammalian ribonucleotide reductase is a nuclear membrane associated glycoprotein. Biochem. cell Biol., *68*: 880-888, 1990.

34. Cory, J.G. and Chiba, P. Combination chemotherapy directed at the components of nucleoside diphosphate reductase. In: J.G. Cory and A.H. Cory (eds.), Inhibitors of ribonucleoside diphosphate reductase activity, pp. 245-264, New York: Pergamon press. 1989.

35. Sato, A., Bacon, P.E., and Cory, J.G. Studies on the differential mechanisms of inhibition of ribonucleotide reductase by specific inhibitors of the non-heme iron subunit. Adv. Enzyme Regul., *22*: 231-241, 1984.

36. Cory, J.G., Lasater, L., and Sato, A. Effect of iron chelating agents on inhibitors of ribonucleotide reductase. Biochem. Pharmacol., *30*: 979-984, 1981.

37. Sahlin, M., Sjöberg, B-M., Backes, G., Loehr, T.M., and Loehr, J.S. Activation of the iron containing B2 protein of ribonucleotide reductase by hydrogen peroxide. Biochem. Biophys. Res. Commun., *167*: 813-818, 1990.

38. Lam, K-y., Fortier, D.G., Thomson, J.B., and Sykes, A.G. Kinetics of inactivation of the tyrosine radical of the B2 subunit of E.coli ribonucleotide reductase. J. Chem. Soc. ,Chem. Commun., 658-660, 1990.

39. Lam, K-y., Fortier, D.G., and Sykes, A.G. Redox reactivity of the tyrosine radical and FeIII2 of the B2 subunit of E.coli ribonucleotide reductase. J. Chem. Soc. ,Chem. Commun., 1019-1021, 1990.

40. Ehrenberg, A. and Reichard, P. Electron spin resonance of the iron-containing protein B2 from ribonucleotide reductase. J. Biol. Chem., *247*: 3485-3488, 1972.

41. Gerez, C. and Fontecave, M. Reduction of the small subunit of Escherichia coli ribonucleotide reductase by hydrazines and hydroxylamines. Biochemistry, *31*: 780-786, 1992.

42. Lepoivre, M., Chenais, B., Yapo, A., Lemaire, G., Thelander, L., and Tenu, J-P. Alterations of ribonucleotide reductase activity following induction of the nitrite-generating pathway in adenocarcinoma cells. J. Biol. Chem., *265*: 14143-14149, 1990.

43. Lepoivre, M., Fieschi, F., Coves, J., Thelander, L., and Fontecave, M. Inactivation of ribonucleotide reductase by nitric oxide. Biochem. Biophys. Res. Commun., *179*: 442-448, 1991.

44. Cosentino, G., Lavallee, P., Rakhit, S., Plante, R., Gaudette, Y., Lawetz, C., Whitehead, P.W., Duceppe, J-S., Franette, C.L., Dansereau, N., Guilbault, C., Langelier, Y., Gaudreau, P., Thelander, L., and Guindon, Y. Specific inhibition of ribonucleotide reductases by peptides corresponding to the C-terminal of their second subunit. Biochem. cell Biol., *69*: 79-83, 1991.

45. Climent, I., Sjöberg, B-M., and Huang, C.Y. Carboxyl-terminal peptides as probes for Escherichia coli ribonucleotide reductase subunit interaction: Kinetic analysis of inhibition studies. Biochemistry, *30*: 5164-5171, 1991.

46. Stubbe, J. Ribonucleotide reductases: amazing and confusing. J. Biol. Chem., *265*: 5329-5332, 1990.

47. Stubbe, J. Ribonucleotide reductases. Adv. Enzymol., *63*: 349-419, 1992.

48. Collins, S.J. . Blood, *70*: 1233, 1987.

49. Hyde, J.S., Newton, M.E., Strangeway, R.A., Camenisch, T.G., Froncisz, W. Electron paramagnetic resonance Q-band bridge with GaAs field effect transistor signal amplifier and low-noise Gunn diode oscillator. Rev. Sci. Instrum., *62*: 2969-2975, 1991.

50. Hyde, J.S., Gierula, M.P., Jesmanowicz, A., and Antholine, W.E. Pseudo field modulation in EPR spectroscopy. Appl. Magn. Reson., *1*: 483-496, 1990.

51. Hyde, J.S., Jesmanowicz, A., Ratke, J.J., and Antholine, W.E. Pseudomodulation: A computer based strategy for resolution enhancement. J. Magn. Reson., *96*: 1-13, 1992.

52. Steeper, J.R. and Steuart, C.D. A rapid assay for CDP reductase activity in mammalian cell extracts. Anal. Biochem., *34*: 123-130, 1970.

53. Cory, J.G. and Carter, G.L. Leukemia L1210 cell lines resistant to ribonucleotide reductase inhibitors. Cancer Res., *48*: 839-843, 1988.

54. Cory, J.G., Russell, F.A., and Mansell, M.M. A convenient assay for ADP reductase activity using Dowex-1-borate columns. Anal. Biochem., *55*: 449-456, 1973.

55. Berglund, O. and Eckstein, F. Synthesis of ATP- and dATP- substituted sepharoses and their application in the purification of phage-T4-induced ribonucleotide reductase. Eur. J. Biochem., *28*: 492-496, 1972.

56. Knorre, D.G., Kurbatov, V.A., and Samukov, V.V. General method for the synthesis of ATP gamma-derivatives. FEBS Lett., *70*: 105-108, 1976.

57. Hopper, S. Ribonucleotide reductase of rabbit bone marrow. Methods Enzymol., *51*: 237-246, 1978.

58. Harriman, A. Further comments on the redox potentials of tryptophan and tyrosine. J. Phys. Chem., *91*: 6102-6104, 1987.

59. Stubbe, J. Protein radical involvement in biological catalysis? Annu. Rev. Biochem., *58*: 257-285, 1989.

60. Karthein, R., Dietz, R., Nastainczyk, W., and Ruf, H.H. Higher oxidation states of prostaglandin H synthase- EPR study of a transient tyrosyl radical in the enzyme during the peroxidase reaction. Eur. J. Biochem., *171*: 313-320, 1988.

61. Kulmacz, R.J., Ren, Y., Tsai, A-L., and Palmer, G. Prostaglandin H synthase: Spectroscopic studies of the interaction with hydroperoxides and indomethacin. Biochemistry, *29*: 8760-8771, 1990.

62. Lassman, G., Odenwaller, R., Curtis, J.F., DeGray, J.A., Mason, R.P., Marnett, L.J., and Eling, T.E. Electron spin resonance investigation of tyrosyl radicals of prostaglandin H synthase - Relation to enzyme catalysis. J. Biol. Chem., *266*: 20045-20055, 1991.

63. Barry, B.A., El-Deeb, M.K., Sandusky, P.O., and Babcock,

G.T. Tyrosine radicals in photosystem II and related model compounds Characterization by isotopic labeling and EPR spectroscopy. J Biol Chem, *265*: 20139-20143, 1990.

64. Whittaker, M.M. and Whittaker, J.W. A tyrosine-derived free radical in apogalactose oxidase. J. Biol. Chem., *265*: 9610-9613, 1990.

65. Feher,G. Sensitivity considerations in microwave paramagnetic resonance absorption techniques. The Bell System Technical Journal, *36*: 449-484, 1957.

66. Petering, D.H. and Antholine, W.E. Copper toxicity: speciation and reactions of copper in biological systems. In: E. Hodgson, J.R. Bend and R.M. Philpot (eds.), Reviews in biochemical toxicology 9, pp. 225-270, New york: Elsevier Science Publishing Co., Inc.. 1988.

67. Aust, S.D., Lee, L.A., and Thomas, C.E. Role of metals in oxygen radical reactions. J. Free Radical Biol. Med., *1*: 3-25, 1985.

68. Byrnes, R.W., Mohan, M., Antholine, W.E., Xu, R.X., and Petering, D.H. Oxidative stress induced by a copper-thiosemicarbazone complex. Biochemistry, *29*: 7046-7053, 1990.

69. Saryan, L.A., Mailer, K., Krishnamurti, C., Antholine, W.E., and Petering, D.H. Interaction of 2-formylpyridine thiosemicarbazonato copper(II) with Ehrlich ascites tumor cells. Biochem. Pharmacol., *30*: 1595-1604, 1981.

70. Antholine, W.E. and Taketa, F. Effects of 2-formylpyridine monothiosemicarbazonato copper(II) on red cell components. J. Inorg. Biochem., *20*: 69-78, 1984.

71. Saryan, L.A., Ankel, E., Krishnamurti, C., Petering, D.H., and Elford, H. Comparative cytotoxic and biochemical effects of ligands and metal complexes of α-N-heterocyclic carboxaldehyde thiosemicarbazones. J. Med. Chem., *22*: 1218-1221, 1979.

72. Antholine, W.E. and Taketa, F. Binding of 2-formylpyridine monothiosemicarbazonato copper(II) to rat and normal hemoglobins. J. Inorg. Biochem., *16*: 145-154, 1982.

73. Antholine, W.E., Lyman, S., Petering, D.H., and Pickart,

L. Formation of adducts between cupric complexes of known antitumor agents and Ehrlich ascites tumor cells. In: K.D. Karlin and J. Zubieta (eds.), Biological and Inorganic Copper Chemistry, pp. 125-137, New York: Academic press. 1985.

74. Subczynski, W.K., Antholine, W.E., Hyde, J.S., and Petering, D.H. Orientation and mobility of a copper square-planar complex in a lipid bilayer. J. Am. Chem. Soc., *109*: 46-52, 1987.

75. Turner, M.K., Abrams, R., and Lieberman, I. . J. Biol. Chem., *241*: 5777-5780, 1966.

76. Sartorelli, A.C., Agrawal, K.C., and Moore, E.C. Mechanism of inhibition of ribonucleoside diphosphate reductase by α-(N)-heterocyclic aldehyde thiosemicarbazones. Biochem. Pharmacol., *20*: 3119-3123, 1971.

77. Brockman, R.W., Shaddix, S., Stringer, V., and Adamson, D. Proc. Am. Assoc. Cancer Res., *13*: 351, 1972.

78. Carter, G.L. and Cory, J.G. Cross-resistance patterns in hydroxyurea-resistant leukemia L1210 cells. Cancer Res., *48*: 5796-5799, 1988.

79. Narasimhan, J., Antholine, W.E., Chitambar, C.R., and Petering, D.H. Inhibition of iron uptake in HL60 cells by 2-formylpyridine monothiosemicarbazonato Cu(II). Arch. Biochem. Biophys., *289*: 393-398, 1991.

80. Antholine, W.E., Knight, J.M., and Petering, D.H. Inhibition of tumor cell transplantability by iron and copper complexes of 5-substituted 2-formylpyridine thiosemicarbazones. J. Med. Chem., *19*: 339-341, 1976.

81. Chitambar, C.R. and Zivkovic, Z. Uptake of gallium-67 by human leukemic cells: Demonstration of transferrin receptor-dependent and transferrin-independent mechanisms. Cancer Res., *47*: 3929-3934, 1987.

82. Antholine, W.E., Gunn, P., and Hopwood, L.E. Combined modality of 2-formylpyridine monothiosemicarbazonato copper(II) and radiation. Int. J. Rad. Oncol. Biol. Phys., *7*: 491-495, 1981.

83. Deziel, M.R. and Girotti, A.W. . J. Biol. Chem., *255*: 8192-8198, 1980.

84. Beutler, E. . In: Red Cell Metabolism: A Manual of Biochemical Methods, pp. 38, New York: Grune & Stratton.

1975.

85. Peisach, J. and Blumberg, W.E. . Arch. Biochem. Biophys., *165*: 691, 1974.

86. Antholine, W.E., Knight, J.M., Whelan, H., and Petering, D.H. Studies of the reaction of 2-formylpyridine thiosemicarbazone and its iron and copper complexes with biological systems. Mol. Pharmacol., *13*: 89-98, 1977.

87. Sjöberg, B-M., Karlsson, M., and Jörnvall, H. Half-site reactivity of the tyrosyl radical of ribonucleotide reductase from Escherichia coli. J. Biol. Chem., *262*: 9736-9743, 1987.

88. Sturrock, A., Alexander, J., Lamb, J., Craven, C.M., and Kaplan, J. Characterization of a transferrin-independent uptake system for iron in HeLa cells. J. Biol. Chem., *265*: 3139-3145, 1990.

89. McClarty, G.A., Chan, A.K., Choy, B.K., and Wright, J.A. Increased ferritin gene expression is associated with increased ribonucleotide reductase gene expression and the establishment of hydroxyurea resistance in mammalian cells. J. Biol. Chem., *265*: 7539-7547, 1990.

90. Klausner, R.D. and Harford, J.B. Cis-trans models for post-transcriptional gene regulation. Science, *246*: 870-872, 1989.

91. Theil, E.C. Regulation of ferritin and transferrin receptor mRNAs. J. Biol. Chem., *265*: 4771-4774, 1990.

92. Kraker, A., Krezoski, S., Schneider, J., Minkel, D., and Petering, D.H. Reaction of 3-ethoxy-2-oxybutyraldehyde bis(thiosemicarbazonato) Cu(II) with Ehrlich cells. J. Biol. Chem., *260*: 13710-13718, 1985.

93. Takahashi, K., Takita, J., and Umezawa, H. . J. Antibiot., *40*: 348-353, 1987.

94. Foster, B.J., Clagett-Carr, K., Hoth, D., and Leyland-Jones, B. Gallium nitrate: The second metal with clinical activity. Cancer Treat. Rep., *70*: 1311-1319, 1988.

95. Warrell, R.P.,Jr. Clinical trials of gallium nitrate in patients with cancer-related hypercalcemia. Semin. Oncol., *18*: 26-31, 1991.

96. Harris, W.R. and Pecoraro, V.L. Thermodynamic binding constants for gallium transferrin. Biochemistry, *22*:

292-299, 1983.

97. Larson, S.M., Rasey, J.S., Allen, D.R., Nelson, N.J., Grunbaum, Z., Harp, G.D., and Williams, D.L. Common pathway for tumor cell uptake of Gallium-67 and Iron-59 via a transferrin receptor. J. Natl. Cancer Inst., *64*: 41-53, 1980.

98. Chitambar, C.R. and Seligman, P.A. Effects of different transferrin forms on transferrin receptor expression, iron uptake and cellular proliferation of human leukemic HL60 cells: Mechanisms responsible for the specific cytotoxicity of transferrin-gallium. J. Clin. Invest., *78*: 1538-1546, 1986.

99. Latimer, W.M. The oxidation state of the elements and their potentials in aqueous solutions. In: , Englewood Cliffs, New Jersy: Prentice-Hall. 1982.

100. Chitambar, C.R., Matthaeus, W.G., Antholine, W.E., Graff, K., and O'Brien, W.J. Inhibition of leukemic HL60 cell growth by transferrin-gallium: Effects on ribonucleotide reductase and demonstration of drug synergy with hydroxyurea. Blood, *72*: 1930-1936, 1988.

101. Chitambar, C.R., Narasimhan, J., Guy, J., Sem, D.S., and O'Brien, W.J. Inhibition of ribonucleotide reductase by gallium in murine leukemic L1210 cells. Cancer Res., *51*: 6199-6201, 1991.

102. Wright, J.A., Alam, T.G., McClarty, G.A., Tagger, A.Y., and Thelander, L. Altered expression of ribonucleotide reductase and role of M2 gene amplification in hydroxyurea-resistant hamster, mouse, rat and human cell lines. Somatic Cell Mol. Genet., *13*: 155, 1987.

103. Urena, E., Garcia de Torres, A., Pavon, J.M.C., and Aziza, J.L.G. Determination of traces of gallium in biological materials by fluorometry. Anal. Chem., *57*: 2309-2311, 1985.

104. Scott, N., Carter, D.E., and Fernando, Q. Separation and determination of parts-per-billion concentrations of gallium in biological materials. Anal. Chem., *59*: 888-890, 1987.

105. McClarty, G.A., Chan, A.K., Engstrom, Y., Wright, J.A., and Thelander, L. Elevated expression of M1 and M2 components and drug-induced posttranscriptional modulation of ribonucleotide reductase in a hydroxyurea-resistant mouse cell line. Biochemistry, *26*: 8004-8011, 1987.

106. Morlein, S.M., Welch, M.J. The chemistry of gallium and indium as related to radiopharmaceutical production. Int. J. Nucl. Med. Biol., *8*: 277-287, 1981.

107. Seligman, P.A., Klausner, R.D., and Heubers, H.A. Molecular mechanisms of iron metabolism. In: G. Stamatoyannopoulos, A.W. Nienhuis, P. Leder and P. Majerus (eds.), The Molecular Basis of Blood Disease, pp. 219-244, Philadelphia, PA: W.B. Saunders. 1987.

108. Lederman, H.M., Cohen, A., Lee, J.W.W., Freedman, M.H., and Gelfand, E.W. Deferoxamine: A reversible S-phase inhibitor of human lymphocyte proliferation. Blood, *64*: 748-753, 1984.

109. Taetle, R., Castognola, J., and Mendelsohn, J. Mechanisms of growth inhibition by anti-transferrin receptor monoclonal antibodies. Cancer Res., *46*: 1759-1763, 1986.

110. Chitambar, C.R. and Narasimhan, J. Targeting iron-dependent DNA synthesis with gallium and transferrin-gallium. Pathobiology, *59*: 3-10, 1991.

111. Cory, J.G. and Chiba, P. Combination chemotherapy directed at the components of nucleoside diphosphate reductase. Pharmac. Ther., *29*: 111-127, 1985.

112. Lundberg, J.L. and Chitambar, C.R. Interaction of gallium nitrate with fludarabine and iron chelators: effects on the proliferation of human leukemic HL60 cells. Cancer Res., *50*: 6466-6470, 1990.

113. Sato, A., Carter, G.L., Bacon, P.E., and Cory, J.G. Effects of combinations of drugs having different modes of action of action at the ribonucleotide reductase site on growth of L1210 cells in culture. Cancer Res., *42*: 4353-4357, 1982.

114. Cory, J.G. Ribonucleotide reductase as a chemotherapeutic target. Adv. Enzyme Regul., *27*: 437-455, 1988.

115. Choy, B.K., McClarty, G.A., Chan, A.K., Thelander, L., and Wright, J.A. Molecular mechanisms of drug resistance involving ribonucleotide reductase: Hydroxyurea resistance in a series of clonally related mouse cell lines selected in the presence of increasing drug concentrations. Cancer Res., *48*: 2029-2035, 1988.

116. Donehower, R.C. Hydroxyurea. In: B. Chabner (ed.), Pharmacologic Principles of Cancer Treatment, pp.

269-275, Philadelphia: W.B. Saunders. 1982.

117. Carter, G.L., Thompson, D.P., and Cory, J.G. Mechanisms of drug resistance to inhibitors directed at the individual subunits of ribonucleotide reductase. Cancer Commun., *1*: 13-20, 1989.

118. Chitambar, C.R., Zivkovic-Gilgenbach, Z., Narasimhan, J., and Antholine, W.E. Development of drug resistance to gallium nitrate through modulation of cellular iron uptake. Cancer Res., *50*: 4468-4472, 1990.

119. Fujioko, S. and Silber, R. Leukocyte ribonucleotide reductase: Studies in normal subjects and in subjects with leukemia or pernicious anemia. J. Lab. Clin. Med., *77*: 59-64, 1971.

This dissertation was prepared under the direction of the chairman of the candidate's supervisory committee and has been approved by all members of that committee. It was submitted to the Associate Dean, The Graduate School, Medical College of Wisconsin and was approved as a partial fulfillment of the requirements for the degree of Doctor of Philosophy:

Committee in Charge:

Chairman

Associate Dean for Graduate Studies